AD-A049 040 IIT RESEARCH INST CHICAGO ILL F/G 6/21
RELATIVE STRUCTURAL CONSIDERATIONS FOR PROTECTION FROM INJURY A--ETC(U)
JUN 77 A LONGINOW, A WIEDERMANN DCPA01-75-C-0325
UNCLASSIFIED IITRI-J6365 NL

1 OF 2
AD
A049040

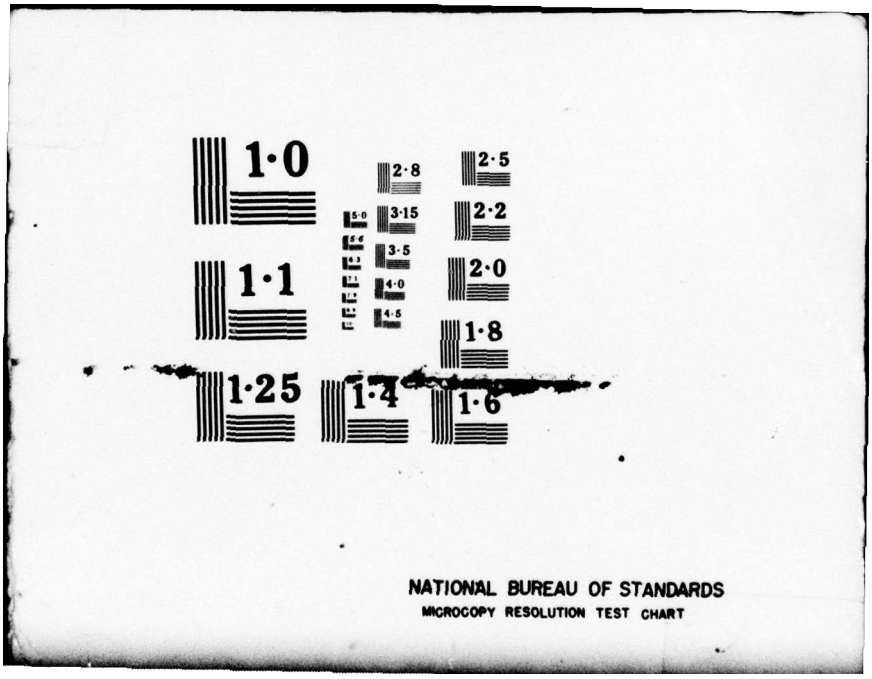
1·0
1·1
1·25
2·8
3·15
3·5
4·0
4·5
5·0
2·5
2·2
2·0
1·8
1·4
1·6
NATIONAL BUREAU OF STANDARDS
MICROCOPY RESOLUTION TEST CHART

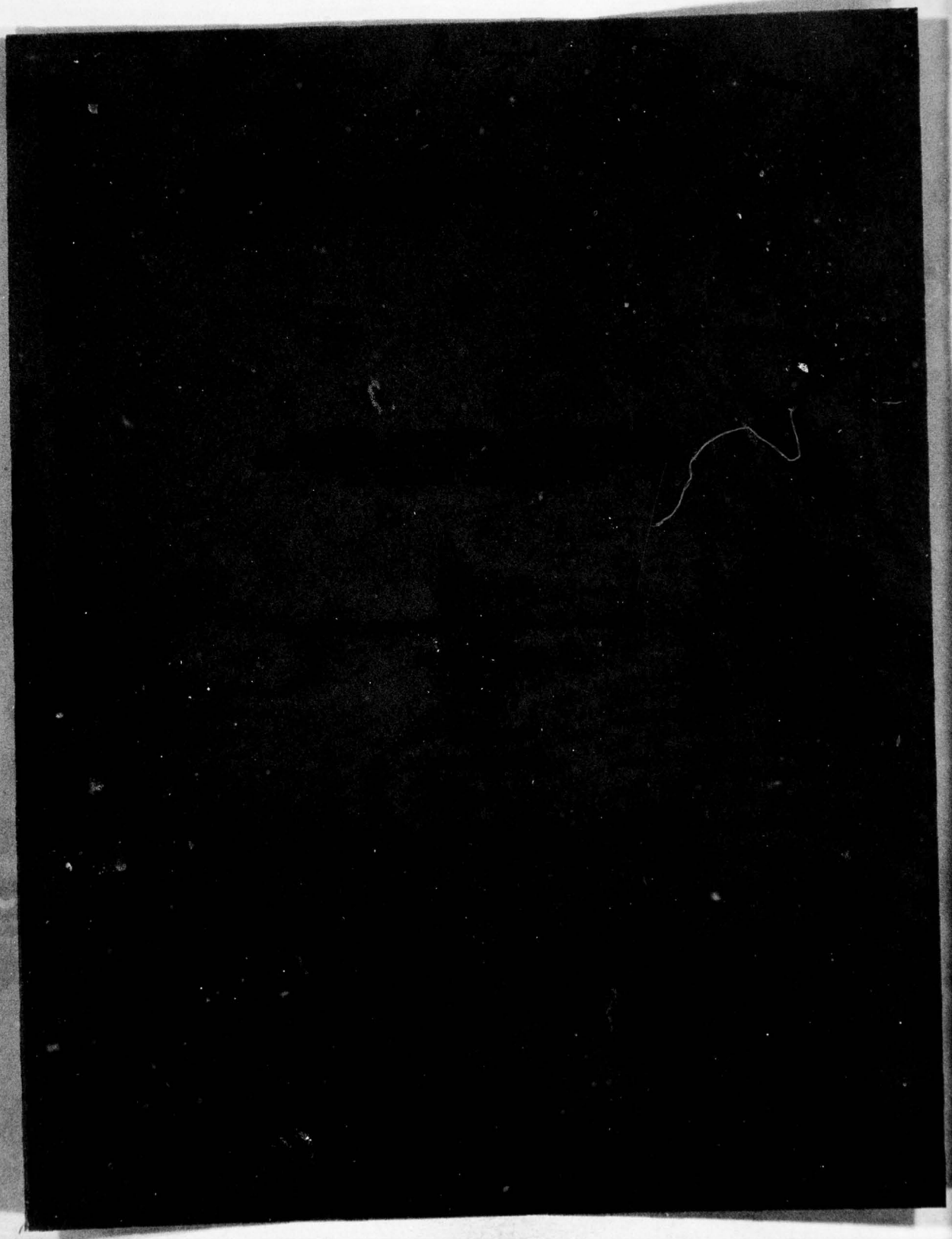

RELATIVE STRUCTURAL CONSIDERATIONS FOR PROTECTION FROM INJURY AND FATALITY AT VARIOUS OVERPRESSURES

Summary

DCPA Contract DCPA01-75-C-0325

FINAL REPORT

by

A. Longinow

A. Wiedermann

for

Defense Civil Preparedness Agency
Washington, D.C. 20301

June 1977

RELATIVE STRUCTURAL CONSIDERATIONS FOR PROTECTION FROM INJURY AND FATALITY AT VARIOUS OVERPRESSURES

SUMMARY

The emphasis of the study reported was on the survivability of people located in conventional buildings when subjected to the direct effects of nuclear weapons. The objective was to gain a better understanding of the inherent protective capabilities of such buildings. The study was based upon the conditions of a 1 MT surface burst with the building (shelter) located in the Mach region. Results produced can be used, in conjunction with the results of previous studies (Ref. 1,2), to identify and classify best available shelter space. Specific topics considered are described in the paragraphs that follow.

People Survivability in Basements

To gain a better understanding as to levels of protection inherent in basements of highrise buildings, a series of survivability analyses were performed. These were full basements with reinforced concrete peripheral walls and two-way overhead slabs supported on steel beams. Building parameters considered constitute a representative range of spans, design live loads and material properties. The hazard load environment consisted of primary and secondary effects of blast. Primary casualty mechanisms were impact and the trapping of people due to the failure and collapse of the overhead slab.

In the previous study (Ref. 1) basements of multistory reinforced concrete buildings with flat slab and flat plate floor systems were analyzed in a similar fashion. The results of this effort add one more basement category to the catalog of those examined in the light of a nuclear weapon attack.

Flow Induced Translational Effects in Basement Shelters

The major task of this portion of the study dealt with generating the description of the transient velocity field within a given basement shelter and then using it to determine the response of individuals located within. The velocity field was generated using

existing procedures and is an update and extension of that previously reported in Ref. 1. The following parameters were considered:

- Basement Size (Plan Area)
- Basement Aspect Ratio
- Size of Inlet(s) (Entranceway(s))
- Location of Inlet(s)

External, free field overpressures specifically include 2, 6, 10 and 15 psi.

Using the transient flow fields and the shelter parameters described, calculations were performed to determine impact velocities that would be experienced by individuals when coming in contact with shelter walls. A simple, two-dimensional (plan) drag model was used to simulate individuals. Results indicate that:

- Most severe impact conditions result when individuals are located in the jet. Outside the jet boundary, they are substantially reduced.
- Many of the wall impacts occur at very shallow angles and hence the normal component is rather low. However, since such an impact does not materially impede the motion, the second impact may be more severe than the first. The influence of the second impact was not considered.
- Most individuals will impact the front wall, i.e., the wall which contains the entranceway. This suggests that some improvement in survivability can be achieved by appropriately treating this surface.
- The influence of room size on impact velocities is to make the translation-impact environment in the larger shelters more severe. The reason is in part due to the fact that the duration of the intense flow is longer and therefore there is more time to accelerate the individuals.
- Results show that the location of the single inlet significantly influences the percent of floor area (related to the initial location of individuals) which produces impacts in excess of a given intensity. The most severe conditions noted exist for a configuration in which the entranceway is located at the edge of the front wall.

Tumbling Characteristics in Shelters

Two closely related problems were considered in this task. The first examines the influence of anthropometric variation of shelterees on the general nature of the blast translation problem (in a tumbling mode) and the severity of the resulting impact with the floor and walls of the shelter. In addition to this, the influence of occupant orientation with height to the airflow is examined briefly. The tumbling mode is examined since it is the primary response mode in a blast wind environment. The "tumbling man" computer model (Ref. 1) was used to simulate individuals. Translation parameters studied included:

- Velocity variation of the center of gravity of individuals
- Time to first impact
- Distance traveled before first impact
- Magnitude of the impact velocity
- Portion of the body impacted, i.e., head, feet.

Results indicate that:

- differences in the response due to anthropometric variations are generally small and therefore relatively unimportant,
- head/floor impact occurs at approximately 0.5 sec after the start of translation process
- the onset of head/floor impact occurs in the fairly narrow range of wind velocities of 200 fps to 250 fps.
- the impact velocity experienced by individuals is relatively independent of the intensity of the wind field being about 16 fps.
- the displacement of the center of gravity at the time of impact is in the range of about 22 ft to 56 ft. Therefore, in large shelters most impacts will be with the floor.

The second problem considered examined the tumbling characteristics of individuals in a series of representative flow environments.

Three wind fields characterized by equilateral triangles of equal impulse but varying peak and duration were used in conjunction with the "tumbling man" computer model.

Response parameters studied were again velocity, variation of the center of gravity, time to first impact, distance traveled before first impact, portion of the body impacted and impact velocity. Results obtained indicate that:

- wave details are of little, if any, significance on response;
- for the eight cases considered, with two exceptions, the head impact velocities achieved were consistently 22.6 fps and therefore, mostly independent of the waveform and peak magnitude of the wind field.

Results indicate that the hazard to shelter occupants results more from the fact that the individual will fall over when subjected to a blast wind field, than the hazard being proportional to the intensity of the disturbance.

People Survivability in Upper Stories

Previous studies on people survivability in the upper stories of highrise buildings with strong (arching) masonry walls have not considered the overturning of the building as a failure and casualty mechanism. Results of an analysis effort reported in Ref. 1 has indicated that this can be an important failure mechanism and should be considered. A nominal effort was devoted in this study to the task of examining the consequence of this failure mechanism on people survivability. A preliminary analysis method was formulated and was used to tentatively update previous (Ref. 2) results. Chapter 5 contains a discussion and results of this effort.

REFERENCES

1. Longinow, A., et al., Debris Motion and Injury Relationships in All Hazard Environments, for Defense Civil Preparedness Agency, Contract DCPA01-74-C-0251, DCPA Work Unit 1614 E, IIT Research Institute, July 1976.

2. Longinow, A., "Survivability in a Direct Effects Environment (Analysis of 50 NFSS Buildings), for Defense Civil Preparedness Agency, Contract DAHC20-73-C-0227, IIT Research Institute, July 1974.

UNCLASSIFIED

SECURITY CLASSIFICATION OF THIS PAGE (When Data Entered)

REPORT DOCUMENTATION PAGE

READ INSTRUCTIONS BEFORE COMPLETING FORM

1. REPORT NUMBER

2. GOVT ACCESSION NO.

3. RECIPIENT'S CATALOG NUMBER

(9)

4. TITLE (and Subtitle)

(6) RELATIVE STRUCTURAL CONSIDERATIONS FOR PROTECTION FROM INJURY AND FATALITY AT VARIOUS OVERPRESSURES.

5. TYPE OF REPORT & PERIOD COVERED

Final Report. ~~6/17/75 - 5/18/77~~

6. PERFORMING ORG. REPORT NUMBER

(14) IITRI-J6365

14 June 75-18 May 77.

7. AUTHOR(s)

(10) A. Longinow, A. Wiedermann

8. CONTRACT OR GRANT NUMBER(s)

(15) DCPA01-75-C-0325 new

9. PERFORMING ORGANIZATION NAME AND ADDRESS

IIT Research Institute
10 West 35th Street
Chicago, Illinois 60616

10. PROGRAM ELEMENT, PROJECT, TASK AREA & WORK UNIT NUMBERS

11. CONTROLLING OFFICE NAME AND ADDRESS

Defense Civil Preparedness Agency
Washington, D.C. 20301

(11)

12. REPORT DATE

June 1977 ✓

13. NUMBER OF PAGES

124

14. MONITORING AGENCY NAME & ADDRESS (if different from Controlling Office)

(12) 133p.

15. SECURITY CLASS. (of this report)

Unclassified

15a. DECLASSIFICATION/DOWNGRADING SCHEDULE

16. DISTRIBUTION STATEMENT (of this Report)

Approved for public release; distribution unlimited.

17. DISTRIBUTION STATEMENT (of the abstract entered in Block 20, if different from Report)

18. SUPPLEMENTARY NOTES

19. KEY WORDS (Continue on reverse side if necessary and identify by block number)

Civil Defense, Nuclear Weapons, Personnel Shelter, Blast Effects, Casualties, Survivors, Damage, Impact.

20. ABSTRACT (Continue on reverse side if necessary and identify by block number)

This report contains the results of a study concerned with producing casualty (injury and fatality) relationships for people located in conventional buildings when subjected to the direct effects produced by nuclear weapons.

People survivability estimates for people located in conventional basements of multistory buildings subjected to blast effects of megaton

→ next page

DD FORM 1 JAN 73 1473 EDITION OF 1 NOV 65 IS OBSOLETE

UNCLASSIFIED

SECURITY CLASSIFICATION OF THIS PAGE (When Data Entered)

175 350

range nuclear weapons are presented. Results are for full basements with two-way reinforced concrete overhead floor systems supported on steel beams.

The transient velocity field that may exist in such basements is modeled and used to determine the response of individuals located within. Two models having different levels of sophistication are used to simulate individuals. Results are used in part to gauge the adequacy of the simpler model. The more sophisticated model is subsequently used to examine two closely related problems. The first considers the influence of anthropometric variation of individuals on the general nature of the blast translation problem (in the tumbling mode) and the severity of the resulting impact with floor and walls. The second examines the tumbling characteristics of individuals in a series of representative flow environments.

A nominal effort was devoted to the task of examining the consequence of tall building overturning when subjected to blast on people survivability. A preliminary analysis method was formulated and used to tentatively update results where this failure mechanism was not considered.

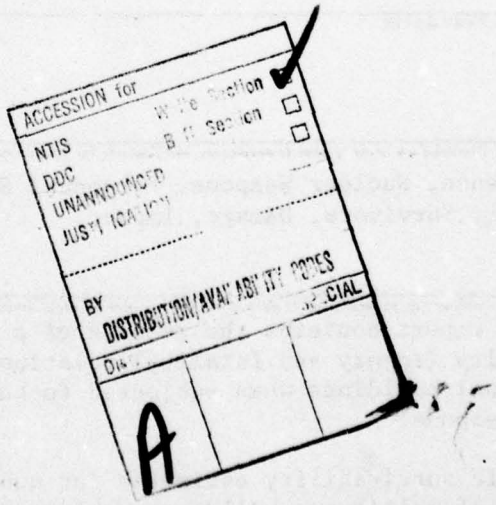

RELATIVE STRUCTURAL CONSIDERATIONS FOR PROTECTION FROM INJURY AND FATALITY AT VARIOUS OVERPRESSURES

DCPA Contract DCPA01-75-C-0325

FINAL REPORT

by

A. Longinow

A. Wiedermann

for

Defense Civil Preparedness Agency
Washington, D.C. 20301

June 1977

DCPA Review Notice

This report has been reviewed in the Defense Civil Preparedness Agency and approved for publication. Approval does not signify that the contents necessarily reflect the views and policies of the Defense Civil Preparedness Agency.

FOREWORD

This is the final report on IITRI Project J6365, entitled, "Relative Structural Considerations for Protection from Injury and Fatality at Various Overpressures". The study described was performed for Defense Civil Preparedness Agency (DCPA) under contract DCPA01-75-C-0325. The effort was initiated June 17, 1975 and completed May 18, 1977.

The study was performed in the Structural Analysis Section, Engineering Research Division of IIT Research Institute. The following personnel provided technical contributions to this effort. A. Longinow, A. Wiedermann and D. Oldham. The study was monitored by Mr. D. A. Bettge of DCPA. The numerous useful suggestions provided by Mr. Bettge in the course of this effort are gratefully acknowledged.

Respectfully submitted,
IIT RESEARCH INSTITUTE

A. Longinow
Project Engineer

APPROVED:

K. E. McKee
Director of Research
Engineering Division

TABLE OF CONTENTS

LIST OF ILLUSTRATIONS

ILLUSTRATIONS (concluded)

LIST OF TABLES

CHAPTER 1
SUMMARY AND CONCLUSIONS

The emphasis of the study reported herein was on the survivability of people located in conventional buildings of the National Fallout Shelter Survey (NFSS) type when subjected to the direct effects of megaton-range nuclear weapons. The overall objective is to gain an understanding as to the inherent capabilities of conventional buildings in providing protection to the urban population in the event of a nuclear weapon attack. Results can be used to identify and classify best available shelter space. The topics considered are described in the following paragraphs. Detailed discussion is provided in subsequent chapters.

1.1 PEOPLE SURVIVABILITY IN CONVENTIONAL BASEMENTS

To gain a better understanding as to the levels of protection afforded by existing conventional basements of high rise buildings against the effects of blast, a series of survivability analyses for people located in basements of steel framed buildings was performed.

Floor systems considered are two-way slabs supported on steel beams. Slab design parameters constitute a representative (real world) range of spans, design live loads and material properties. The hazard load environment represents the blast effects of a single, megaton-range nuclear weapon. Structural analyses of slab response were based on current state of the art techniques backed by experimental results, most of which were generated by Waterways Experiment Station (WES) at the request of Defense Civil Preparedness Agency (DCPA). People survivability analyses were performed using the results of the structural analysis. Casualty mechanisms considered were impact and the trapping of people due to the failure and collapse of the overhead slab. Slab collapse mechanisms and corresponding overpressure levels were identified with the aid of structural analyses.

In a previous study, (Ref. 1) basements of multistory reinforced concrete buildings with flat slab and flat plate floor systems were considered in a similar fashion. The results of this effort add one more building basement category to the catalog of those examined in the light of a nuclear weapon attack. Predicted failure overpressures for all slabs considered correlate most directly with design live load.

Upper and lower bound estimates of total survivors and injured survivors were obtained for each type of floor system as a function of free field overpressure. Results are compared and discussed in Chapter 2.

1.2 FLOW INDUCED TRANSLATIONAL EFFECTS IN BASEMENT SHELTERS

The major task of this effort dealt with generating the description of the transient velocity field within the shelter and then using it to determine the response of individuals located within. The transient velocity field was generated using existing procedures and is an update and extension of that previously reported in Ref. 1. The following parameters and their ranges were considered.

The study was based upon the conditions of a 1MT surface burst with the shelter located in the Mach region. External, free field overpressures considered specifically include 2, 6, 10 and 15 psi.

Shelters considered are square with Volume to Entranceway Area (V/A) ratios in the range from 500 ft to 4000 ft. Shelter (room) parameters studied include room size, room configuration, i.e., aspect ratio, entranceway size and entranceway location. Single and multiple entranceways were considered.

Using the transient flow fields and the shelter parameters described, calculations were performed to determine impact velocities that would be experienced by individuals when coming in contact with shelter walls. Results for shelters having a centrally located entranceway are described first.

As would be expected, the most severe impact conditions result when individuals are located in the jet. Outside the jet boundary they are substantially reduced. Many of the wall impacts occur at very shallow angles and hence the normal component is rather low. However, since such an impact does not materially impede the motion, the second impact may be more severe than the first. The influence of the second impact was not considered in this study.

Most individuals will impact the front wall, i.e., the wall which contains the entranceway. This suggests that some improvement in survivability can be achieved by appropriately treating this surface and avoiding the placement of objects along this wall which could be hazardous to impacting individuals.

The influence of room size on impact velocities is to make the translation-impact environment in the larger shelters more severe. The reason is in part due to the fact that the duration of the intense flow is longer and therefore there is more time to accelerate the individuals.

Results show that the location of the single inlet (entranceway) significantly influences the percent of floor area (related to the initial location of individuals) which produces impacts in excess of a given intensity. The most severe conditions noted exist for a configuration in which the entranceway is located at the edge of the front wall. When compared to that of the same shelter but with the opening centrally located, the affected floor area was increased by a factor of 2.7.

Rooms identical in all respects. i.e., volume, entranceway area, entranceway area location, except that the aspect ratio is different were examined to gauge the influence of this parameter on impact velocities. Results indicate that the influence of inlet location is predominant. That of the overpressure level is moderate while room aspect ratio does not appear to be significant.

The multiple inlet problem applies primarily to large shelters. The number of inlets was made proportional to room size which corresponds approximately to one inlet per 2400 sq ft of floor area. As in the previous cases, edge located inlets significantly increase

the hazard over that produced by centrally located inlets. Room aspect ratio is not a significant parameter.

Decreasing the size of the entranceway area by a factor of two, resulted in the reduction of the affected floor area by roughly a factor of two.

1.3 TUMBLING CHARACTERISTICS IN SHELTERS

Chapter 4 is concerned with the tumbling characteristics of individuals in shelters produced by blast winds when closures are not provided or when their capacity is exceeded by the blast. Two closely related problems are considered. The first examines the influence of anthropometric variation of shelterees on the general nature of the blast translation problem (in a tumbling mode) and the severity of the resulting impact with the floor and walls of the shelter. In addition to this, the influence of occupant orientation with height to the airflow is examined briefly. The tumbling mode is examined since it is the primary response mode in a blast wind environment.

Anthropometric data on the general population are fairly limited. IITRI examination of the existing data base indicates that sample sizes tend to be small and mostly involve the young adult male. However, for purposes of this effort the available data are adequate. The reference point was taken as that of an average adult male. A series of simple scaling relationships were established so as to bracket a 90 to 95 percentile of the adult male population. To make the picture more complete, limited anthropometric estimates were also made for women, teenagers, and children. Using existing computer programs the response of this group of individuals was evaluated when subjected to step-pulse wind velocites in the range of zero to 500 fps. Translation parameters studied included:

Velocity variation of the center of gravity

Time to first impact

Distance traveled before first impact

Magnitude of the impact velocity

Portion of the body impacted, i.e., head, feet.

Results indicate that:

- differences in the response due to anthropometric variations are generally small and therefore relatively unimportant,
- head/floor impact occurs at approximately 0.5 sec after the start of translation process
- the onset of head/floor impact occurs in the fairly narrow range of wind velocities of 200 fps to 250 fps.
- the impact velocity experienced by individuals is relatively independent of the intensity of the wind field being about 16 fps.
- the displacement of the center of gravity at the time of impact is in the range of about 22 ft to 56 ft. Therefore in large shelters most impacts will be with the floor.

The second problem considered in Chapter 4 examined the tumbling characteristics of individuals in a series of representative flow environments with the object of estimating the influence in flow variations on response of individuals and of evaluating the adequacy or limitations of the simple drag translation model used in Chapter 3.

Three wind fields characterized by equilateral triangles of equal impulse but varying peak and duration were used in conjuction with the "tumbling man" computer model to evaluate the influence of these parameters. Five other cases were considered to study the influence of pulse shape. Again, triangular pulses were used. Response parameters studied were again velocity, variation of the center of gravity, time to first impact, distance traveled before first impact, portion of the body impacted and impact velocity. Results obtained indicate that:

- wave details are of little, if any, significance on response;
- for the eight cases considered, with two exceptions, the head impact velocities achieved were consistently 22.6 fps and therefore, mostly independent of the wave form and peak magnitude of the wind field.
- a comparison of results for the two simulation models, i.e., tumbling block and the drag model indicates that agreement was generally adequate for situations in which the time of motion or the overall displacement are not excessive. The limits are estimated at 1 to 2 sec of time motion and displacements not in excess of about 20 fps.

Results of this study indicate that the hazard to shelter occupants results more from the fact that the individual will fall over when subjected to a blast wind field, than the hazard being proportional to the intensity of the disturbance. This is borne out by the following.

Simple loss of balance followed by unaided fall with impact to the head results in an impact velocity of about 22.8 fps for an average adult. Results of this effort indicate that individuals subjected to a "zero rise time - no decay" wind field with magnitudes up to at least 500 fps will be tumbled and will impact (on the head) with a velocity of about 16 fps, essentially independent of blast wind magnitude.

When the pulse is triangular with durations of up to 0.6 sec and wind velocities are in the same range magnitude as above, the head impact velocity was determined to be fairly consistently 22.6 fps.

It appears, therefore, that at least as far as large open shelters are concerned, a great deal can be done with very little to increase the survivability of initially standing occupants subjected to blast winds in the range of magnitudes considered in this study. By providing a padded surface on the floor the threshold of fatality (about 21 fps) may be reduced to simple injury or less.

1.4 PEOPLE SURVIVABILITY IN UPPER STORIES

Previous studies on people survivability in the upper stories of highrise buildings with strong (arching) masonry walls have not considered the overturning of the building as a failure and casualty mechanism. Results of an analysis effort reported in Ref. A2 has indicated that this can be an important failure mechanism and should be considered. A nominal effort was devoted in this study to the task of examining the consequence of this failure mechanism on people survivability. A preliminary analysis method was formulated and was used to tentatively update previous (Ref. 11) results. Chapter 5 contains a discussion and results of this effort.

CHAPTER 2

PEOPLE SURVIVABILITY IN CONVENTIONAL BASEMENTS

This chapter contains the results of analyses that were performed to gain a better understanding as to the levels of protection afforded by conventional basements against the effects of blast produced by the detonation of megaton-range nuclear weapons. Conventional basements considered are those in engineered buildings. This, therefore, excludes single- and two-family residences which are generally not engineered.

Protection in such basements depends on a number of parameters which include:

1. Type of overhead floor system used in the building; involves the type of slab, design live load, span lengths, aspect ratio, end conditions, material strengths and workmanship.
2. Size of basement - volume and floor area
3. Degree of basement exposure; can range from a subbasement with few protected apertures to a partial basement with one or several exposed basement walls and many large apertures.
4. Design criteria and age of structure; refers to the specific design code provisions as to type of concrete, steel, the placement of reinforcement, details, allowable live load reductions, and the degree of deterioration at the footings and elsewhere experienced since construction.

In this study we consider multistory, steel-framed buildings. The floor system consists of two-way reinforced concrete slabs supported on steel beams. There is no exposure of the basement walls, nor are there windows to the basement. The V/A ratio is large, i.e., the subject is large basements with proportionally small entranceway areas. This precludes the production of significant casualties by blast winds entering basements through failed or open entranceways. Thus, the primary casualty mechanism is impact which is produced by spalled chunks of concrete from the overhead slab and the collapse of the slab itself. The influence of blast winds on the survivability of people in basement areas is discussed in Chapter 3 and 4 of this report.

In the previous study, (Ref. 1) basements of multistory reinforced concrete framed buildings with flat plate and flat slab floor systems were considered in a similar fashion. The results of this effort add one more building basement category to the catalog of those examined in the light of a nuclear weapon attack.

Engineering data on floor systems and other relevant physical aspects of existing buildings was not readily available for sufficiently large and representative samples of buildings in the course of this effort. For this reason it became necessary to first design a set of floor systems for representative ranges of design loads, span lengths and material properties. The designs were subsequently analyzed when subjected to the effects of blast produced by megaton-range nuclear weapons. Specific parameters considered and the design approach taken is discussed.

2.1 DESIGN

Typical, square interior panels (see Figure 2.1) were designed in accordance with ACI 318-63 (Ref. 2). The designs are based on all combinations of the following parameters:

Span: 12, 16, 20, 24 and 28 ft
Ultimate compressive stress of concrete: 3000 and 4000 psi
Yield strength of reinforcing steel: 40,000 and 60,000 psi
Design live load: 50, 80, 100, 125, 200 and 250 psf

As in the previous study (Ref. 1) the design was based on a minimum volume of concrete through the use of minimum slab thicknesses. This approach is assumed to yield a reasonable-cost structure if not the least-cost structure, which would be dependent on actual construction costs at the time of construction.

Slab design was performed using the ACI Method 2, (see Appendix A of Ref. 2). The design live load acting on the slab was assumed to be the nominal live load reduced as provided for in the Chicago Building Code (Ref. 3) for beams, girders and trusses. This building code allows the following live load reductions for these structural members.

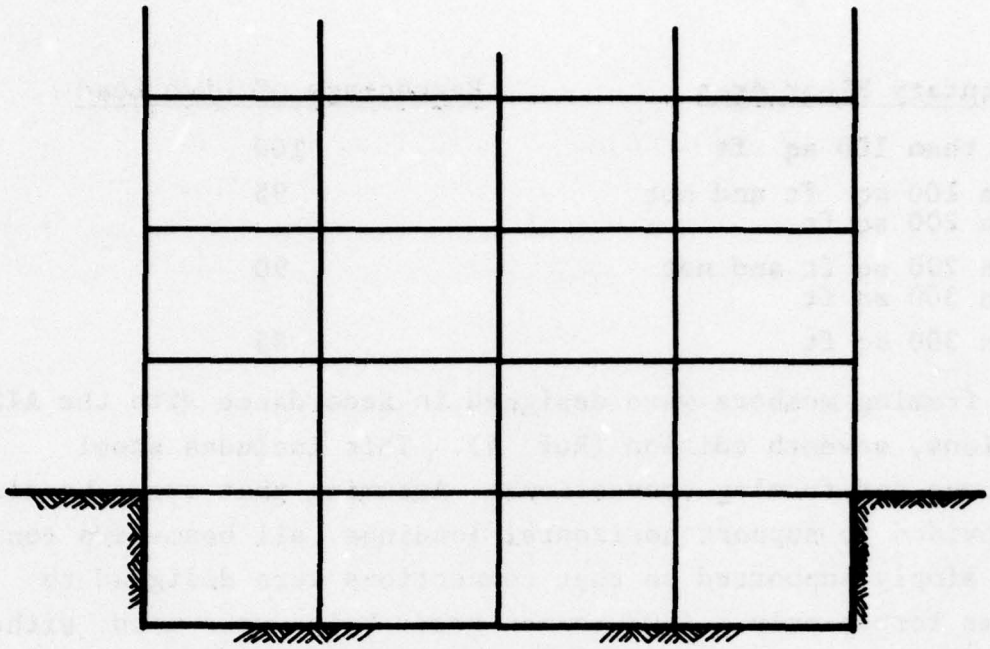

(a) Building Elevation

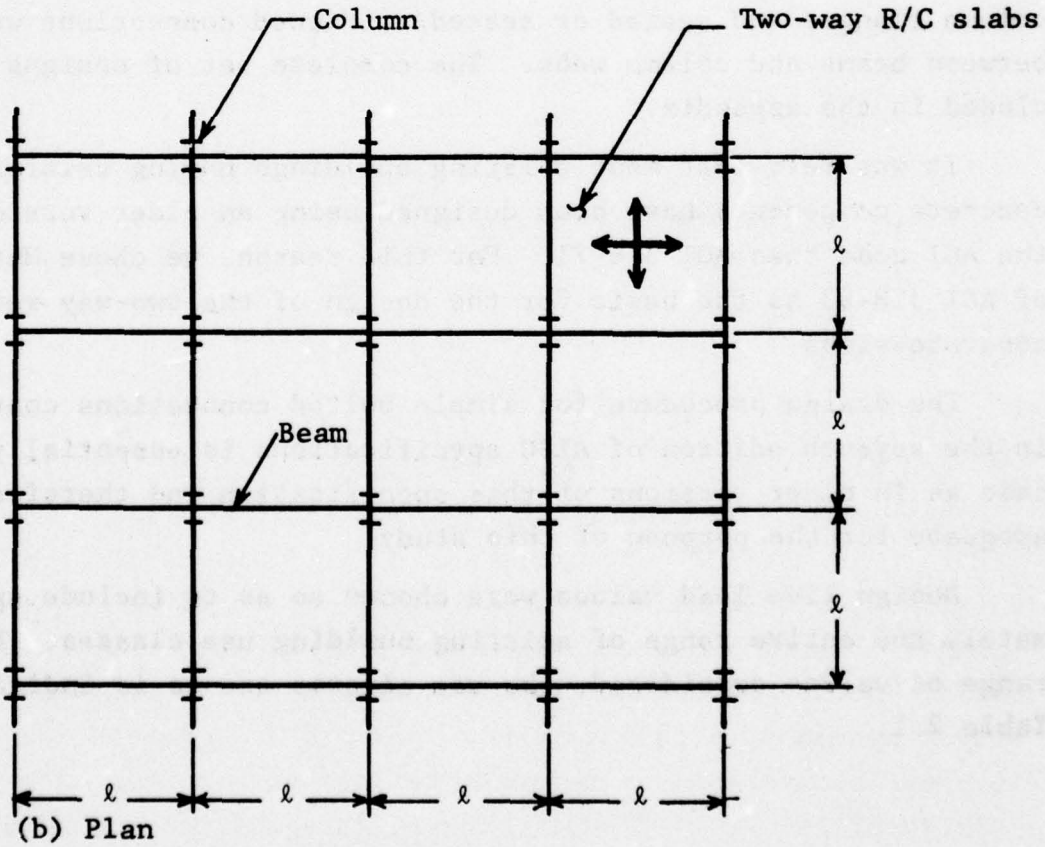

(b) Plan

Figure 2.1 Framing Plan

Tributary Floor Area	Percentage of Live Load
• Not more than 100 sq ft	100
• More than 100 sq ft and not more than 200 sq ft	95
• More than 200 sq ft and not more than 300 sq ft	90
• More than 300 sq ft	85

Steel framing members were designed in accordance with the AISC specifications, seventh edition (Ref. 4). This includes steel beams, columns and framing connections. Assuming that cross-bracing will be provided to support horizontal loadings, all beams are considered as simply supported so that connections were designed to resist shear forces only. A307 common grade bolts were used, either 3/4 inch or 1 inch diameter as needed. Connection angles were of A36 steel. Standard framed connections were used between beams and column flanges and seated or seated/stiffened connections were used between beams and column webs. The complete set of designs is included in the appendix.

It was felt that most existing buildings having reinforced concrete components have been designed using an older version of the ACI code than ACI 318-71. For this reason, we chose Method II of ACI 318-63 as the basis for the design of the two-way reinforced concrete slabs.

The design procedure for simple bolted connections contained in the seventh edition of AISC specifications is essentially the same as in older versions of this specification and therefore, adequate for the purpose of this study.

Design live load values were chosen so as to include approximately the entire range of existing building use classes. For the range of values considered, the use classes are as is indicated in Table 2.1.

TABLE 2.1

DESIGN LIVE LOAD AND BUILDING USE CLASSES

Design Live Load psf	Building Use Classes
40 - 60	Hotel, guestrooms, library reading rooms, private apartments, corridors of residential buildings, classrooms
80	Offices
100	Restaurants, passenger car garages, gymnasiums, office building lobbies, hotel public rooms, school corridors, first floor areas of retail stores, theater corridors and lobbies
125	Manufacturing, light storage warehouses, wholesale stores
200 - 250	Heavy storage warehouses

2.2 ANALYSIS

The set of two-way floor systems described was analyzed with the object of determining collapse overpressures when subjected to the blast effects of a single, megaton-range nuclear weapon in its Mach region.

Theory and experimental data indicate that floor systems of the type considered will fail either in flexure of the slab or the supporting beams or shear failure of the connections. Shear failure of the slabs is not expected to be a prime failure mechanism.

Overpressures producing failure in the slab and the supporting beams were determined using procedures described in Chapters 7 and 8 of Ref. 5 and Chapter 7 of Ref. 6. Failure criteria used are described in the following paragraphs.

For the purpose of estimating the number of survivors, two levels of structural failure are considered for reinforced concrete slabs and steel beams, i.e., incipient failure and ultimate failure (collapse). Loads producing incipient failure are defined herein as the minimum values of flexural or shear resistance of the structural member. Thus in the case of a simply supported steel beam,

incipient flexural failure is defined as the dynamic load required to produce a plastic hinge at midspan. As indicated in Figure 2.2 this occurs when μ (ductility ratio y_m/y_y) is equal to 1. Ultimate collapse is assumed to occur when $\mu = 8$ (Ref. 5).

For two-way reinforced concrete slabs, incipient flexural failure is defined as the dynamic, uniformly applied load required to produce plastic moments for a minimum load yield pattern. When expressed in terms of a resistance function, this occurs when deflection y_f (see Figure 2.3) is reached. Ultimate collapse depends on whether the reinforcement is capable of developing membrane resistance, then flexural failure is indicated by a limiting ductility ratio, resulting in a collapse deflection of

$$y_m = \frac{0.10}{p} y_e \leq 30\, y_e \qquad (2.1)$$

where y_e is the equivalent yield deflection of the slab based on a bilinear resistance function and p is the tensile steel ratio. When the slab is capable of developing membrane resistance, then failure is indicated by a limiting deflection of

$$y_{ft} = 0.15\, L_s \qquad (2.2)$$

where L_s is the length of the slab in the long direction (Ref. 7).

Beam connections were analyzed to determine their ultimate capacity by analyzing each possible failure mechanism. Failure is assumed to occur and collapse is assumed to follow when either one or several of the following conditions is produced.

(a) Combined shear capacity of the bolts
(b) Bearing capacity of the beam web
(c) Bearing capacity of column web or flange
(d) Bearing capacity of simple connection support angles

In the case of seated connections, the contribution of the top angle in resisting shear is ignored. The ultimate capacity of connections is expressed in terms of dynamic uniform load applied to the slab. Procedure used in analyzing connections was taken from Ref. 8.

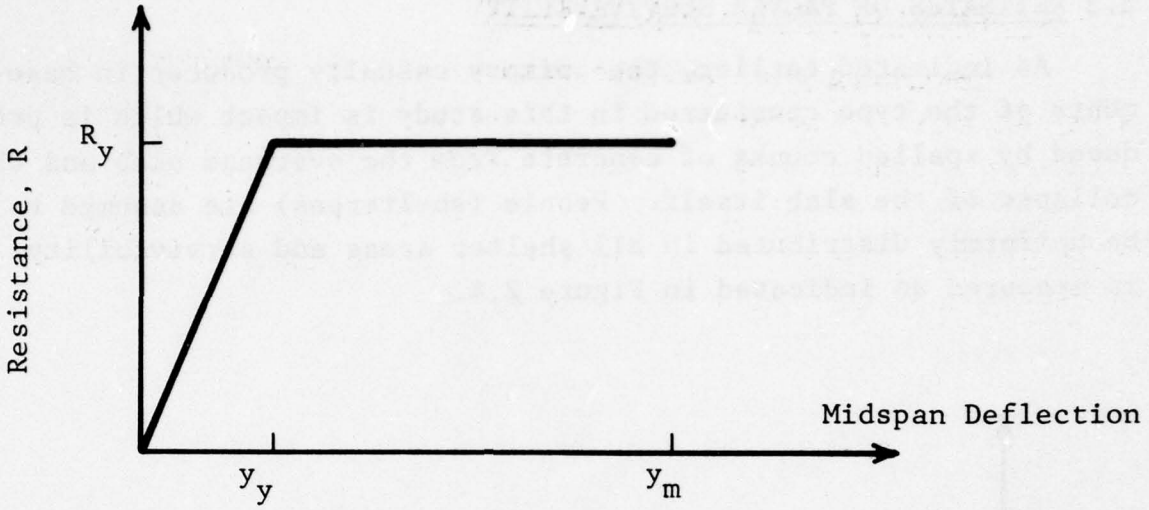

Figure 2.2 Resistance Function for a Simply Supported Beam

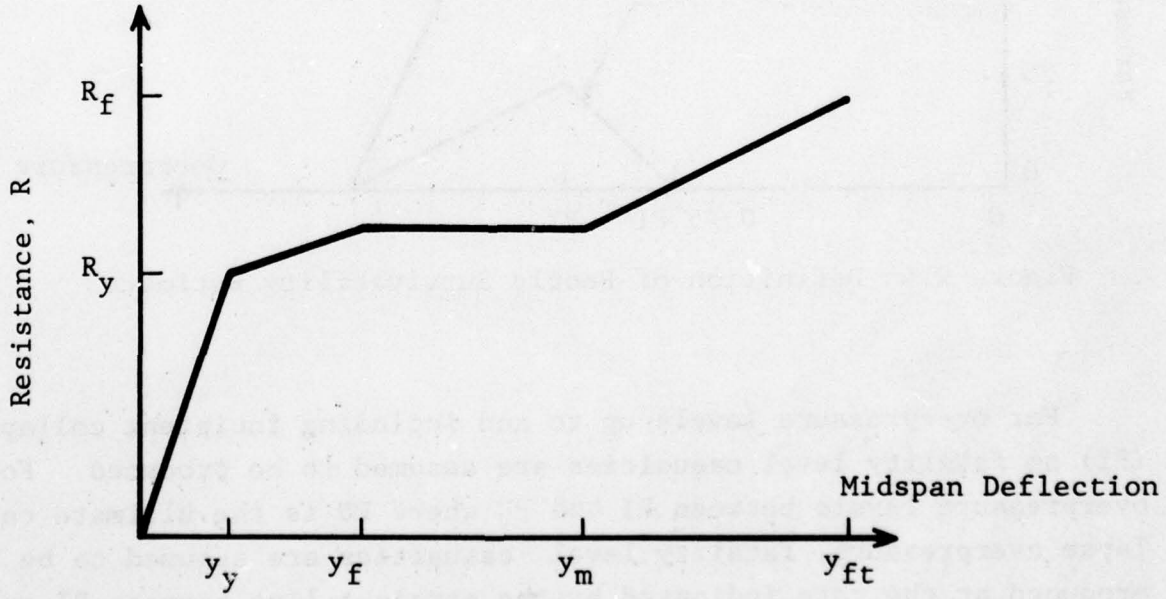

Figure 2.3 Resistance Function for a Reinforced Concrete Two-Way Slab

2.3 ESTIMATES OF PEOPLE SURVIVABILITY

As indicated earlier, the primary casualty producer in basements of the type considered in this study is impact which is produced by spalled chunks of concrete from the overhead slab and the collapse of the slab itself. People (shelterees) are assumed to be uniformly distributed in all shelter areas and survivability is measured as indicated in Figure 2.4.

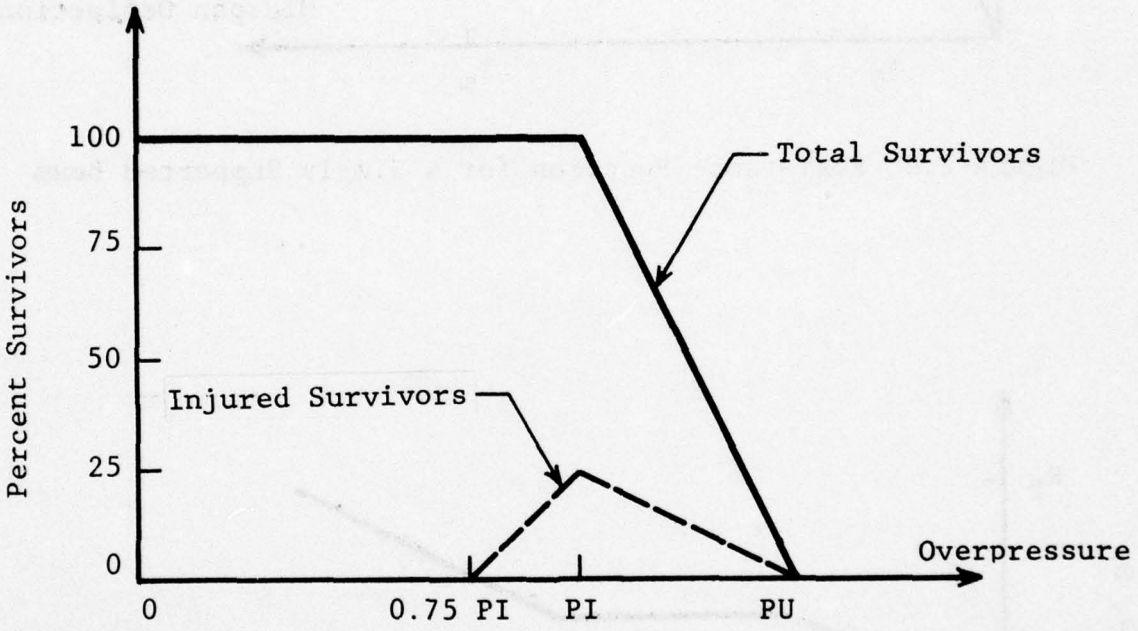

Figure 2.4 Definition of People Survivability Estimate

For overpressure levels up to and including incipient collapse (PI) no fatality level casualties are assumed to be produced. For overpressure levels between PI and PU where PU is the ultimate collapse overpressure, fatality level casualties are assumed to be produced at the rate indicated by the straight line between PI and PU. Nonfatal injuries are assumed to begin at 3/4 PI, reach a maximum at 25 percent and to decrease at a linear rate to PU. Recoverable injuries are assumed to be produced by spalled chunks

of concrete from the overhead slab. The fact that spallation occurs is indicated by tests such as those of Ref. 9.

For the set of slabs considered in this effort and that of the previous effort (Ref. 1), the upper and lower bounds on PI and PU are summarized in Table 2.2.

TABLE 2.2
BOUNDS ON PI* AND PU*

PI		PU		Structural Member**
Lower Bound	Upper Bound	Lower Bound	Upper Bound	
0.57	0.81	1.80	2.40	FP
0.70	2.74	1.10	4.20	FS
0.56	3.38	0.60	13.50	CAPS
0.87	3.40	2.07	7.50	C/S
0.60	1.60	1.13	3.00	SB
-	-	1.30	6.40	Conn

* PI - Incipient Collapse Overpressure
PU - Ultimate Collapse Overpressure

** FP - Flat plate
FS - Flat slab with drop panel and no capital
CAPS - Flat slab with drop panel and capital
C/S - Two-way R/C slab on steel beams
SB - Steel beam
Conn - Bolted connections

Corresponding people survivability estimates are given in Figure 2.5 and 2.6. Figure 2.5 was reproduced from Ref. 1. It depicts the people survivability potential in large, full basements of reinforced concrete framed buildings with flat plate and flat slab floor systems.

It will be noted that survivable injury is higher (up to 50 percent) in basements with flat slab floor systems. This is due to larger quantities of debris that is produced by the failure (spallation) of drop panels which are generally unreinforced.

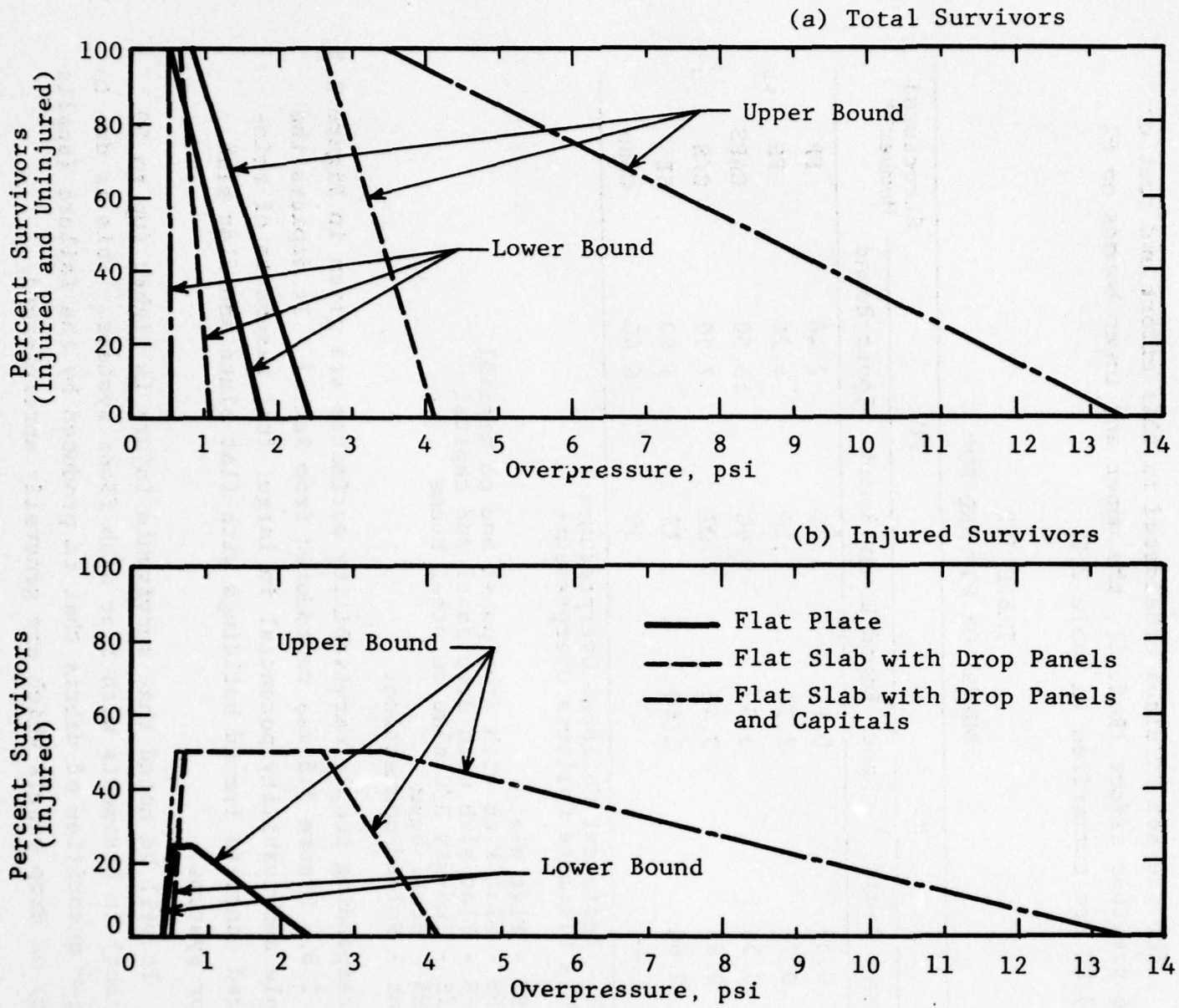

Figure 2.5 Upper and Lower Bound Estimates of Survivability and Injury (Two-Way Slabs)

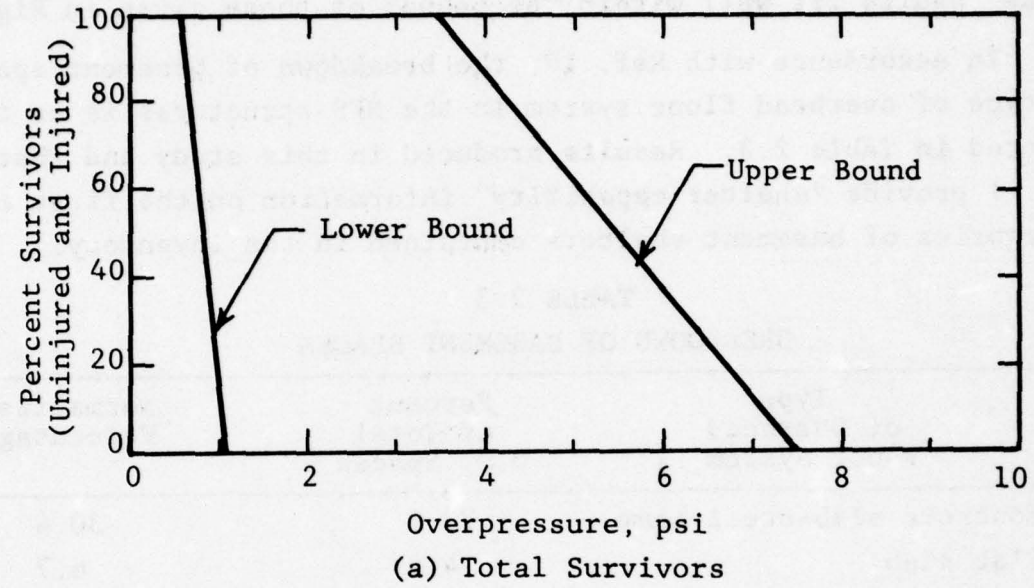

(a) Total Survivors

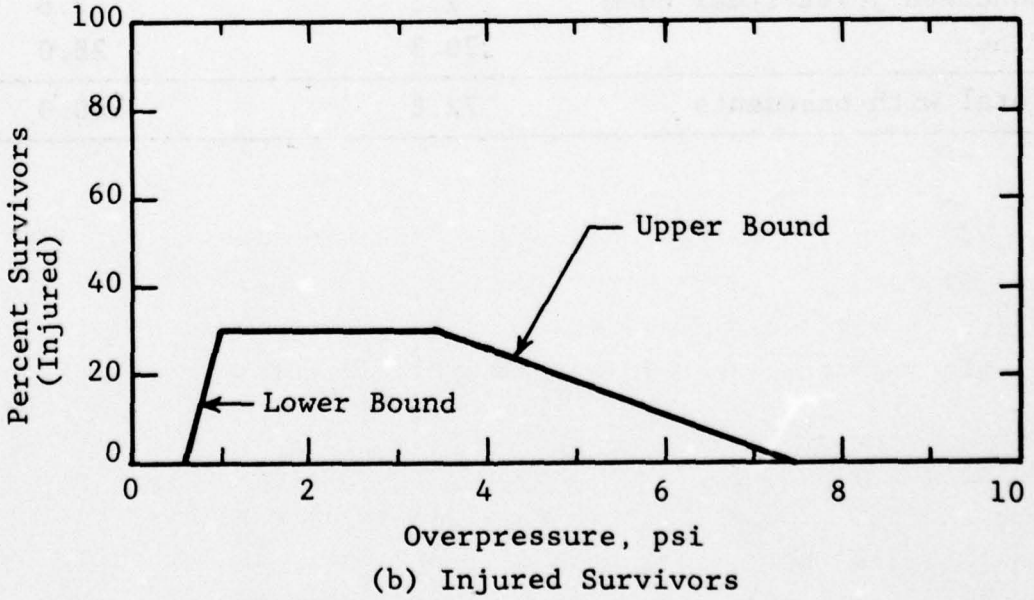

(b) Injured Survivors

Figure 2.6 Upper and Lower Bound Estimates of Survivability and Injury (Two-Way Slabs on Steel Beams)

Results for basement shelters in steel framed buildings with two-way reinforced concrete floor systems are shown in Figure 2.6. These results fit well within the bounds of those given in Figure 2.5.

In accordance with Ref. 10, the breakdown of basement spaces by type of overhead floor system in the NFS structures is as indicated in Table 2.3. Results produced in this study and that of Ref. 1 provide "shelter capability" information on the first three categories of basement shelters contained in the inventory.

TABLE 2.3

BREAKDOWN OF BASEMENT SPACES

Type of Overhead Floor System	Percent of Total U.S. Spaces	Normalized Percentages
1. Concrete slab-steel beam	22.1	30.4
2. Flat slab	4.9	6.7
3. Flat plate	5.7	7.8
4. Concrete slab-concrete beam	16.9	23.2
5. Concrete joist-concrete beam	0.8	1.1
6. Concrete joist-steel beam	2.1	2.8
7. Other	20.3	28.0
Total with basements	72.8	100.0

CHAPTER 3

FLOW INDUCED TRANSLATIONAL EFFECTS IN BASEMENT SHELTERS

3.1 BACKGROUND

In this chapter the results of an effort to establish the probability of survival for personnel within conventional basement type shelters when subjected to blast wind induced translating effects generated by an atmospheric burst of a nominal, megaton-range nuclear weapon in its Mach region are presented.

The detonation of a large nuclear weapon within the atmosphere generates a rather well defined blast wave system which propagates outward from the burst point. This blast wave system will interact with the ground plane and its perturbations (hills, structures, etc.) altering the local blast environment to some extent. This blast environment is characterized by the presence of a shock discontinuity across which the air pressure increases. The pressure level then decreases, decaying down below the atmospheric level (entering the so-called negative phase) and then increases again, yet more slowly, until the ambient pressure level is reached. The air motion also undergoes a similar oscillatory (outward-inward) pattern. Structure geometries and orientations, shielding effects, and shelter entrance locations and configurations will further distort the fine details of the local blast environment.

Ultimately, the blast wave energy will propagate within an open shelter and induce a variety of rather intense flow regimes within the shelter. Personnel and objects located within these shelters will respond to the environment, in part, by being transported in some fashion (tumbled, slid, etc.) until the adverse environment is relieved or an impact with a wall or other object occurs. The nature and intensity of an impact, if one occurs, will be dependent upon the many variables defining the explosion, the shelter, the object, and the location of the object and other objects within the shelter. The survivability of personnel to such impacts will be a function of the nature and intensity of the impact

or perhaps impacts and the complicated interactions of other adverse physiological effects such as blast overpressure exposure.

The current study is based upon the conditions of a 1 MT nuclear weapon surface burst with the shelter located in the Mach region. This restriction is not a limiting one as other weapon yields and burst conditions can be readily treated. However, as an effort to establish a measure of the survivability levels of personnel in shelters some restrictions and simplifications are required. The survivability question is a complex one and if an adequate prediction is to be made, then a comprehensive effort coupled with some attempt (perhaps experimental observations) to verify the more important aspects of this complex problem will have to be made. The basic elements of the problem can be categorized by these steps or criteria:

(a) Injury and fatality criteria
(b) Impact and bounce conditions
(c) Complete description of the transient air velocity field within the shelter
(d) Development or adaptation of adequate translational models
(e) Adequate selection of pertinent shelter parameter values.

In many instances these steps can be undertaken at several levels of sophistication and precision. Initially simple models and/or criteria can be used or established to obtain a rough estimate of the survivability levels for typical conditions of interest and to identify the critical aspects of the overall problem. Such a procedure is used in this effort.

The transient velocity field which will exist within the shelter will depend upon the geometry of the shelter and the size and location of the inlet opening or openings. Furthermore, the mass flow rate of air into and out of the interior shelter region or cavity will be a significant factor. The latter effect is a function of the V/A ratio of the shelter, where the pertinent area is the total inlet area. This effect will also be dependent upon the free-air blast environment.

Any attempt to define the transient velocity field within a shelter will have to be limited to relatively simple configurations such as rectangular rooms. Since the openings or inlets will frequently occupy nearly the entire vertical height of the room, and since the plan (horizontal) dimensions of a room are generally much larger than the vertical height, the flow within the shelter will take place primarily in the horizontal plane. A two-dimensional flow model should be adequate to define the blast induced velocity field and the basement shelter can then be characterized simply by its width, W and its length, H. The inlet area can be connected to an equivalent inlet width, B by dividing the inlet area by the room height. Initially, the location of the inlet was restricted to the central location on one wall which is called the front wall. The identification of the back and side walls follows naturally. Such a symmetric geometry leads to the inclusion of the case where the axis of symmetry (across which no flow of air occurs) can be treated as a wall. The width of this reduced room and of the inlet correspond to the related half-widths of the full room, and the inlet will now be located at one extreme end of the front wall.

Many rooms which differ somewhat from these two geometric cases can be converted to these geometries by neglecting some small geometric perturbations and by utilizing average or effective values for some of the shelter parameters. The basic geometry (a rectangular room with one centrally located inlet on the front wall) can be combined with identical modules to yield more complex configurations which contain multiple but similar openings. Figure 3.1 illustrates a variety of room configurations which can be treated. The use of the basic geometry and its variant forms will provide a range of configurations which correspond to most shelter geometries of interest.

A number of distinct shelter sizes have been selected for this study. Three large shelters were selected from Ref. 11 and two small basement shelters considered in Ref. 1 were included to cover a rather wide range of probable sizes. Dimensions and parameter values for this range of shelter sizes are

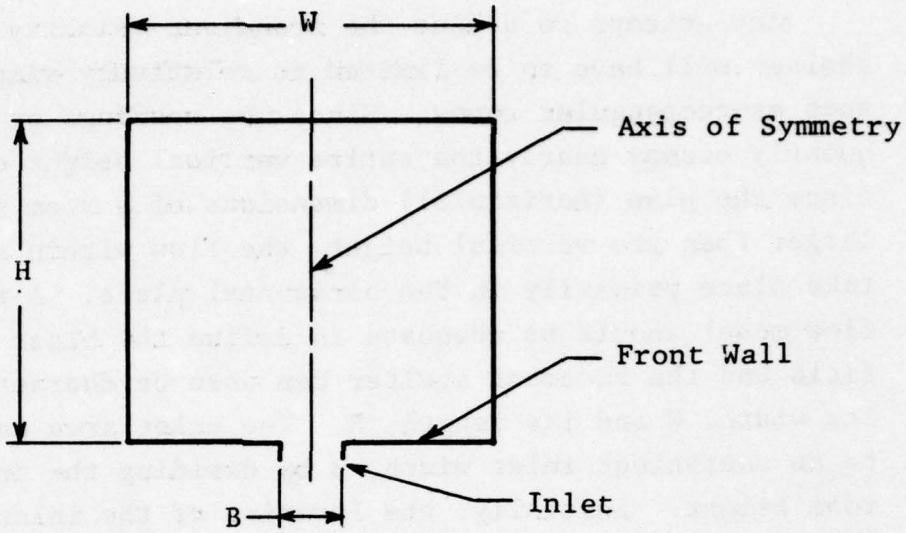

(a) Basic Geometry

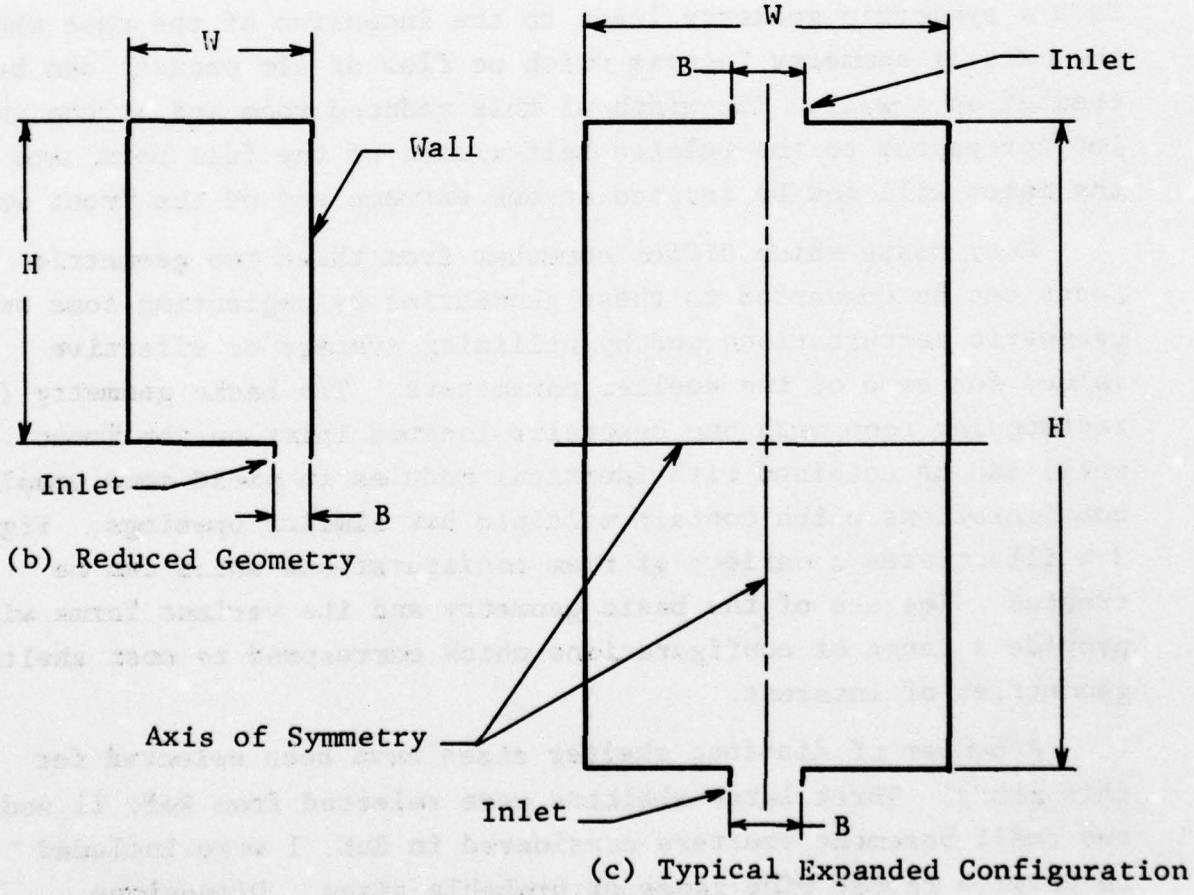

(b) Reduced Geometry

(c) Typical Expanded Configuration

Figure 3.1 Room Configurations

presented in Table 3.1. In most cases several inlet area values were selected, however, multiple inlets will generally exist for the larger shelters. The number of inlets and/or their locations are not specifically defined at this stage. The fact that the rooms selected are square is of no particular significance. Other aspect ratios can be included at a future time. The sizes of the inlet areas were generally selected to obtain a desired V/A ratio. This parameter will generally be larger for the larger shelter sizes.

TABLE 3.1

SELECTED SHELTERS

Case	Volume, V (ft^3)	Dimensions (ft x ft x ft)	Inlet Area, A (ft^2)	V/A Ratio (ft)
A	4.0×10^5	200 x 200 x 10	400.	1000
B1	10^5	100 x 100 x 10	25.	4000
B2	10^5	100 x 100 x 10	100.	1000
C1	3.6×10^4	60 x 60 x 10	10.	3600
C2	3.6×10^4	60 x 60 x 10	50.	720
D1	2048	16 x 16 x 8	2.05	1000
D2	2048	16 x 16 x 8	4.10	500
E1	6270	28 x 28 x 8	6.27	1000
E2	6270	28 x 28 x 8	12.54	500

Since the overall mass flow rate aspect of this problem is only dependent on one shelter variable (the V/A ratio) auxiliary calculations were made for a range of this variable (from 200 to 4000 ft) and for a nominal range of peak free field overpressure levels. Recall, that the weapon size and burst condition have already been fixed. The overpressure values treated specifically include 2, 6, 10 and 15 psi. The cavity filling computer code of Ref. 12 was used for these calculations after some minor modifications needed to obtain the desired details were made. The inlet flow velocity histories corresponding to an overpressure of 10 psi are presented in Figure 3.2. At somewhat high overpressures

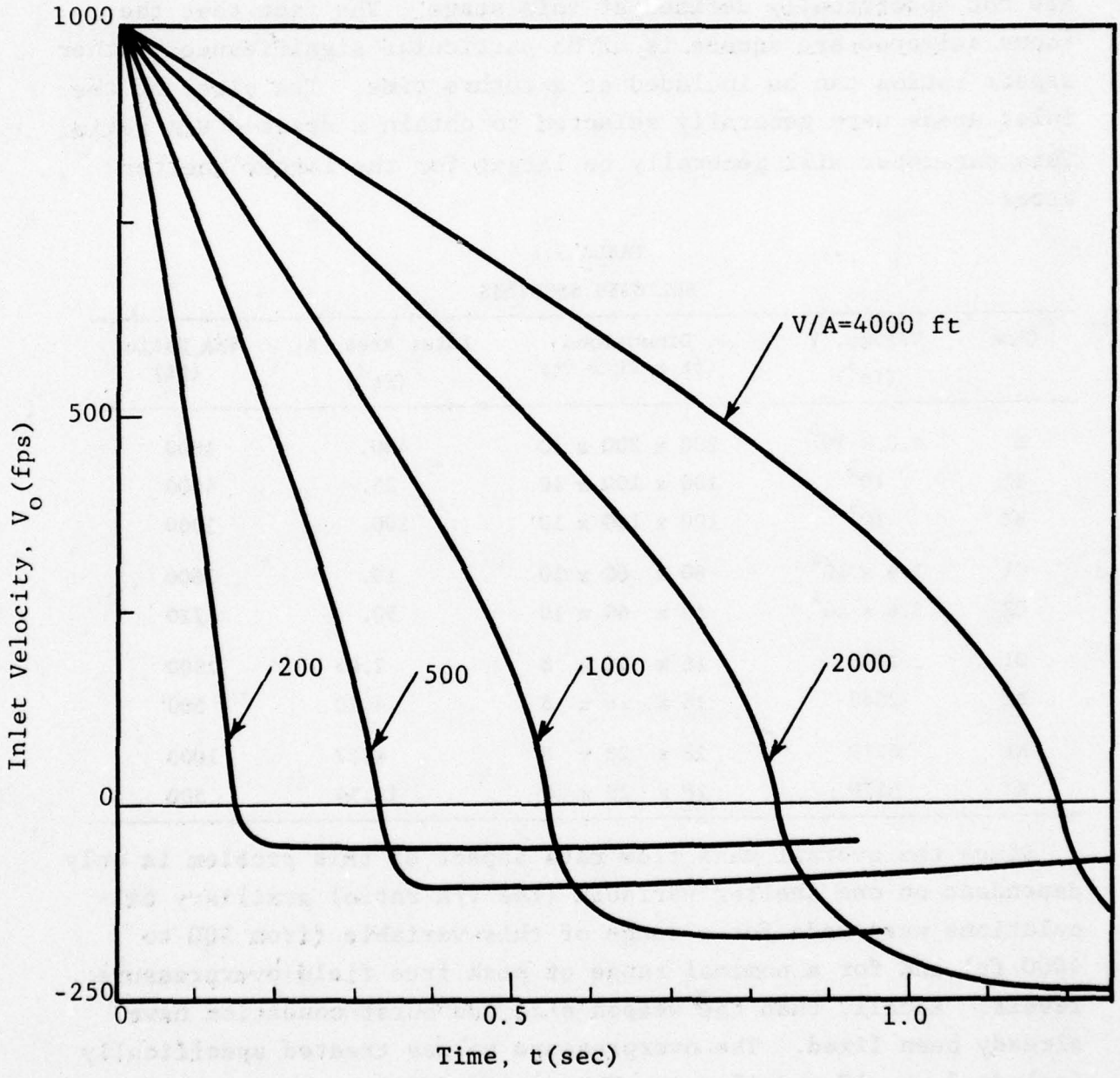

Figure 3.2 Inlet Flow Velocity Histories, p_i=10 psi

the flow is initially choked and remains so for a short period of time. In those instances the inlet velocity remains constant for an appropriate period of time at a value of approximately 1100 fps. In this study standard ambient conditions for both pressure and temperature were used. This approximation is adequate since these variables are not very influential over their conventional ranges.

The inlet flow velocity histories shown in Figure 3.2 are similar to those of the other overpressure levels with the exception that the initial value is lower for lower overpressure levels. The mass flow rate reaches a value of zero when the cavity (shelter) overpressure reaches its maximum value. The interior pressure increases from the time of shock arrival in a manner which can be described to be, very roughly, linear in form and then decays like and at essentially the same value as the outside free field overpressure decays. This pressure decay period corresponds to the outflow (negative inlet velocity) interval shown in Figure 3.2. It lasts until the end of the positive phase duration of the overpressure which for the overpressure levels indicated is in the range of 2 to 3 seconds. The peak magnitude of the inlet flow velocity is smaller during the outflow period than it is during the inflow period. During the negative phase of the overpressure the air within the shelter will continue to flow out of the region, however, at a substantially reduced rate. It would appear that, as a first order approximation, the inlet flow velocity can be set equal to zero during this late time period and thus enable the analyst to terminate the inlet flow in some reasonable manner.

These cavity filling calculations have provided for a reasonable estimate of the inlet flow velocity histories for the range of overpressure of general interest. They also provide additional flow details. The air density within the cavity will vary somewhat as the cavity pressure varies, but over a narrower percentage range. Therefore, for the current study a constant value is used. The standard ambient density is used in subsequent transport calculations although a value modified slightly to account for the

overpressure level could also be applied. The cavity filling calculations also provide the maximum or peak pressure which exists within the shelter. This information for the range of shelter parameters of interest is shown in Figure 3.3. This figure illustrates the variation of peak average pressure within the shelter as a function of external free field overpressure and the V/A ratio. These pressure levels are too low to produce noticeable casualties by themselves. Assuming "fast rising" pressure, the LD_{50} (50 percent probability of mortality value for man) is 61.5 psi (see p 28, Ref. 13).

The major task of this effort dealt with generating an adequate description of the transient velocity field within the basement shelter and then to imposing this environment on objects within and subsequently observing the resulting translational effects. This has been done using a simple drag type translational model. The calculations were carried out until an impact occurred at one of the room boundaries. Only the initial impact was considered. The conversion of this observed impact condition into a statement of survivability or injury level, although not explicitly made in this report must involve some appropriate impact criteria. The criteria presented in Figures 4 and 5 (Ref. 1) should be adequate for initial estimates of survivability. It is apparent that multiple impact conditions may be common in the shelter environment, hence the rebound or "bounce" aspect of the problem must be introduced in some manner.

At the present time a simple approach has been formulated, but not applied since the transport calculations were stopped after the first impact occurred. The approach which was formulated was that of using an analytical expression, specifically an exponential decay form, to reduce the normal component of the rebound velocity when normalized by the normal component of the impact velocity. The exponential factor involves the normal component of the impact velocity and an appropriate critical velocity. A value of 50 fps was selected initially for this critical velocity. In this manner the rebound velocity is treated as a function of the impact velocity. The final selection of the analytical form

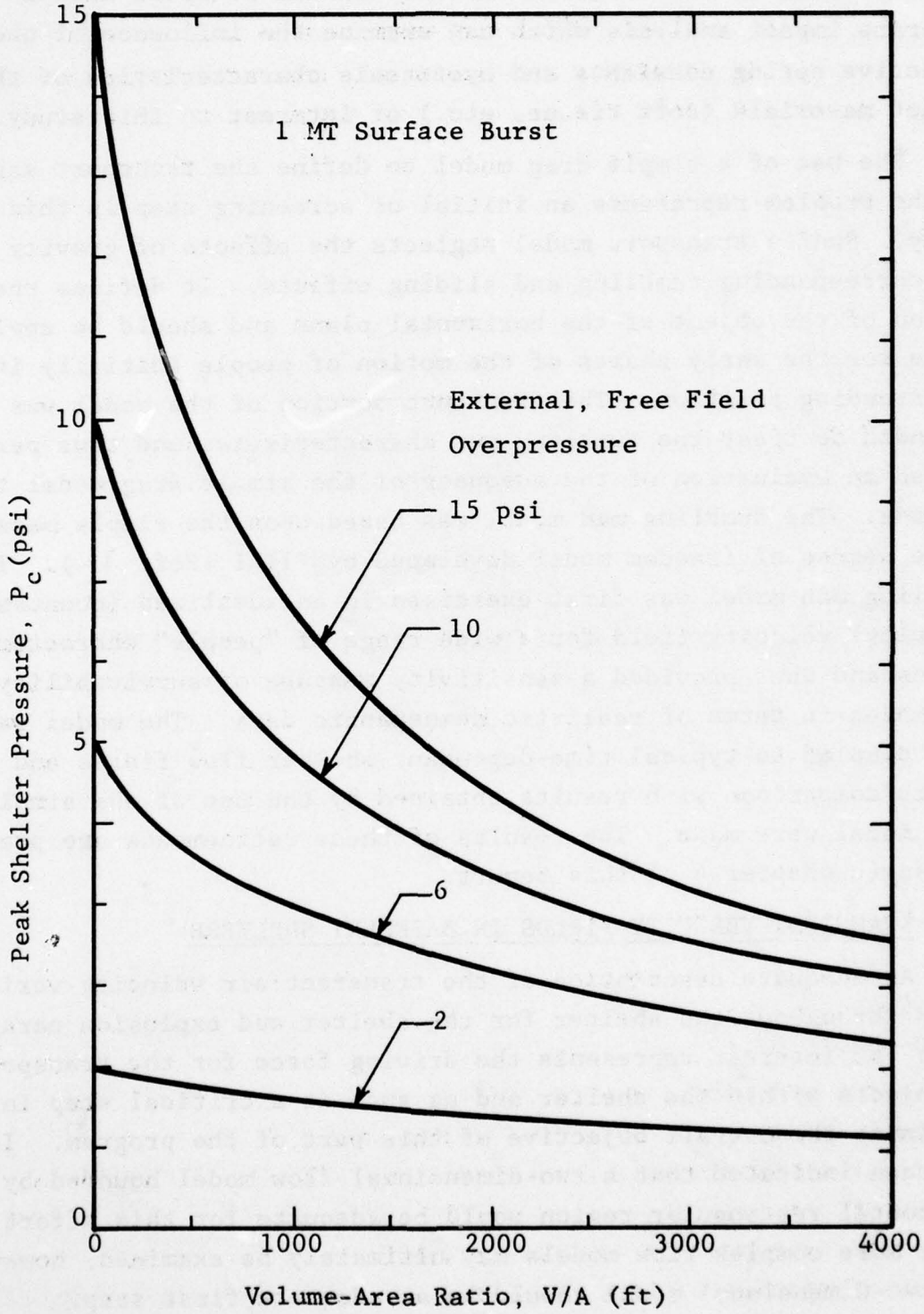

Figure 3.3 Peak Pressure Environment in Shelter

and the value of the critical velocity should be based upon a separate impact analysis which can examine the influence of the effective spring constants and hysteresis characteristics of the impact materials (soft tissue, etc.) of interest to this study.

The use of a simple drag model to define the transport aspect of the problem represents an initial or screening step in this study. Such a transport model neglects the effects of gravity and the corresponding tumbling and sliding effects. It defines the motion of the object of the horizontal plane and should be applicable for the early phases of the motion of people initially in the standing position. The transport portion of the model was extended to treat the tumbling man characteristics and thus permitted an evaluation of the adequacy of the simple drag model to be made. The tumbling man model was based upon the simple mass, three degree of freedom model developed by IITRI (Ref. 14). This tumbling man model was first exercised in an idealized (constant velocity) velocity field for a wide range of "people" characteristics and thus provided a sensitivity measure of survivability estimates in terms of realistic demographic data. The model was then coupled to typical time-dependent shelter flow fields and a direct comparison with results obtained by the use of the simple drag model were made. The results of these refinements are presented in chapter 4 of this report.

3.2 TRANSIENT VELOCITY FIELDS IN BASEMENT SHELTERS

An adequate description of the transient air velocity variations throughout the shelter for the shelter and explosion parameters of interest represents the driving force for the transport of objects within the shelter and as such is a critical step in attaining the overall objective of this part of the program. It has been indicated that a two-dimensional flow model bounded by a horizontal rectangular region would be adequate for this effort. Other more complex flow models may ultimately be examined; however, the two-dimensional model should be an adequate first step.

There are several approaches which could be followed to obtain

the needed flow details. One method would be to use an appropriate gas dynamic or hydrocode capability to numerically integrate the governing flow equations in a forward time stepping manner and thus carry the solution to some late time point in the flow process. A number of such solutions have been obtained for basement type shelter geometries (Ref. 15, 16 and 17) for overpressure levels of general interest. Such solutions are relatively expensive to obtain. The flow solution could be obtained simultaneously with the solution of a transport problem (for one or more objects) and then redone for other transport conditions. Or, a given solution could be stored on tape and used repeatedly for a wide variety of transport problems.

The storage requirements for a single velocity field solution (one shelter geometry at one overpressure level) would be rather large since such solutions frequently involve about 1000 node points (the spatial coordinates) and perhaps well over 1000 time steps. This many time steps would be needed to carry the solution out far enough in time. Undoubtedly, some economies could be generated by curve fitting over coarser intervals in either space or time (or both). However, at least two parameter values would have to be stored at each storage unit. It appears at this time that for the many overpressure levels of interest and the wide variety of shelter sizes and geometries which may be examined, the described approaches are not economically feasible and were therefore beyond the scope of this study. The use of such an approach may be appropriate as an accuracy check or at least as a consistency check on other methods. The accuracy of these numerical solutions is limited; however, these types of solutions should be quite adequate for the goal of survivability prediction.

Experimental methods have been used in the past to obtain solutions of such complex transient multidimensional gas dynamic flows. The scaled shock tube type experiments were generally limited to obtaining information relating to pressure variations. Very little success was achieved in observing flow velocities of air particles. Nonetheless such experiments did provide an

insight into a number of complex phenomena, such as shock diffraction effects and vortex growth and transport.

The approach which was selected for obtaining a description of the transient air velocity throughout a shelter is that of synthesizing the velocity field analytically by using a number of functional terms to define the magnitude of the velocity vector components. The bases for this development are all the known applicable solutions such as the numerical solutions given in Ref. 15 and 16. The adequacy and accuracy of such an approach has not yet been demonstrated; however, the initial results are promising. Accuracy is being sacrificed to some degree but this approach does not permit many flow solutions to be generated at a very low cost. Development of the synthetic process is described and the current state of velocity field approximation development is indicated in the following paragraphs.

Velocity diagrams for three time values (measured by Cycle number which is a time indicator used in Ref. 15) are presented in Figures 3.4 through 3.6. These details were taken from Ref. 15 and correspond to a square shelter with a 25 percent opening in the center of the front wall. The solution was obtained for a specific shock tube condition on a small-scale model; the peak overpressure was approximately 5 psi. The effective duration is such that this solution is applicable to the general range of parameter values of interest to the current problem. These three diagrams are presented to demonstrate the general nature of the flow regimes which will exist within the shelter.

A shock wave will propagate through the inlet, diffract around the geometric features and then propagate out into the shelter interior. In this manner the first motions of the air within the cavity are induced. The details of this initial flow will be influenced, in part, by exterior perturbations and distortions of the local exterior blast environment and by the geometric details of the entranceway. For purposes of the current program these fine, perhaps randomly occurring, details are of secondary importance and can be eliminated by considering a simplified model.

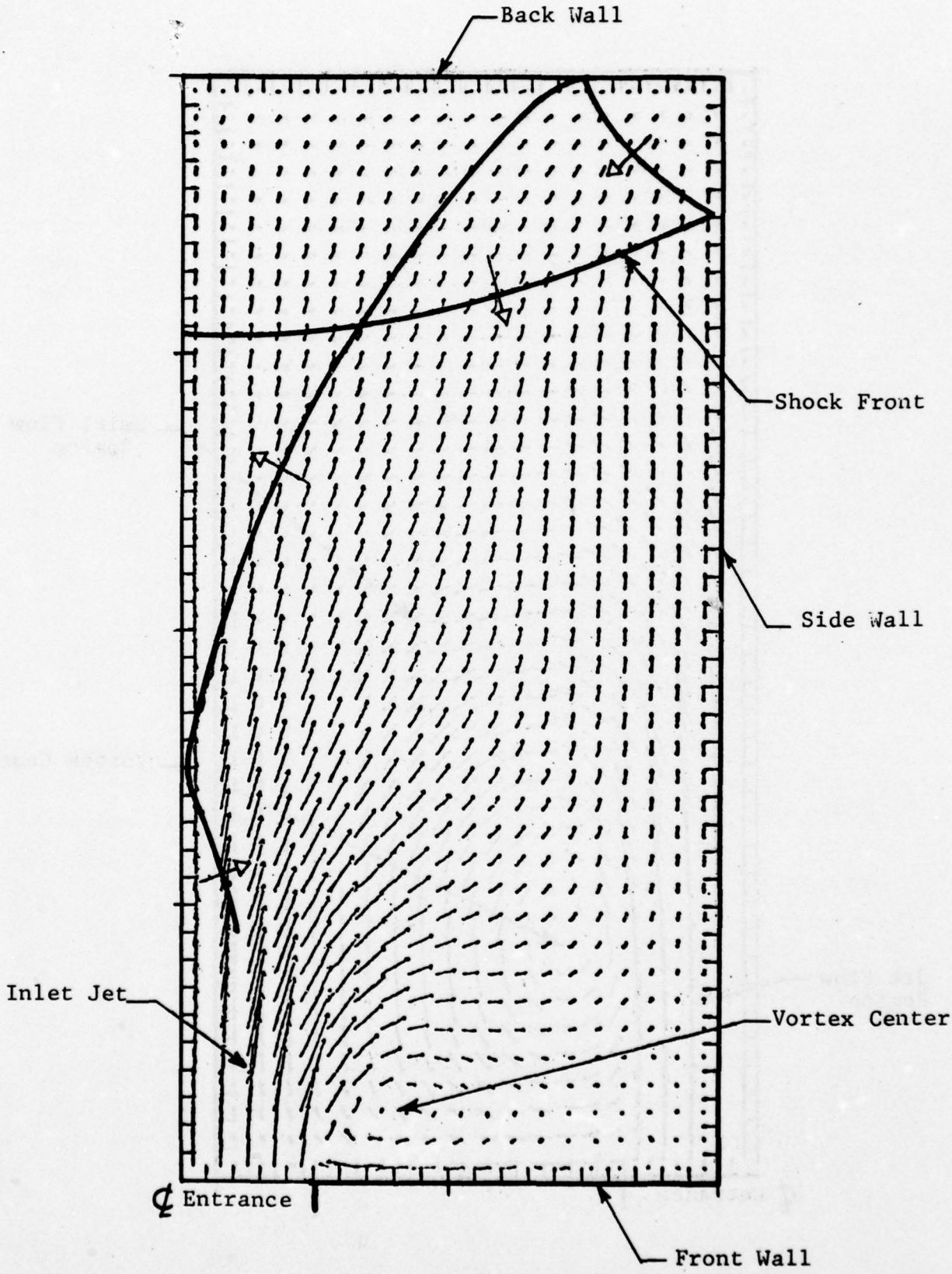

Figure 3.4 Velocity Diagram, Cycle 150

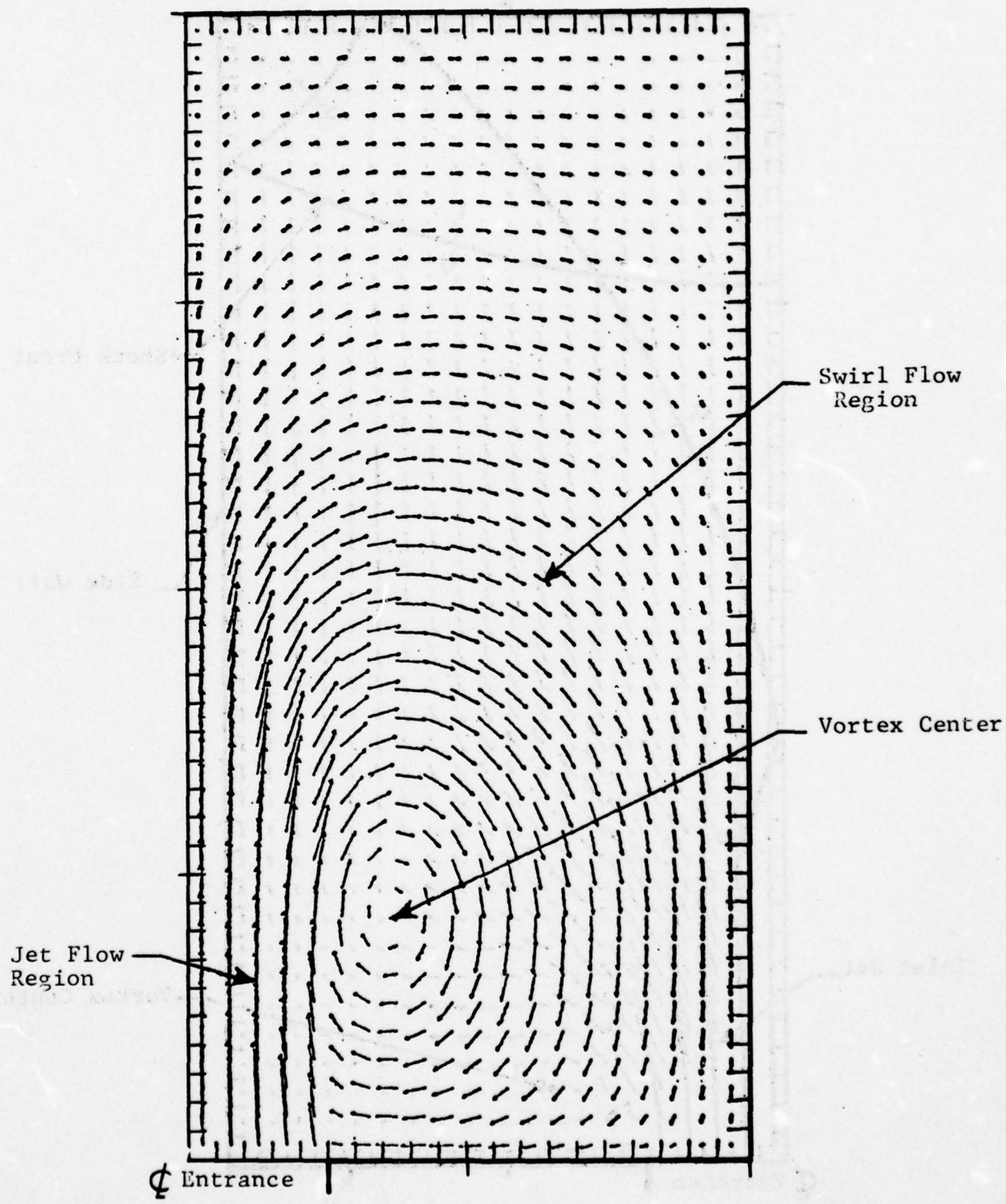

Figure 3.5 Velocity Diagram, Cycle 275

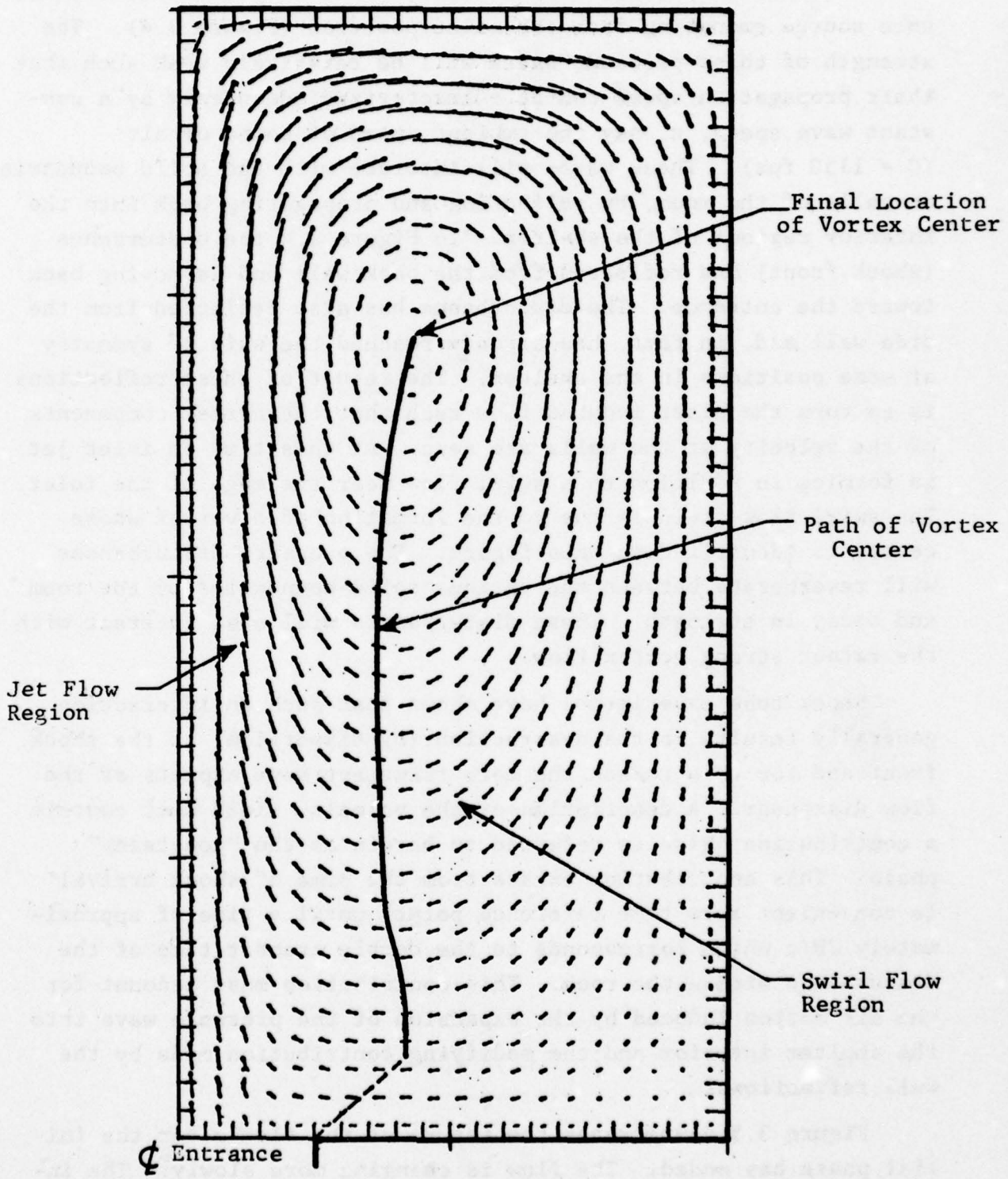

Figure 3.6 Velocity Diagram, Cycle 750

The initial process can be idealized by a cylindrical disturbance source emanating from the inlet position (Figure 3.4). The strength of these pressure waves will be relatively weak such that their propagation speed can be characterized adequately by a constant wave speed, c, say the ambient speed of sound of air (C = 1130 fps). These waves will interact with the solid boundaries or walls of the room, by reflecting and propagating back into the interior regions of the shelter. In Figure 3.4 the disturbance (shock front) has reflected from the back wall and is moving back toward the entrance. The disturbance has also reflected from the side wall and, in fact, has already reached the axis of symmetry at some positions in the shelter. The result of these reflections is to turn the blast induced flow such that the normal components of the velocity at the walls are zero. At this time an inlet jet is forming in addition to a swirl flow near the edge of the inlet. The swirl flow field is due to the formation of a vortex whose center is identified in this figure. The pressure disturbances will reverberate between the various solid boundaries of the room and decay in strength. These disturbances will also interact with the rather strong vortex flow.

Shock tube experiments have shown that such an interaction generally results in the destruction (by dispersion) of the shock front and for this reason the more transient wave aspects of the flow disappear. A description of the velocity field must contain a contribution which is referred to herein as the "nonsteady" phase. This contribution exists from the time of shock arrival (a convenient zero time reference point) until a time of approximately 2H/c which corresponds to the double transit time of the disturbance within the room. This contribution must account for the air motion induced by the expansion of the pressure wave into the shelter interior and the modifying contribution made by the wall reflections.

Figure 3.5 illustrates the nature of the flow after the initial phase has ended. The flow is changing more slowly. The inlet jet is completely formed and extends further into the room.

It has already adjusted to the finite length of the region available to it. The swirl flow region has grown in size and now occupies the entire shelter area. The center of the vortex is moving slowly toward the rear of the shelter. Thus two significant flow features are present at this time interval; a stabilized inlet jet flow and a moving swirl flow region. These naturally form two additional velocity contributing terms in the velocity field model.

Figure 3.6 illustrates the velocity field at a later time. The velocity of the air at the inlet region has decayed substantially. The movement of the vortex center has stopped due to its interaction with the back boundary; the swirl flow has stabilized in position and is decaying in intensity. The path of the vortex center is shown in Figure 3.6 and indicates its rather well defined movement. Similar vector diagrams have been examined from other related numerical solutions and the above described general features are common to each solution. Unfortunately these available numerical solutions were not extended sufficiently in time to define the outflow aspects of the velocity field. It is clear that the jet flow is replaced by some type of sink flow (the sink being located at the inlet of the shelter) and that the intensity of the flows is greatly diminished. The swirl flow may persist for some short time after the outflow begins but no data are currently available to establish this aspect of the flow. If it does exist its intensity will probably be small.

The current velocity field model which was used in this study consists of four components defining (1) the nonsteady blast diffraction effects, (2) the inlet jet flow, (3) the swirl flow, and (4) the outflow flow contributions. These parts have been written in a computer subroutine form for use in subsequent transport calculations. The most significant aspects of these components, and a discussion of the method used to combine the parts are presented in the following paragraphs. Due to the symmetry of the basic geometry the velocity field need only be defined for the reduced geometric case. Each submodel defines the velocity field components U and V at a given time, t and position (x,y).

The velocity components U and V correspond respectively to an orthogonal x and y coordinate system whose origin is at the center of the inlet on the front wall. The positive x-direction is into the room toward the back wall of the shelter, thus $0 \leq x \leq H$. The positive y-direction is from the center of the inlet toward the side wall, thus $0 \leq y \leq W$.

The nonsteady flow submodel is applicable during the time interval $0 \leq t \leq 2H/c$ during which the inlet velocity, V_o, is varying slowly with time (see Figure 3.2). An examination of the available numerical solutions during this early time period indicated that the velocity distribution behind the initially expanding disturbance (i.e., no wall reflections) is primarily radial in direction and increases in intensity from an essentially zero value at the shock front to the inlet value at the origin. The wave shape is relatively constant, and nearly linear, hence a self-similar solution in the variable (R/R_s) can be formulated, where R is the radial distance of the position (x,y) from the origin and R_s is the range of the disturbance. This range is simply the product of the wave speed and the elapsed time (R_s=ct) recalling that the flow starts when t=0.

The development procedure was iterative in nature, being modified as the various submodels were combined and adjusted to obtain a reasonably good comparison over the full field of interest and for the various times at which velocity vector data were available. As a result the self-similar solution for the velocity magnitude, V_n took on the form

$$V_n = V_2\left(1 - \frac{R}{R_s}\right)e^{-\frac{R}{R_s}} \cos(0.8\alpha), \qquad 0 \leq R \leq R_s \qquad (3.1)$$

where V_2 is the contribution of the inlet velocity V_o allocated to the nonsteady flow contribution and α is the position angle measured from the x-axis. The wall reflections are flow adjustments dictated by the physical requirement that the normal component of the velocity at the wall vanish. This requirement could be met easily by using a method of images. Thus the velocity at a given

point could be made up of many vector contributions. Eight sources were selected, two in the x-direction and four in the y-direction. Only two were needed in the x-direction since the applicability of the nonsteady model was prelimited by $t \leq 2H/c$. Four image positions in the y-direction will allow for four reverberations in this direction and thus be applicable to narrow shelters where $H \leq 2W$. Narrower shelter geometries can be treated by increasing the number of source points. For each of the sources used, the velocity contribution vanishes whenever the apparent range (distance from the source) is greater than the disturbance range.

The current jet flow submodel was patterned after the jet model described in Ref. 12. The latter model corresponded to a free standing jet and is applicable for shelters which are very large compared to the inlet width, B, of the jet. These types of jets can be very long, in fact at a distance of 100 B the flow velocity is still approximately 10 percent of the inlet value. Since the shelter sizes and configurations of interest of the order of say 10 B, the back and perhaps the side walls will influence the jet flow field. The analytic form used in Ref. 12 was simplified slightly with respect to the velocity distribution at any distance x from the inlet. The primary influence of the back wall is to decelerate the jet flow such that the velocity vanishes at the back wall. The current version of the jet submodel merely applies a factor (1-x/H) to the free jet solution to satisfy this requirement; the free jet conditions being defined by an inlet magnitude V_1 which represents that portion of the inlet velocity, V_o, that is allocated to the jet flow contribution. The free jet is narrow enough such that side wall interactions will not occur for the shelter aspect ratios (W/H) being considered. An earlier version of the jet submodel was based upon an image procedure to satisfy the zero velocity requirement at both the back and front wall. This model required some 20 to 40 images (i.e., velocity contribution) plus a final correction procedure to obtain flow details similar to those obtained by the current simple version.

The development of the swirl flow submodel represents the most difficult flow regime to model because of its rather longlasting

moving nature and because it covers the entire shelter area. The motion of the vortex center is rather well defined. After a short induction period it moves at a relatively constant speed, until it approaches its final position of approximately 0.7 H. The path occurs at a near constant value of y of approximately 1.8 B for wide rooms. An adjustment was introduced for narrower rooms such that when W approaches B (an unrealistic width) the value of y was equal to B. The speed at which the vortex center moves is approximately 200 to 250 fps for the various solutions and times examined; a value of 225 fps was selected for the current model.

This narrow range of vortex center speed is consistent with vortex motion observations made many years ago while studying shock diffraction effects on objects in shock tube experiments (i.e., approximately 20 percent of the shock velocity). The direction of flow (i.e., the streamlines) in the swirl flow region is roughly elliptical around the center of the vortex and the flow extends rather deeply into the corners. This feature was approximated by selecting a fourth order relationship between the variables Δx and Δy which define the position relative to the vortex center. In this manner the flow direction, the ratio of the velocity components, was defined for every point within the limiting streamline. The velocity was assumed to vanish outside of the limiting streamline, that is at the corner regions. The magnitude of the velocity also depends upon the absolute distance of the position (x,y) from the center of the vortex. The magnitude of the velocity is essentially zero at the vortex center and then increases in a roughly linear fashion until it reaches its maximum magnitude at a distance approximately equal to B. For larger distances the velocity decreases at nearly constant circulation conditions. Finally some minor adjustments were incorporated into the magnitude calculation to reflect the fact that the intensity of the swirl flow increased with vortex center displacement.

The outflow submodel is relatively simple in concept and does not include any swirl flow features. Basically during the outflow phase a sink type of flow should exist. The strength of the sink is given by the value of the inlet velocity. The flow will be primarily radial in direction and the magnitude will decrease with increasing distance from the sink. The magnitude of the velocity should be essentially zero at the walls of the shelter. Two factors were used to reduce the magnitude of the velocity. First a simple finite sink type relationship was used. Specifically this took the form

$$\frac{1}{1 + \frac{D}{2B}} \tag{3.2}$$

where D is the distance from the origin. Secondly a factor to account for the finite size of the room was introduced. This factor took the form

$$(1 - \frac{D}{D_m}) \tag{3.3}$$

where D_m was the maximum room dimension along the ray passing through the point of interest. In this manner the zero velocity condition at the walls was achieved.

In describing some of the above-mentioned submodels, reference was made to a contribution of the inlet velocity which was allocated to the particular flow regime. The intensity of the flow and its variation with time have been keyed to the intensity of the inlet flow. The inlet flow for a given condition was determined from cavity filling calculations. Whenever more than one flow regime coexists and contributes to the inlet flow magnitude the component parts (such as V_1 and V_2 for the jet flow and nonsteady flow contributions) must make up the whole (i.e., equal to V_o). During the nonsteady flow period $0 \leq t \leq 2H/c$ when the jet flow is in a growth phase, the driving velocity for the nonsteady flow was expressed by the relationship

$$V_2 = V_o(1 - \frac{tc}{2H})^2 \tag{3.4}$$

The swirl flow growth was also related to the intensity of the inlet flow; however, since this flow does not directly involve the mass flow at the inlet, its relationship is not necessarily influenced by other flow regimes. The driving velocity, V_3, was defined by the relationships

$$\left.\begin{aligned} V_3 &= V_o \frac{tc}{4H}, \qquad 0 \leq t \leq 4H/c \\ V_3 &= V_o, \qquad 4H/c \leq t \end{aligned}\right\} \tag{3.5}$$

During the outflow period all of the inlet flow velocity is allocated to the outflow submodel since it is the only flow regime which is assumed to exist at that time. Finally, after the positive phase duration of the overpressure has elapsed, the inlet flow is very small and has been assumed to vanish. In this time interval it has been assumed that a quiescent flow state exists within the shelter and thus the velocity is assumed to vanish everywhere.

The above relationships as well as some of the details of the submodels have been developed and further modified to achieve as accurate a comparison with the existing velocity information as possible. Although this development is not necessarily complete, it appears that an acceptable level of accuracy has been achieved. It is difficult to make any blanket statements regarding accuracy; however, the reader is entitled to an impression in this area. For this reason the following estimate of the accuracy is presented. For the vast majority of the flow region, especially where the magnitude of the velocity is the largest, the magnitude of the velocity is accurate to approximately $\pm$25 percent and its direction is accurate to approximately $\pm$ 20 degrees. Uncertainties of these magnitudes will probably exist whenever the conversion of any real life shelter and the related weapon effects details are idealized to arrive at a specific prediction of the flow environment.

3.3 TRANSLATION ENVIRONMENTS IN SHELTERS

The translational effects of objects or people located within the subject shelters has been evaluated by using a simple drag type of translational model and neglecting the effects of gravity, rotation and ground interactions. A computer code was written for this drag type model which called upon the previously mentioned air velocity description subroutines to define the aerodynamic condition at the current location of the object. The inlet flow velocity histories (see Figure 3.2) were curve fitted and a number of parameters were established with which to define this flow as a function of both overpressure and shelter V/A ratio. The current version of the transport code is applicable to the basic, reduced and extended shelter geometries identified in Figure 3.1. In each of these cases the solid walls must be identified so that an impact condition can be identified. The air velocity model does not discriminate between a solid wall and an axis of symmetry, since in both cases the normal component of the velocity at these boundaries is equal to zero. The current code does consider rebound and multiple impact conditions; however, this feature has not been used to evaluate multiple impact conditions within the shelter.

3.3.1 Basic Shelter Configurations

A series of transport impact calculations were made for shelter cases C, D, and E (see Table 3.1) for the condition of a centrally located inlet. The drag characteristics of the object were similar to those used in Ref. 1 for the case of a standing man. The results are presented in Figures 3.7 through 3.13 and are expressed in terms of trajectories and the magnitude of the normal component of the impact velocity for the first impact. The latter value is indicated for a number of initial positions of the object within the shelter and several contours of constant impact intensity are shown. These correspond generally to the 10, 25, 50 and 100 fps values and represent nominal bounds for injury and fatality conditions for both head impact and total body impact conditions. The angle of incidence at the time of impact is evident from the trajectory results. Other available details such as time of impact and velocity history are not included herein.

Note: See Table 3.1 for Shelter Parameters

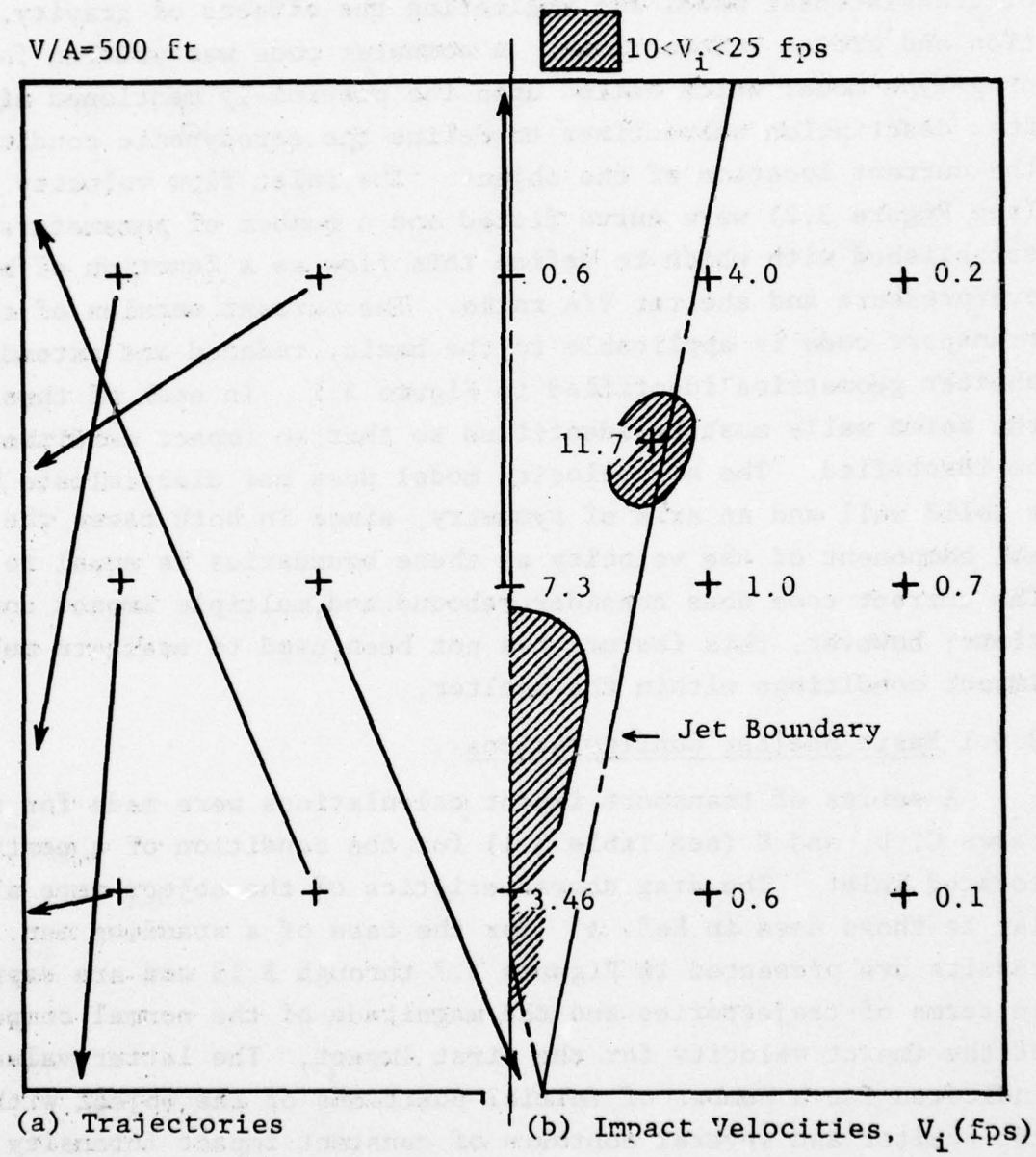

Figure 3.7 Transport Environment, Case E2, 6 psi

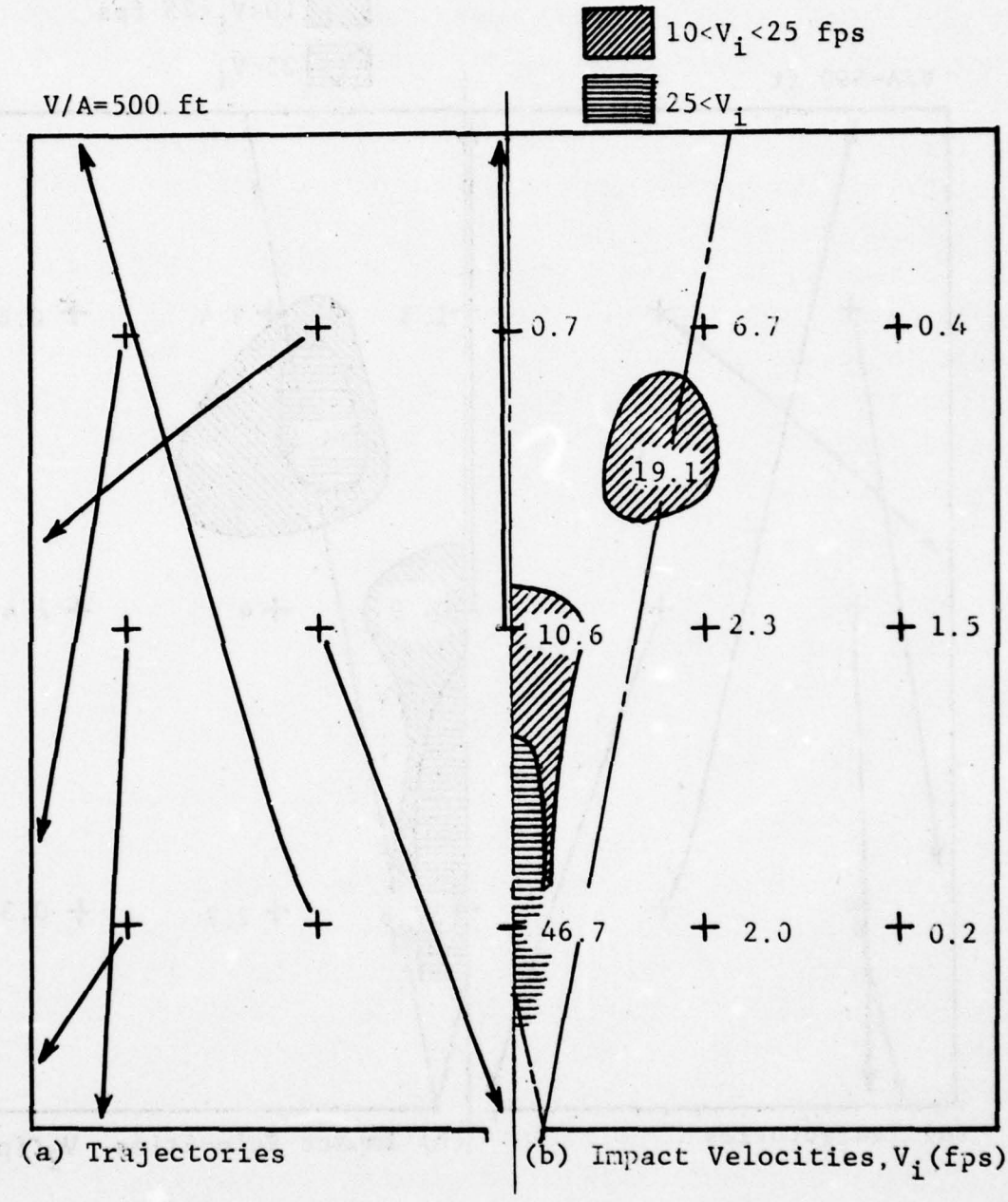

Figure 3.8 Transport Environment, Case E2, 10 psi

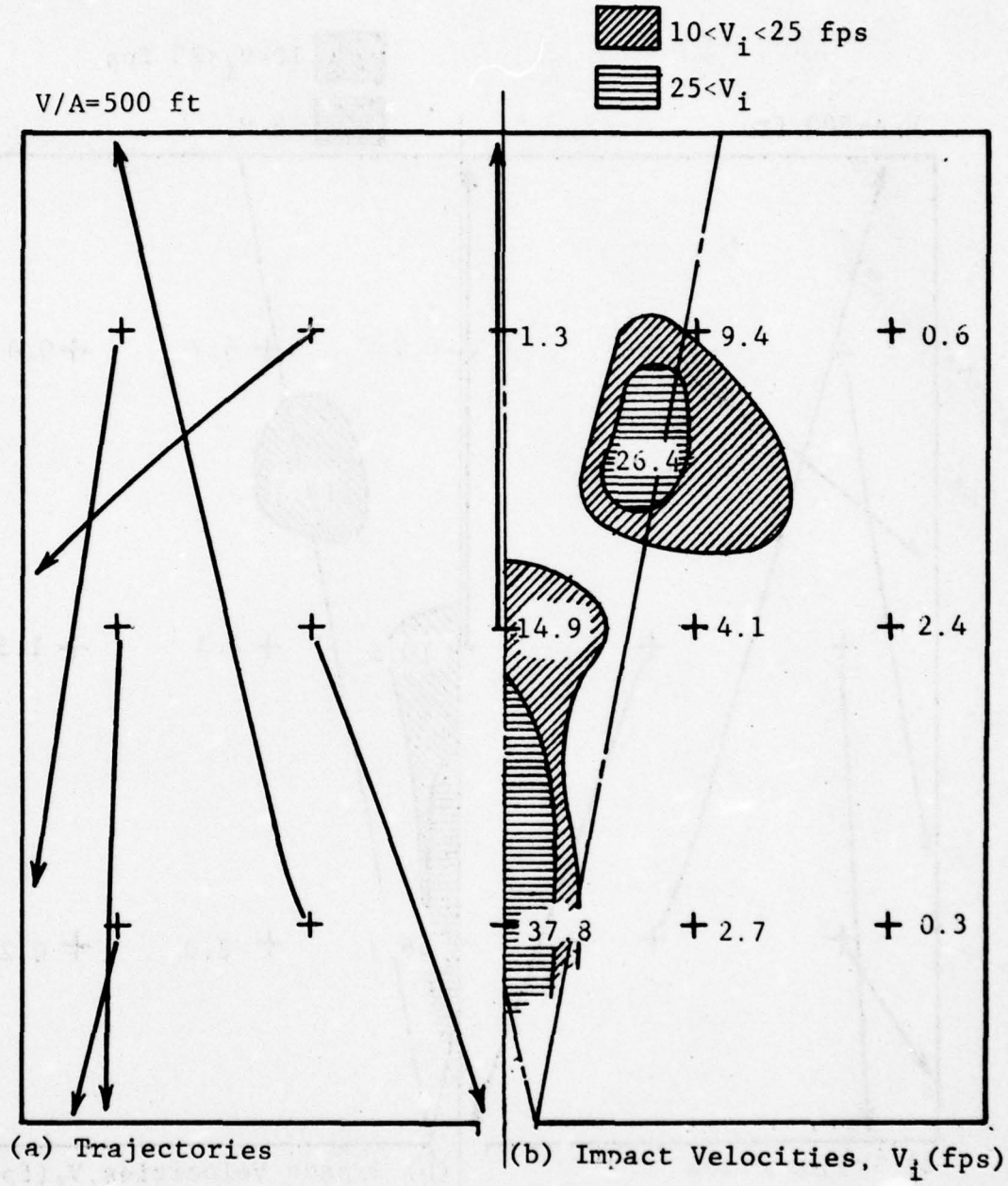

Figure 3.9 Transport Environment, Case E2, 15 psi

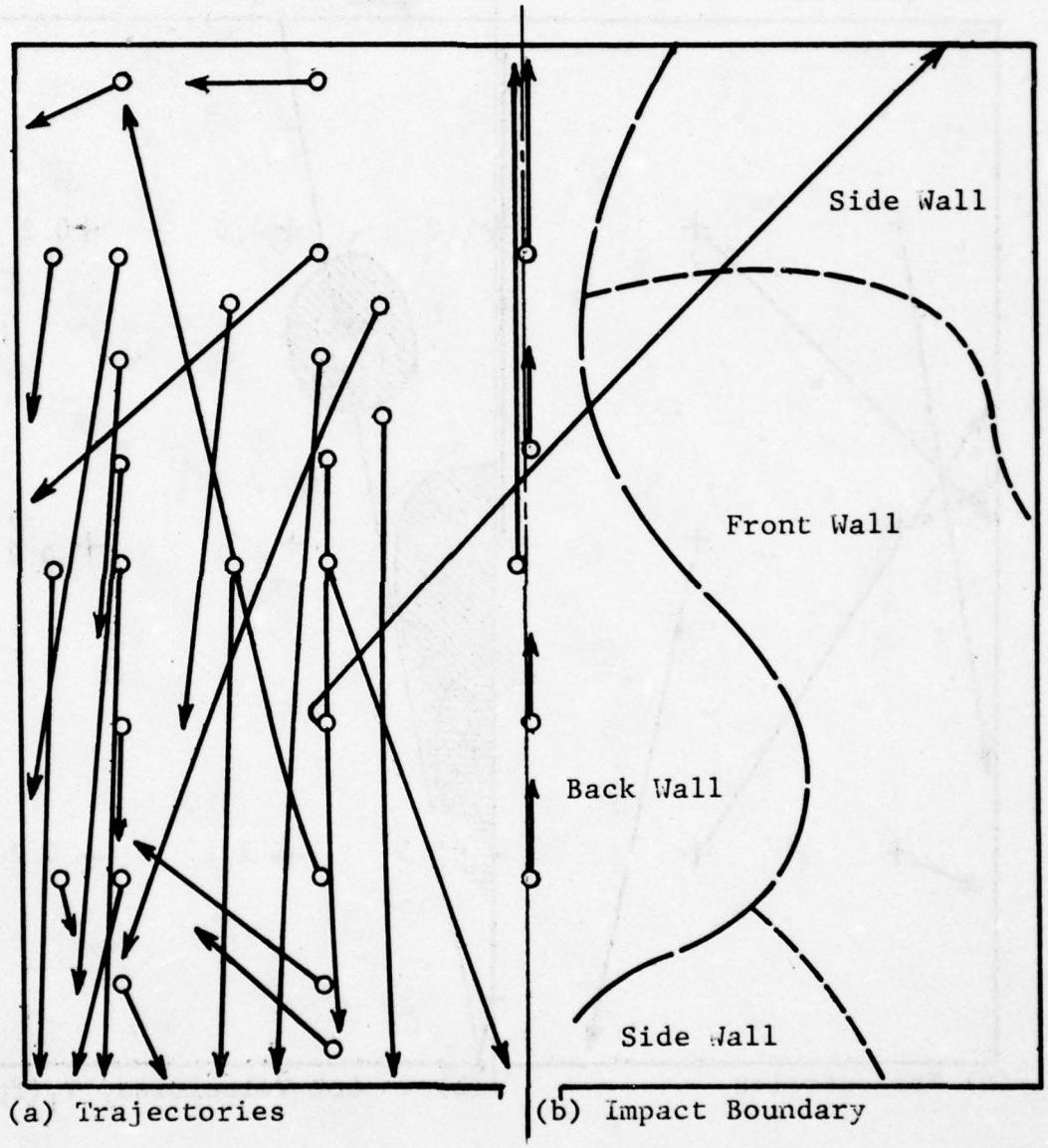

Figure 3.10 Trajectory Details, Case E2, 15 psi

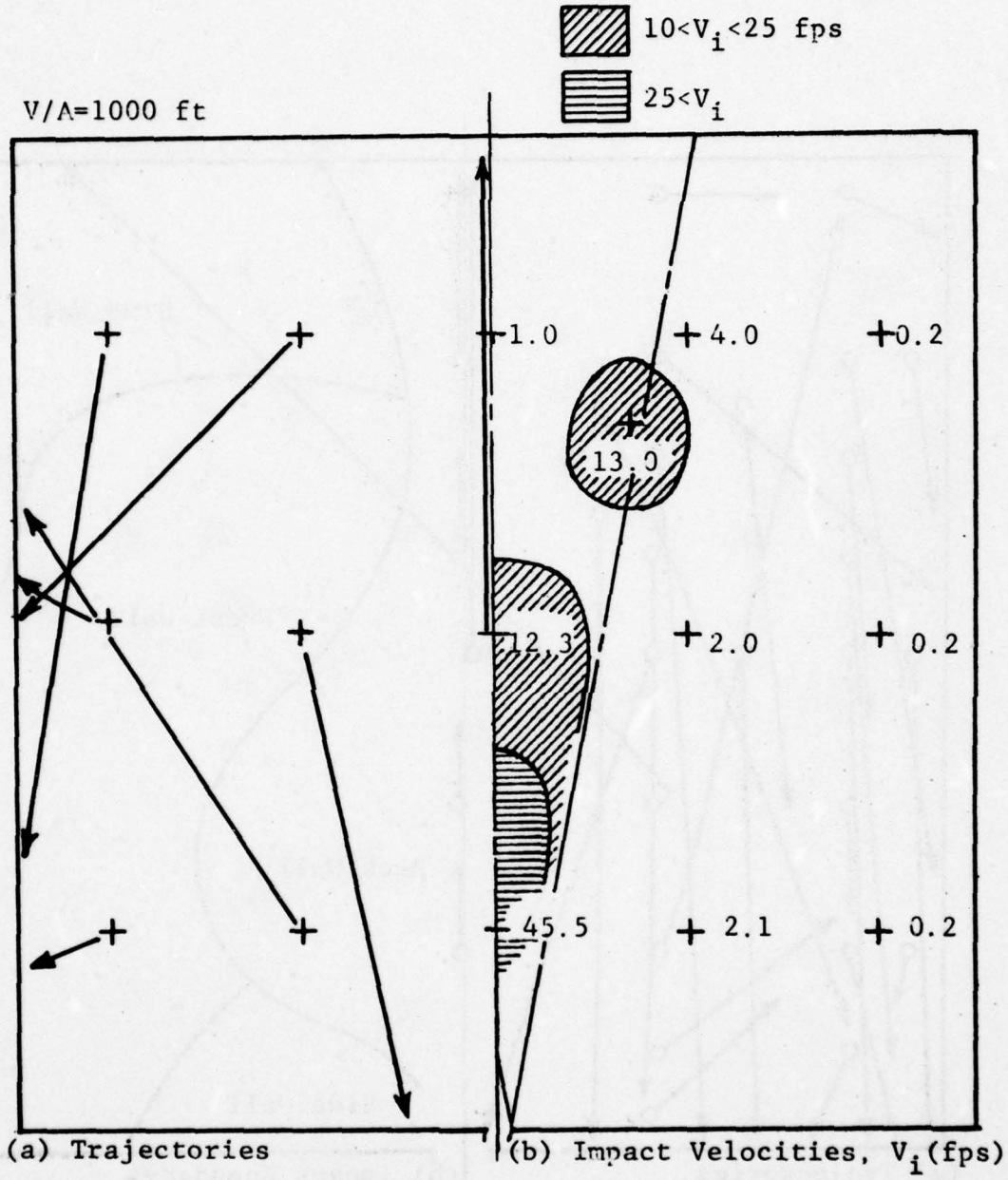

Figure 3.11 Transport Environment, Case E1, 15 psi

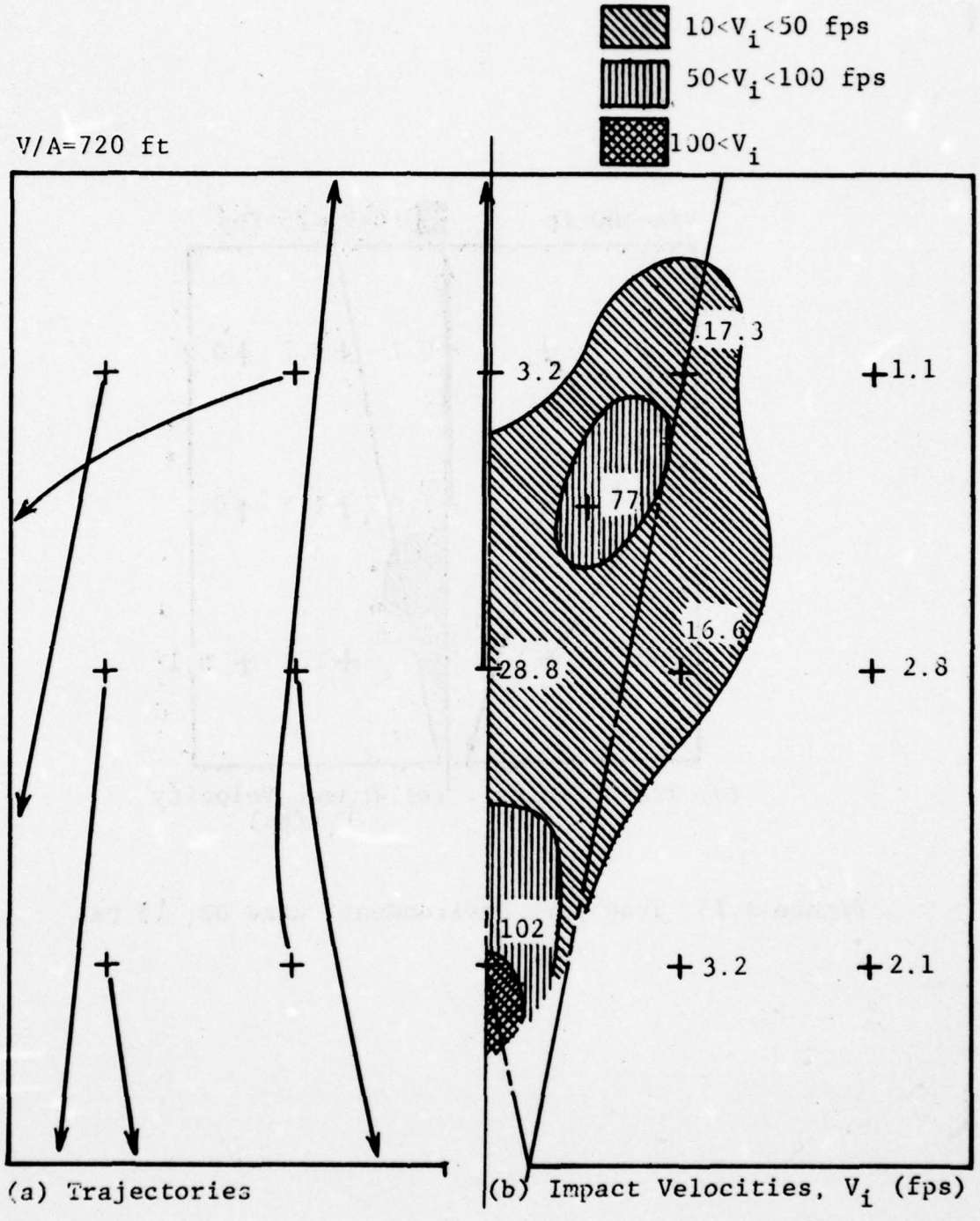

Figure 3.12 Transport Environment, Case C2, 15 psi

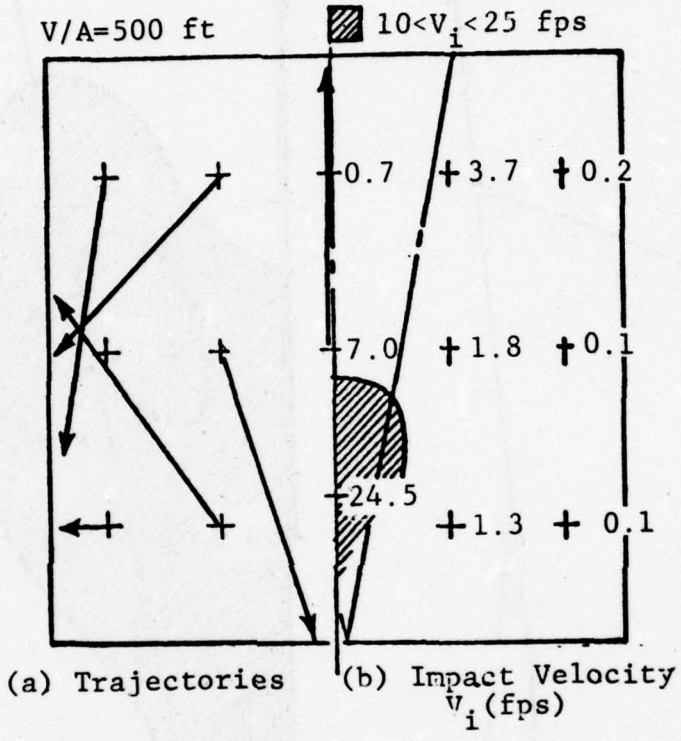

Figure 3.13 Transport Environment, Case D2, 15 psi

Figure 3.7 presents the results for shelter Case E2 when it is exposed to a 6 psi overpressure blast environment. The maximum overpressure which exists in the shelter in this instance is approximately 4.7 psi (see Figure 3.3). The most severe impact conditions result, as expected, from the initial objects position just inside the inlet. These objects move straight back and impact the rear wall. Although the impact velocities for objects located along the axis of symmetry near the back wall may be acceptably low; these objects may be subject to object-to-object impacts from objects closer to the inlet and thus generate an unacceptable impact condition. These calculations show that somewhat less intense impacts occur for another region which is located near the rear of the shelter and at the edge of the jet.

Similar results for this shelter case are shown in Figure 3.8 and 3.9 respectively for the 10 and 15 psi overpressure exposure situation. The peak overpressure within the shelter for the latter case is approximately 10 psi. The intensity of the impact velocity has increased appreciably and the size of the critical area has grown. Figure 3.10 presents some additional trajectory details for the latter condition and identifies the boundary walls at which objects initially located in certain parts of the shelter will impact. Many of the side wall impacts occur at very shallow angles hence the normal velocity component at impact is rather low even though the absolute velocity of the object may be fairly large. This somewhat glancing impact will not significantly impede the motion of the object and a second impact which may be much more severe than the initial one, can be expected to occur. Most of the objects will impact the front wall suggesting that some improvement in survivability can be achieved by appropriately treating that boundary, or conversely by avoiding the placement of hazardous equipment (hazardous from the point of view of impact) along that wall.

The results for shelter Case E1 are presented in Figure 3.11 for an overpressure exposure of 15 psi. This shelter is identical to that of Case E2 except the inlet area and width is smaller by a factor of two. The intensity of the corresponding impacts

is reduced and the size of the critical area is smaller by roughly a factor of two. The influence of the absolute size of the room is shown by the results presented in Figures 3.12 and 3.13. Figure 3.12 presents the results for a larger room (shelter Case C2) and clearly shows that the translation-impact environment is much more severe than that for a smaller shelter. The reason for this may be the fact that the duration of the intense flow is longer and more distance and hence time is available with which to accelerate the object. A tumbling object transport model may yield less severe transport and impact conditions. Figure 3.13 presents results for a small shelter (shelter Case D2), with a rather small inlet, and demonstrates the somewhat milder translation environment when compared to those of the related case (Case E2). Both Cases E2 and D2 have V/A ratios of 500 ft whereas a value of 750 ft occurs for Case C2.

Additional shelter configurations were examined to determine the influence of inlet location and room aspect ratio upon the impact environment. Emphasis was placed upon the impact environment in a small shelter and its variants. Results, show that the location of the single inlet significantly influenced the percentage of the floor area (related to initial object location) which produced impacts in excess of a given intensity. The most severe transport (and impact) conditions noted existed for a configuration in which a single inlet was located at the edge of the front wall. At an overpressure of 15 psi calculations for the reference shelter (Case E2, 38 ft x 28 ft) which has a single inlet located at the center of the front wall indicated that approximately 15 percent of the floor area yielded impacts in excess of 10 fps (the threshold for head injury). The corresponding critical area for the similar shelter (Case E2E, 28 ft x 28 ft) with a single inlet at the edge of the front wall was approximately 40 percent.

Additional results were obtained for this shelter i.e. E2E and for two additional similar shelters for all three overpressure levels. These additional shelters have the same total volume,

the same inlet area, and the same inlet location (the edge of the front wall), but have different room aspect ratios (width to length ratios). These additional shelters are identified as shelter Case E2G (39.6 ft x 19.8 ft) and shelter Case E2H (19.8 ft x 39.6 ft), and correspond to room aspect ratios of 0.5 and 2.0 respectively. The results of these calculations, in terms of several critical impact level contours are presented in Figures 3.14 through 3.22 for shelter Cases E2E, E2G, and E2H and the three overpressure levels. The percent floor area corresponding to impacts in excess of 10 fps are presented in Figure 3.23 as a function of overpressure for the four shelter cases. The influence of inlet location is predominant while room aspect ratio does not appear to be significant. The influence of the overpressure level is moderate.

3.3.2 Multiple Inlet Configurations

The computer model was modified to include the expanded room configurations illustrated in Figure 3.1(c). The basic geometry, and its reduced form can be combined in a variety of ways to treat these expanded configurations by making use of the symmetry conditions of the expanded configurations. Since the front wall does not represent a line of symmetry, the expansion of the basic geometry in the H room direction is limited to two units as shown in Figure 3.1(c). Any number of units can be expanded in the W room direction yielding multiple openings along one or two walls. These openings are all of the same size with the possible exception of the end inlet(s) which will be one-half the nominal size if the inlet is located at the corner.

The multiple inlet shelters will be associated with the larger shelter sizes. Thus shelter B2 was selected for the examination of room size, inlet location, and room aspect ratio. Impact contours for one of the cases studied is presented in Figure 3.24. Four inlets were used for this shelter size. The number of inlets should be somewhat proportional to room size and in the current evaluation this corresponds to one inlet per 2400 ft^2 of floor area.

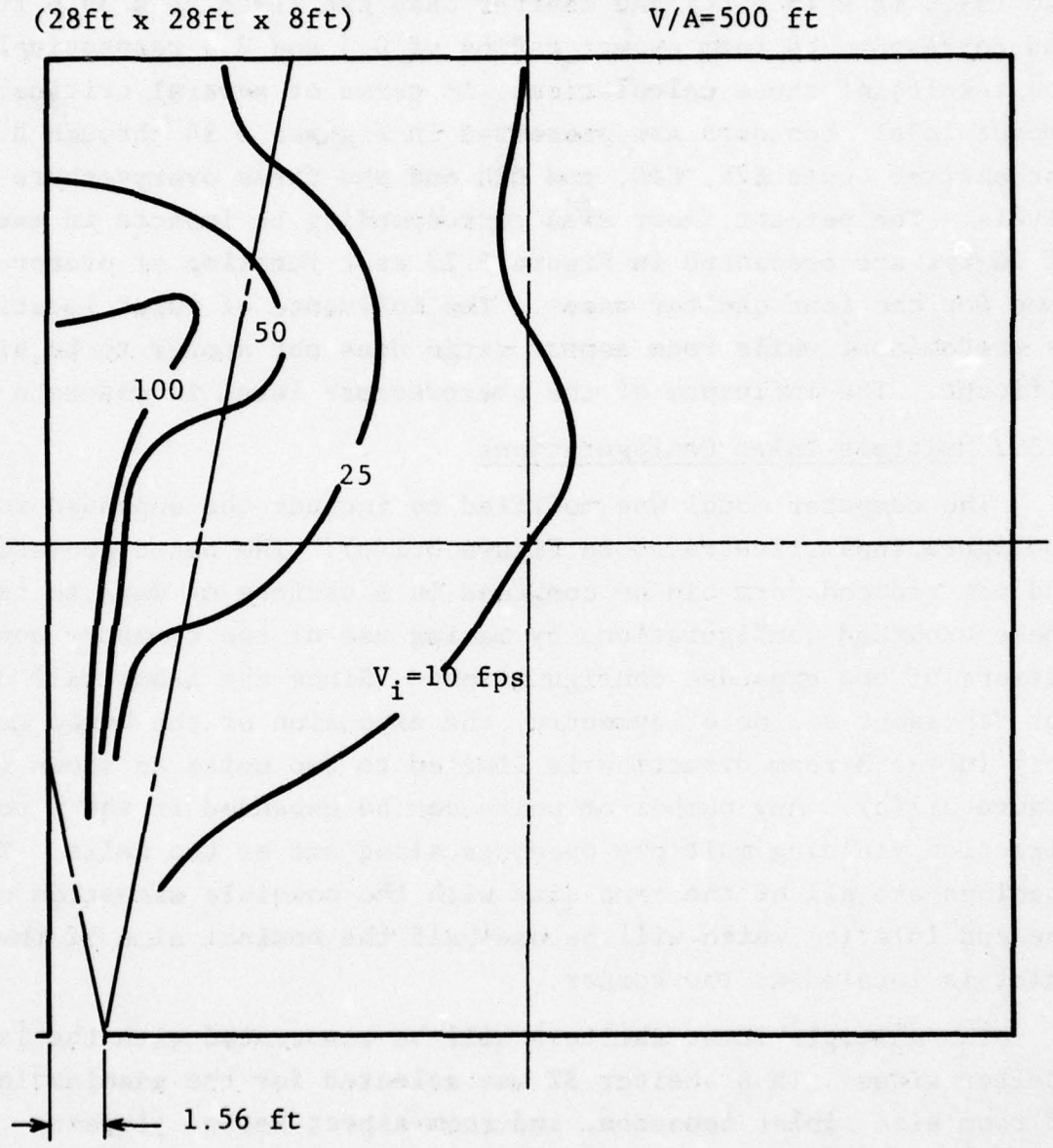

Figure 3.14 Impact Contours for Shelter Case E2E
15 psi Overpressure

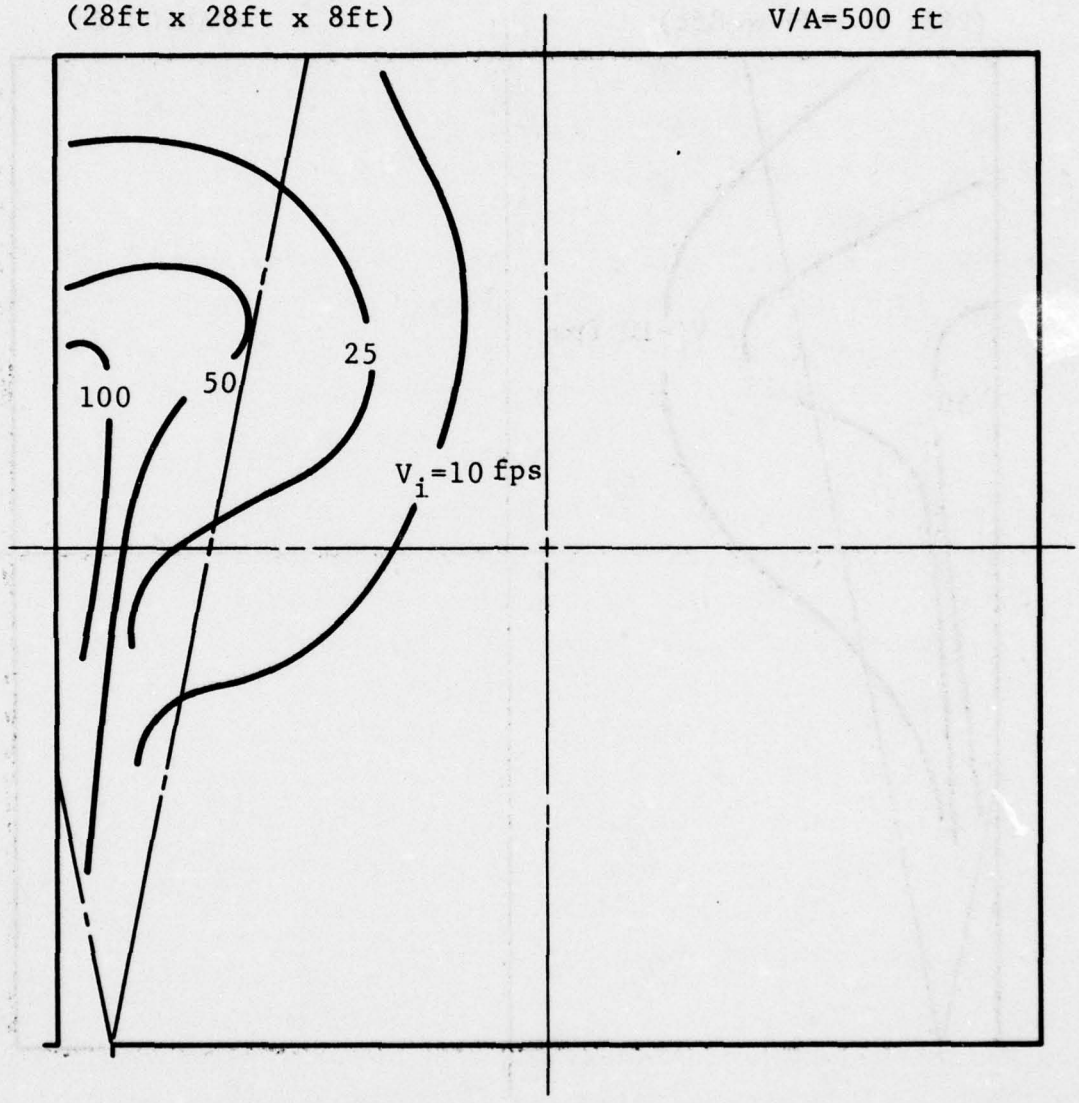

Figure 3.15 Impact Contours for Shelter Case E2E
10 psi Overpressure

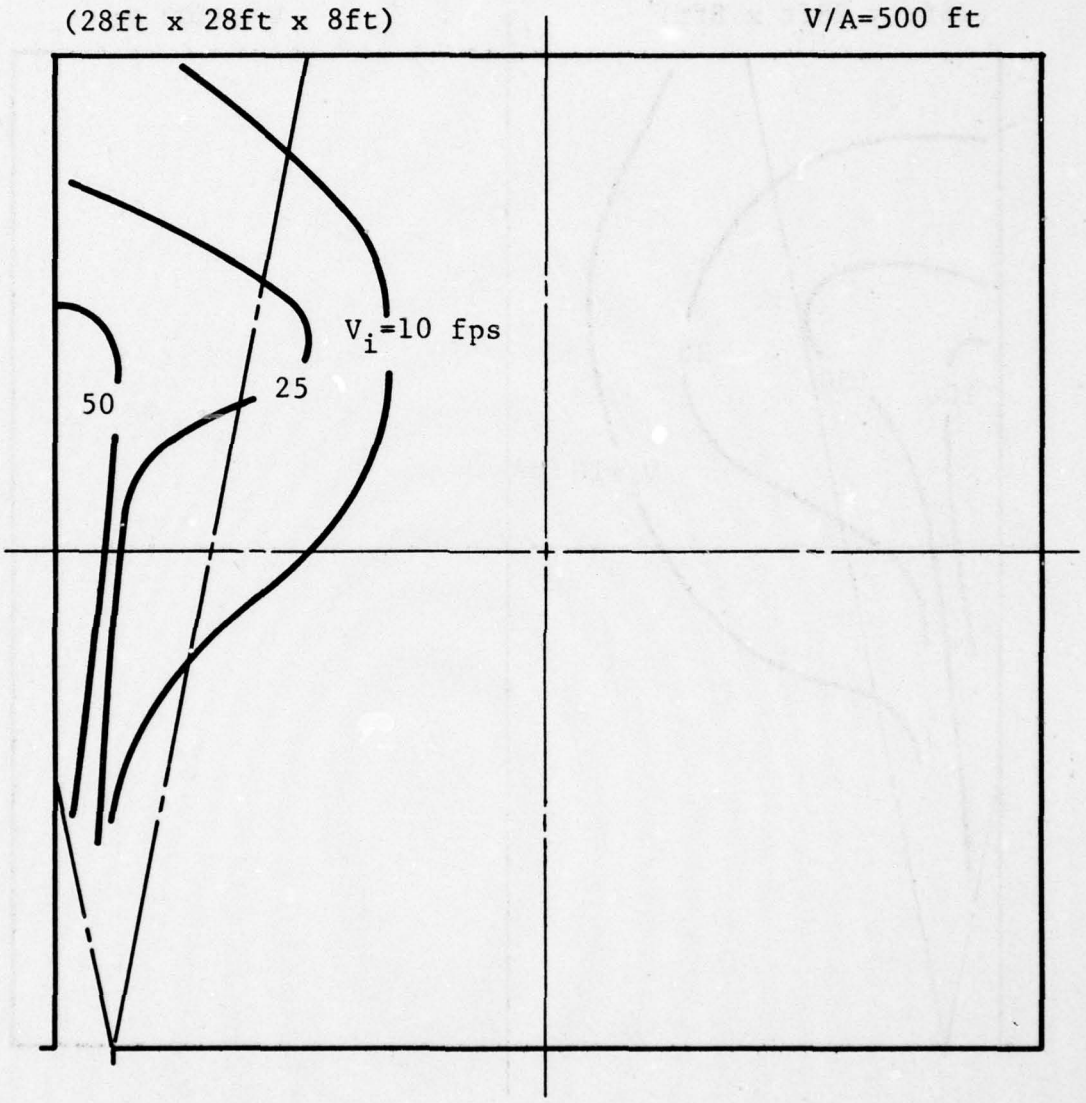

Figure 3.16 Impact Contours for Shelter Case E2E
6 psi Overpressure

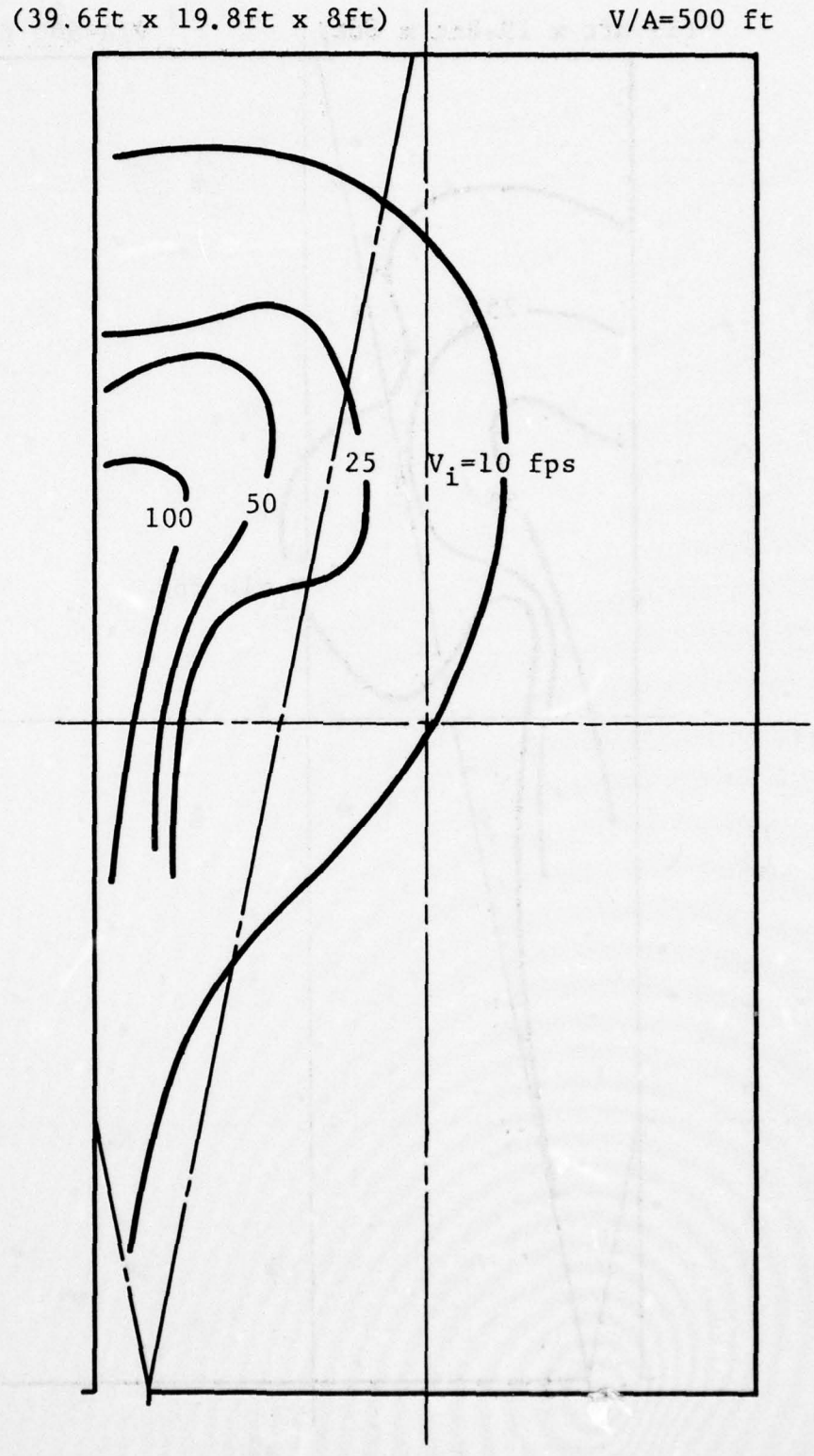

Figure 3.17 Impact Contours for Shelter Case E2G, 15 psi Overpressure

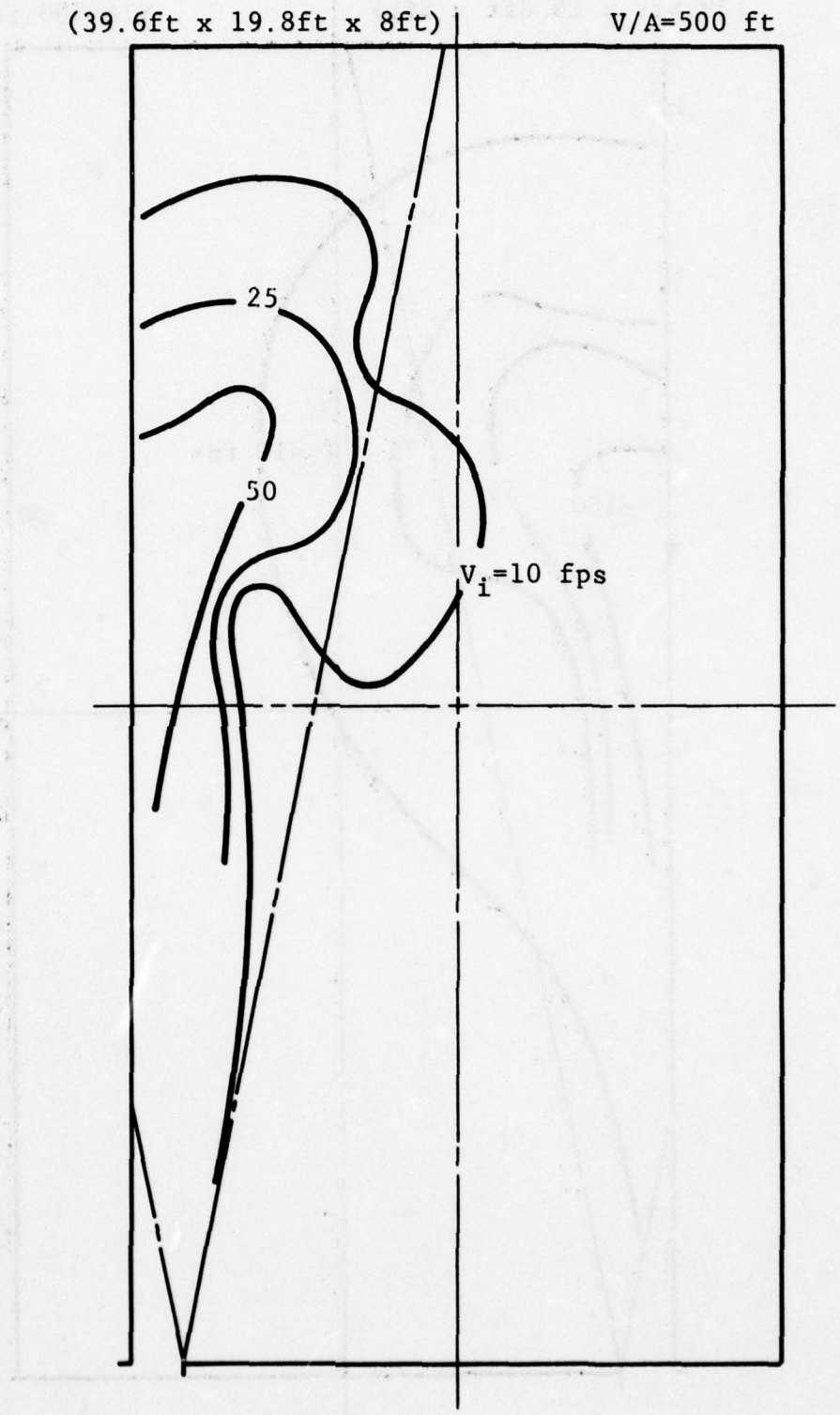

Figure 3.18 Impact Contours for Shelter Case E2G, 10 psi Overpressure

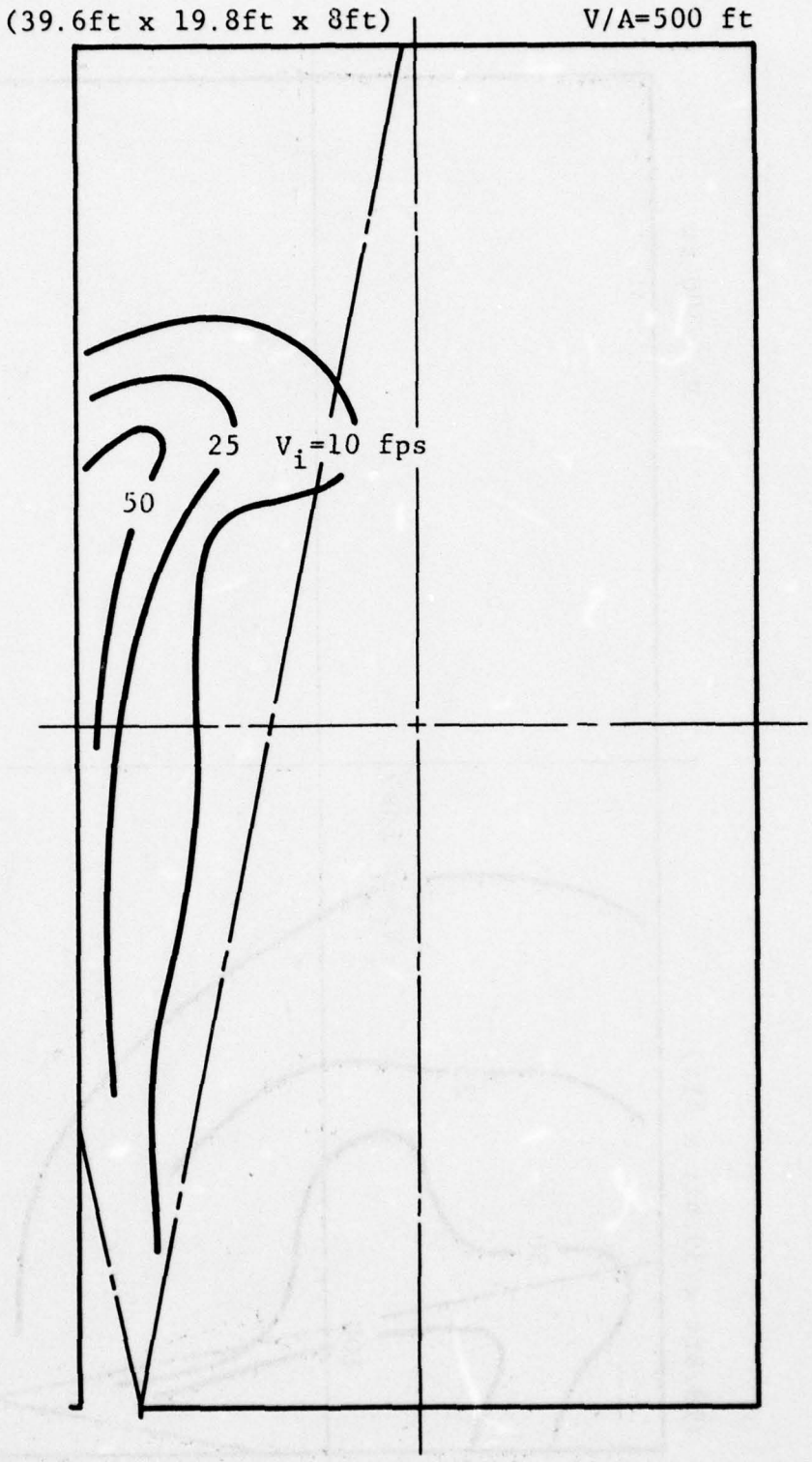

Figure 3.19 Impact Contours for Shelter Case E2G, 6 psi Overpressure

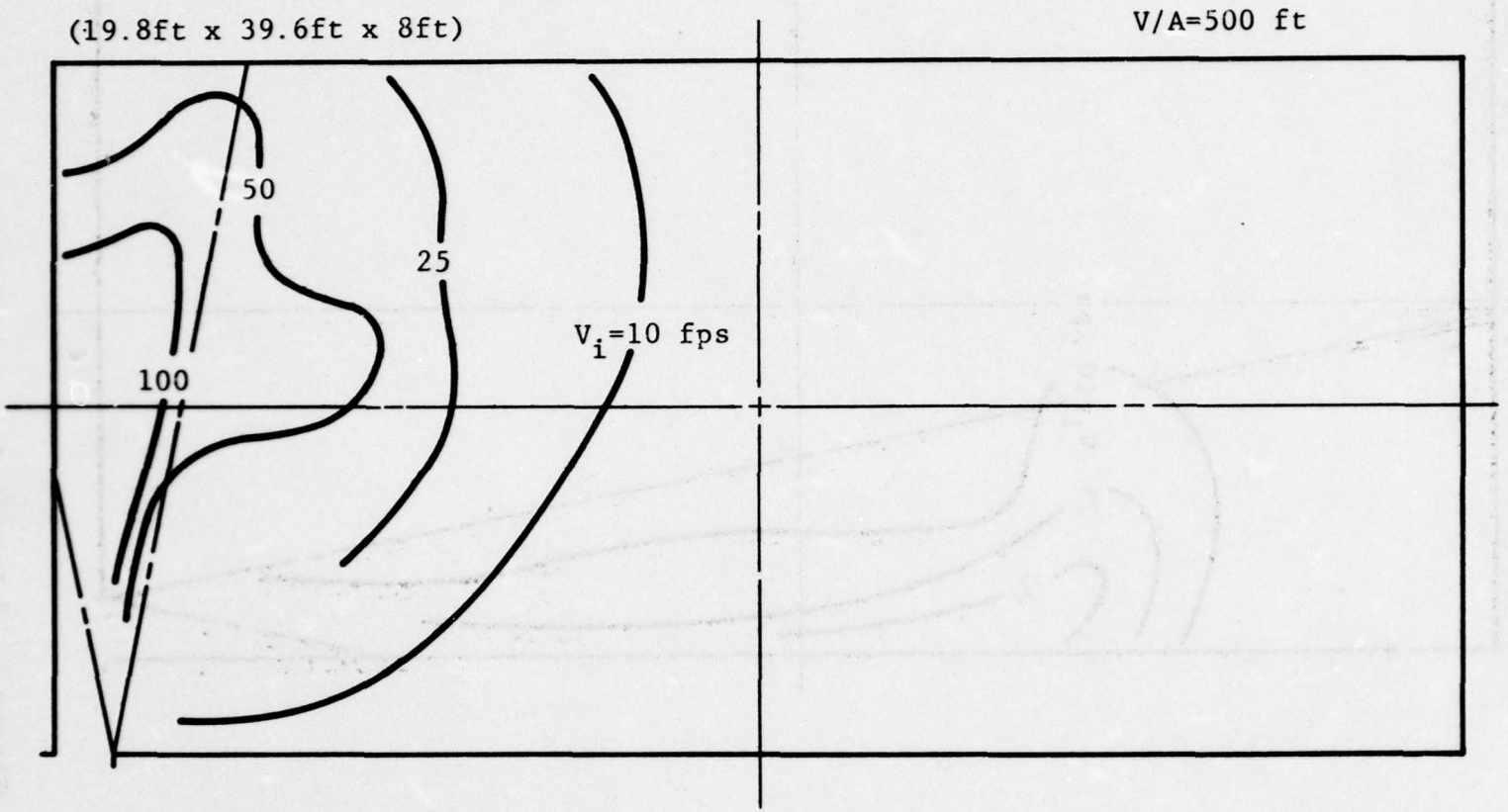

Figure 3.20 Impact Contours for Shelter Case E2H, 15 psi Overpressure

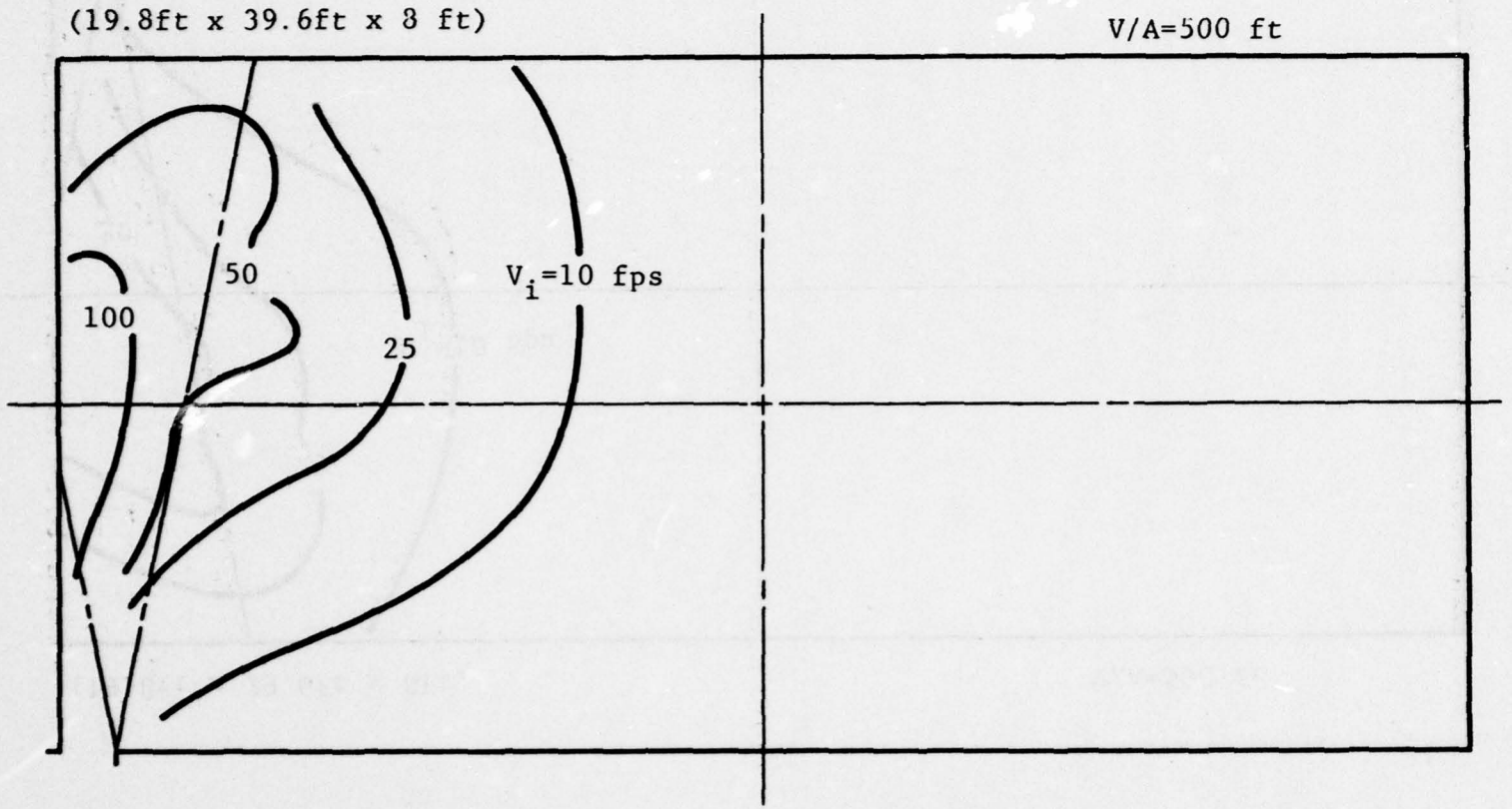

Figure 3.21 Impact Contours for Shelter Case E2H, 10 psi Overpressure

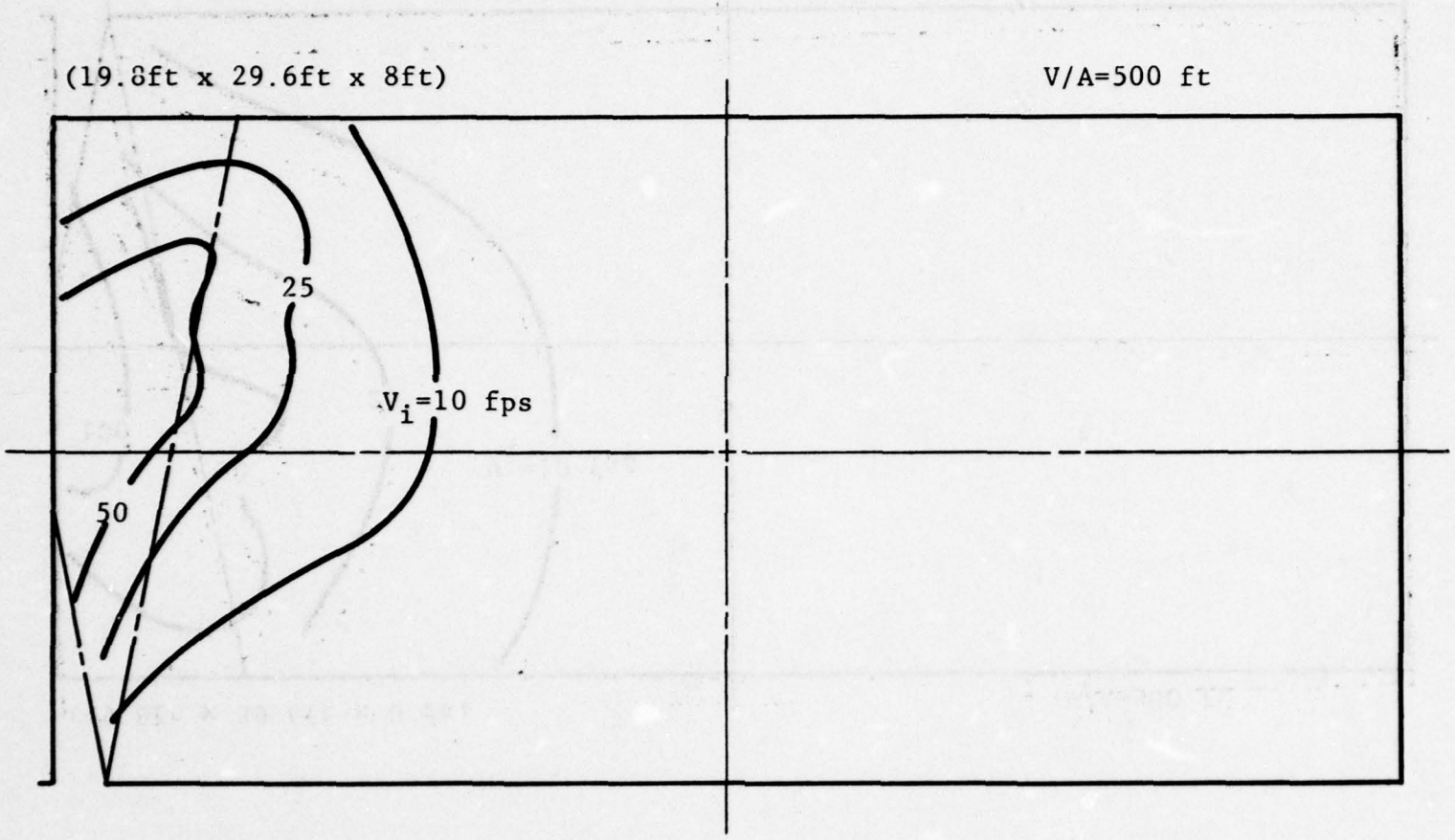

Figure 3.22 Impact Contours for Shelter Case E2H, 6 psi Overpressure

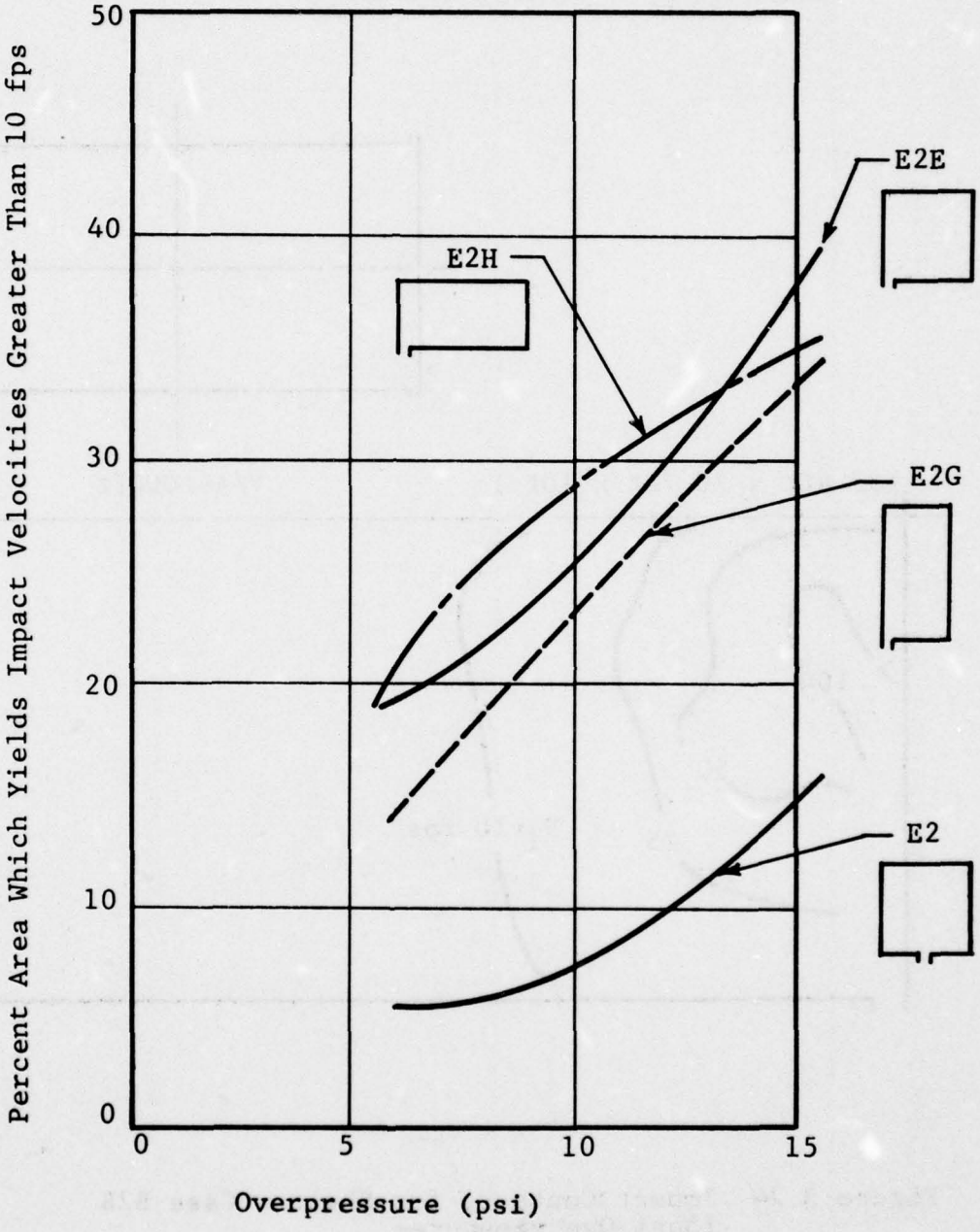

Figure 3.23 Percent Critical Area for Shelter Case E2

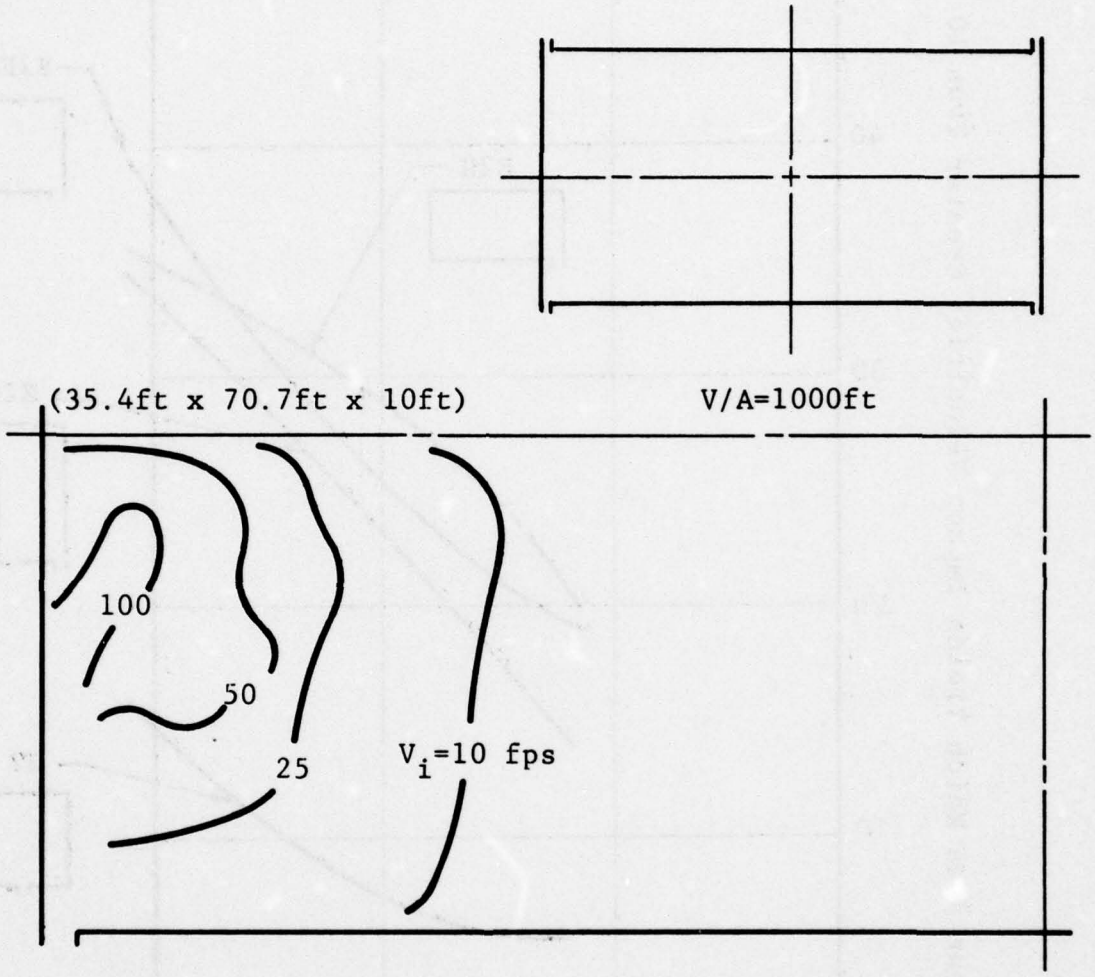

Figure 3.24 Impact Contours for Shelter Case B2B 15psi Overpressure

Thus these room modules correspond roughly to Shelter Case C2, although the V/A ratio is somewhat different.

The results of this evaluation are summarized in Figure 3.25 in terms of the percent floor area corresponding to impacts in excess of 10 fps. These results are similar in form to those obtained for the single inlet configurations, (see Figure 3.23), in that edge located inlets significantly increase the hazard over that produced by centrally located inlets. Room aspect ratio is not a major parameter whereas increasing overpressure produces more severe results as is expected.

3.4 RATING OF SHELTERS FOR BLAST INDUCED EFFECTS

The wall impact results presented in the preceding sections demonstrate the general vulnerability level of shelter occupants due to blast induced translational effects for a variety of blast and shelter parameters. A shelter index has been established with which to rate shelters with respect to the subject injury mechanism as a function of the shelter parameters studied. The specific index chosen is somewhat arbitrary and is therefore intended to serve as a relative measure of the effectiveness of a given set of shelters. The index chosen, I_{10}, is the percent of floor area corresponding to initial occupant locations which produce wall impacts in excess of 10 fps when the shelter is exposed to an overpressure of 15 psi. The results of this definition are presented in Figure 3.26 and the particular shelters examined are appropriately identified. The larger shelters tend to be more hazardous shelters, but for space considerations may be more suitable. The degree of protection possible in such shelters can be increased by eliminating excess inlets, in particular inlets of the edge type. Furthermore the avoidance of certain high flow areas near the inlets will further reduce the general level of potential injuries. It must be noted that many objects may be translated through the shelter space and thus good housekeeping practices are essential in such situations. Finally, the use of padding, especially on floors, should contribute materially to establishing a safer shelter subject to blast induced translational effects.

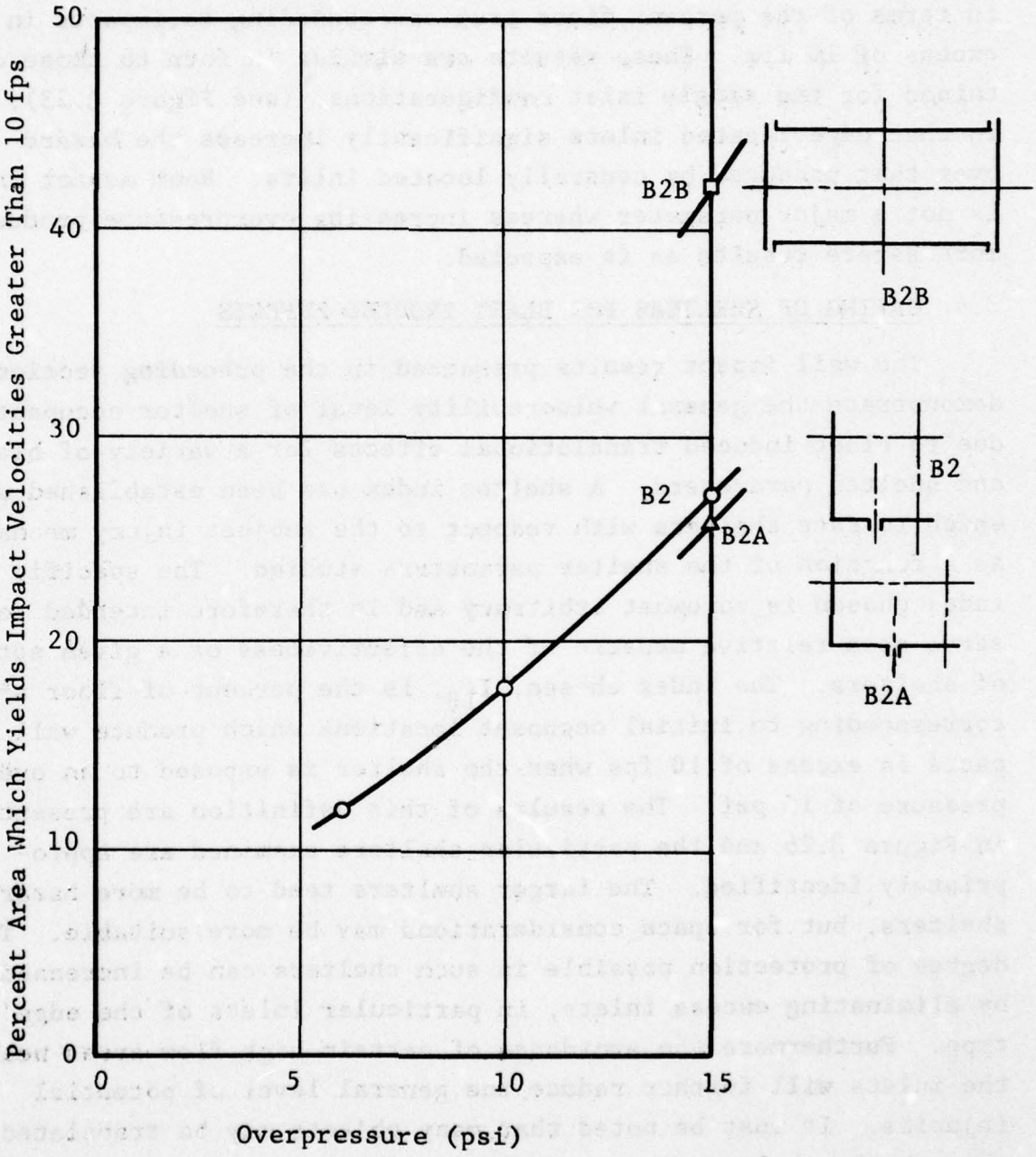

Figure 3.25 Percent Critical Area for Shelter Case B2

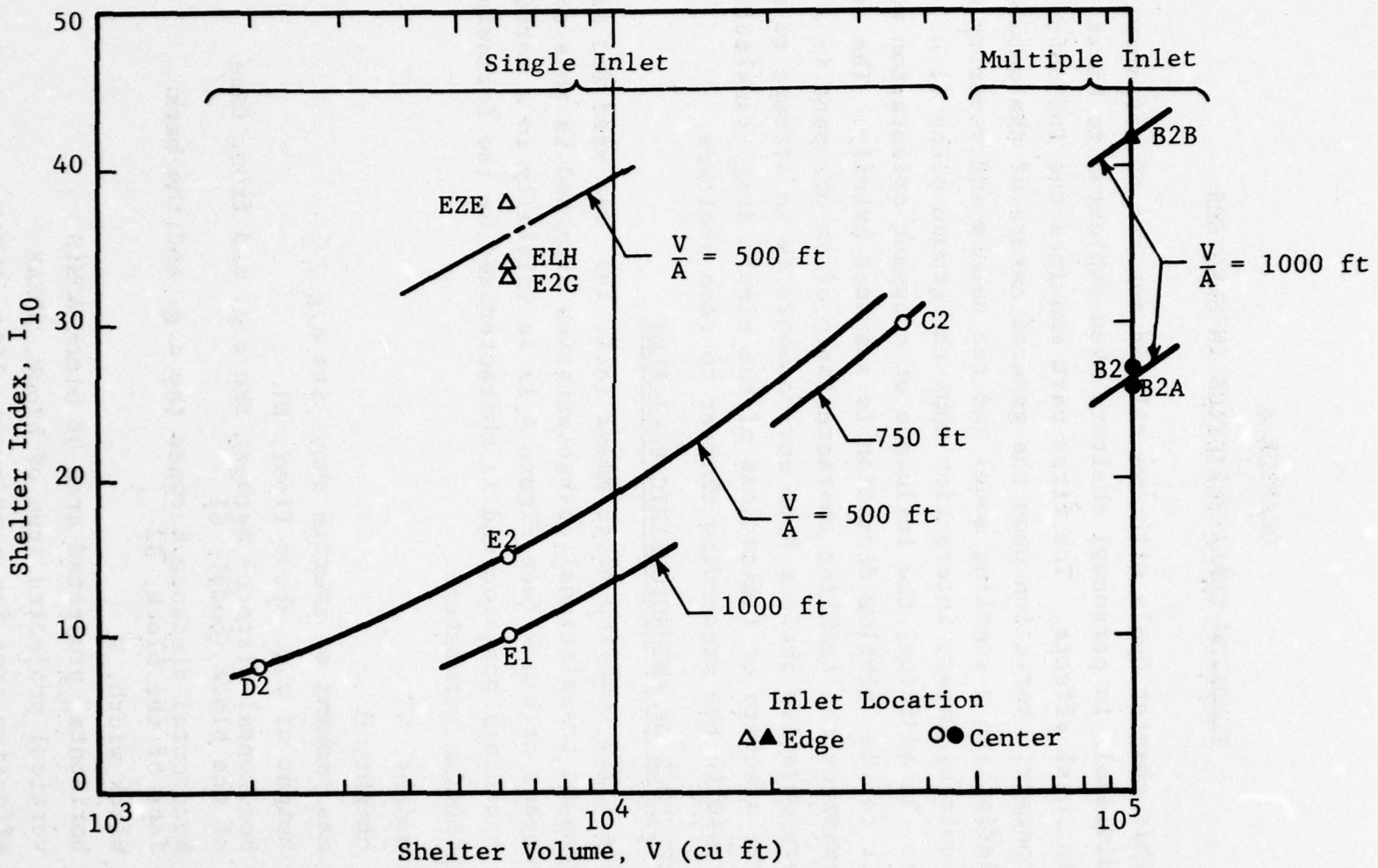

Figure 3.26 Shelter Rating for Blast Induced Translational and Impact Effects

CHAPTER 4

TUMBLING CHARACTERISTICS IN SHELTERS

This chapter deals with two related aspects of the survivability of individuals in personnel shelters when subjected to blast induced translational effects. The first part examines the influence of anthropometric variation upon the general nature of the occupant translation (in a tumbling mode) and the nature and severity of the resulting impact interaction upon the ground plane (i.e., the floor). In addition, the influence of occupant orientation with respect to the airflow direction is examined briefly. The second part examines the tumbling characteristic of an occupant in a series of representative shelter flow environments as an attempt to evaluate the adequacy or limitations of the simple drag translation model used in the preceeding chapter to rate shelters.

4.1 INFLUENCE OF ANTHROPOMETRIC VARIABLES

The IITRI tumbling block model (Ref. 14) was used for all of the occupant translational characteristics examined in this chapter. The occupant or block (see Figure 4.1) is initially in a vertical (i.e., standing) position and is characterized by the following anthropometric parameters:

- weight, WT
- height, H
- mass moment of inertia about its c.g., I
- height of c.g. above floor, D1
- horizontal distance between the c.g. and front face of the block (body), S1
- horizontal distance between the c.g. and the back face of the block, S2
- block width, W
- horizontal projected area of block ADMIN
- vertical projected area of block, ADMAX
- effective area for aerodynamic lift, ALMAX

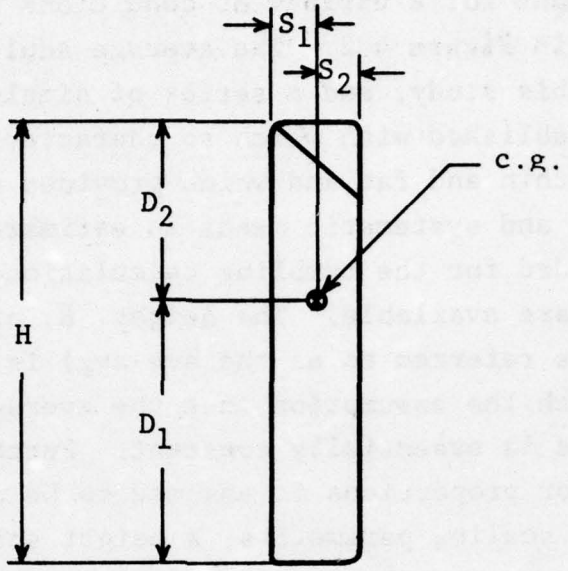

Figure 4.1 Tumbling Block Model

In addition, a series of floor (wall) interaction spring stiffnesses and friction coefficients are utilized. The blast induced or idealized wind field represents the driving force which causes the block to tumble and ultimately interact with some nearby rigid boundary representing the floor or wall. In the first part of this chapter the wind field is idealized as a simple step increase in wind velocity from a no-flow condition to a constant flow value. Thus, the magnitude of the wind velocity is one of the variables examined in this study. A nominal value of the air density was used throughout.

The anthropometric data were obtained from Ref. 18 and clearly document the obvious fact that people come in a wide variety of sizes and shapes, even excluding the influence of sex and age. The anthropometric data are limited in some respects and have a bias in others due to the practical or available sources for such data. Sample sizes are frequently small and tend to involve the young male adult (i.e., the military service candidate) to a large degree. Nonetheless, this data base is adequate for the purposes of this chapter. This data base was examined and the relationship between

height and weight for a variety of conditions was determined and is summarized in Figure 4.2. The average adult male is used as a reference in this study, and a series of simple scaling relationships was established with which to characterize such arbitrary categories as thin and fat and which provides a practical and hopefully adequate and systematic means to estimate the values of those parameters needed for the tumbling calculations and for which new specific data are available. The height, $\overline{H}$, of the average adult male (sometimes referred to as the avg-avg) is used as a reference value along with the assumption that the average body density for all individuals is essentially constant. Furthermore, a linear scale factor for proportions is assumed to be applicable. Thus we can define two scaling parameters; a height scale factor

$$\lambda = \frac{H}{\overline{H}}$$

where H is the height of the individual and $\overline{H}$ the reference value, and a scale factor σ for proportions. A value of $\lambda = 1.08$ was selected for the category "tall", and a value of $\lambda = 0.91$ was selected for the category "short". Similarly values of $\sigma = 0.85$ and $\sigma = 1.15$ were selected for the categories "thin" and "fat", respectively. The following scaling relationships follow from elementary considerations.

$$WT/\overline{WT} = \sigma^2\lambda^3$$

$$I/\overline{I} = \sigma\lambda^4$$

$$D1/\overline{D1} = H/\overline{H} = \lambda$$

$$W/\overline{W} = \sigma$$

$$S1/\overline{S1} = S2/\overline{S2} = \sigma\lambda$$

$$ADMIN/\overline{ADMIN} = \sigma^2\lambda^2$$

$$ADMAX/\overline{ADMAX} = ALMAX/\overline{ALMAX} = \sigma\lambda^2$$

where the ($\overline{\quad}$) quantity represents the reference values for the average adult male.

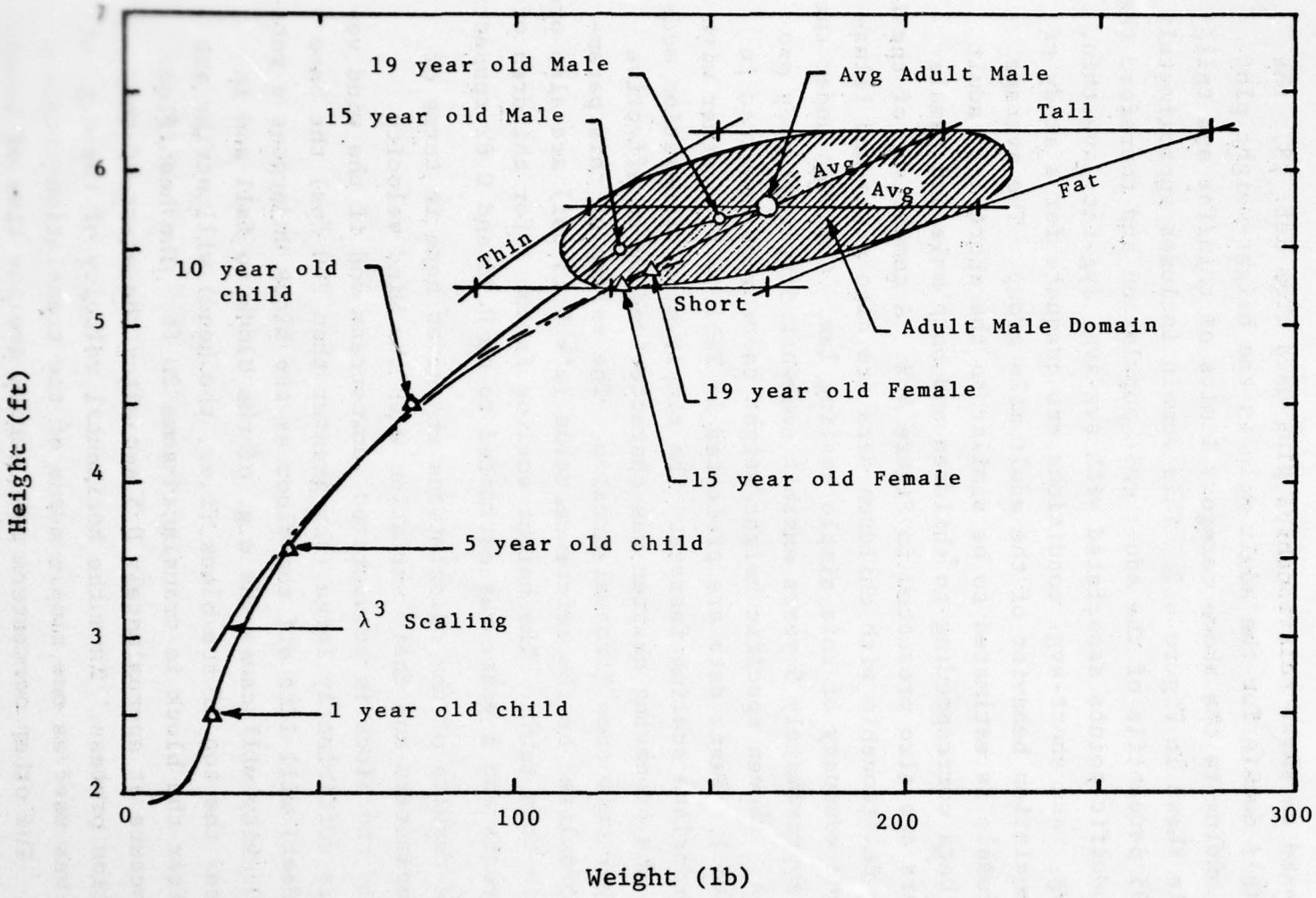

Figure 4.2 Height/Weight Data Summary

Based on these relationships plus data from Ref. 18, the applicable domain for the adult male in the height-weight plot corresponding to the above category limits of thin/fat and tall/short is shown in Figure 4.2. This domain includes approximately 90 to 95 percentile of the adult male population and therefore the five specific points associated with avg-avg, avg-fat, avg-thin, tall-avg, and short-avg, conditions are adequate for a study of the translation behavior of the adult male group. The average adult female is estimated to be similar to the short-avg adult male. Data corresponding to children and both male and female teenagers are also presented in Figure 4.2. A comparison of the λ^3 scaling relationship with children data are also given and illustrate the adequacy of this simple scaling law. Children under the age of approximately 5 years exhibit somewhat different body proportions. Eleven specific height/weight cases were examined in some detail. Basic data are presented in Table 4.1 together with the appropriate scaling factors. The simple drag translation model used in the preceding chapter was characterized by an effective height per unit area (frontal area) ω. The values of this parameter, normalized by the reference value ($\omega' = 0.13$ psi) are also presented in this table. The height scaling factor λ for children of age 10 years and 5 years was estimated to be 0.78 and 0.62 respectively.

The results of the calculations are given here in terms of three parameters and their variation with the wind velocity. Typically the block is accelerated downstream and if the wind velocity is sufficiently large (say greater than 200 fps) the base (i.e., feet) will lift off the floor as the block undergoes a rotation. Gravity will cause the c.g. of the block to fall and in most cases the top of the block (i.e., the head) will strike the floor after the block is translated some 20 ft. The head/floor impact occurs at approximately 0.5 sec after the start of the translation process. Thus the horizontal velocity of the c.g. at 0.5 sec was used as one simple means of the translation-rotation process. The other parameters used herein are the time of impact and the magnitude of the impact (vertical) velocity. If the wind

velocity is low, then the block is translated horizontally, generally bouncing several times on its base, until it eventually falls over.

TABLE 4.1

HEIGHT/WEIGHT CHARACTERISTICS OF INDIVIDUALS*

Category (Shape-Height)	Weight (lb)	Height (ft)	Moment of Inertia (lb sec^2 ft)	λ	σ	$\frac{\omega}{\omega'}$
Avg-Avg	165	5.77	8.58	1.00	1.00	1.00
Avg-Short**	124	5.25	5.88	0.91	1.00	0.91
Avg-Tall	210	6.25	11.81	1.08	1.00	1.09
Thin-Short	90	5.25	5.00	0.91	0.85	0.78
Thin-Avg	119	5.77	7.29	1.00	0.85	0.85
Thin-Tall	152	6.25	10.04	1.08	0.85	0.93
Fat-Short	165	5.25	6.76	0.91	1.15	1.05
Fat-Avg	2.18	5.77	9.87	1.00	1.15	1.15
Fat-Tall	2.78	6.25	13.58	1.08	1.15	1.25
10 yr old child	78	4.50	3.17	0.78	1.00	0.78
5 yr old child	40	3.60	1.30	0.62	1.00	0.62

* The average adult female is similar to avg-short.
**Data for the 11 case studies considered in this chapter.

The horizontal velocity (at 0.5 sec) of the block obtained from the tumbling block model is similar to that obtained from the simple drag model for low wind velocities. This is a result of the fact that friction effects at the base of the block are not effective due to the slight lifting of the block. However, when subjected to larger wind forces the horizontal velocity is degraded substantially when compared to the results of the simple drag model. This is due in part to the lower exposed drag area resulting from the gross rotation of the block. These results are presented in Figure 4.3 and the comparison with the simple drag solution is applicable to the average male adult curve (identified as avg). The corresponding results for the two other male groups as well as for the average adult female and two groups of children are presented in Figures 4.4 and 4.5. Surface blast characteristics including

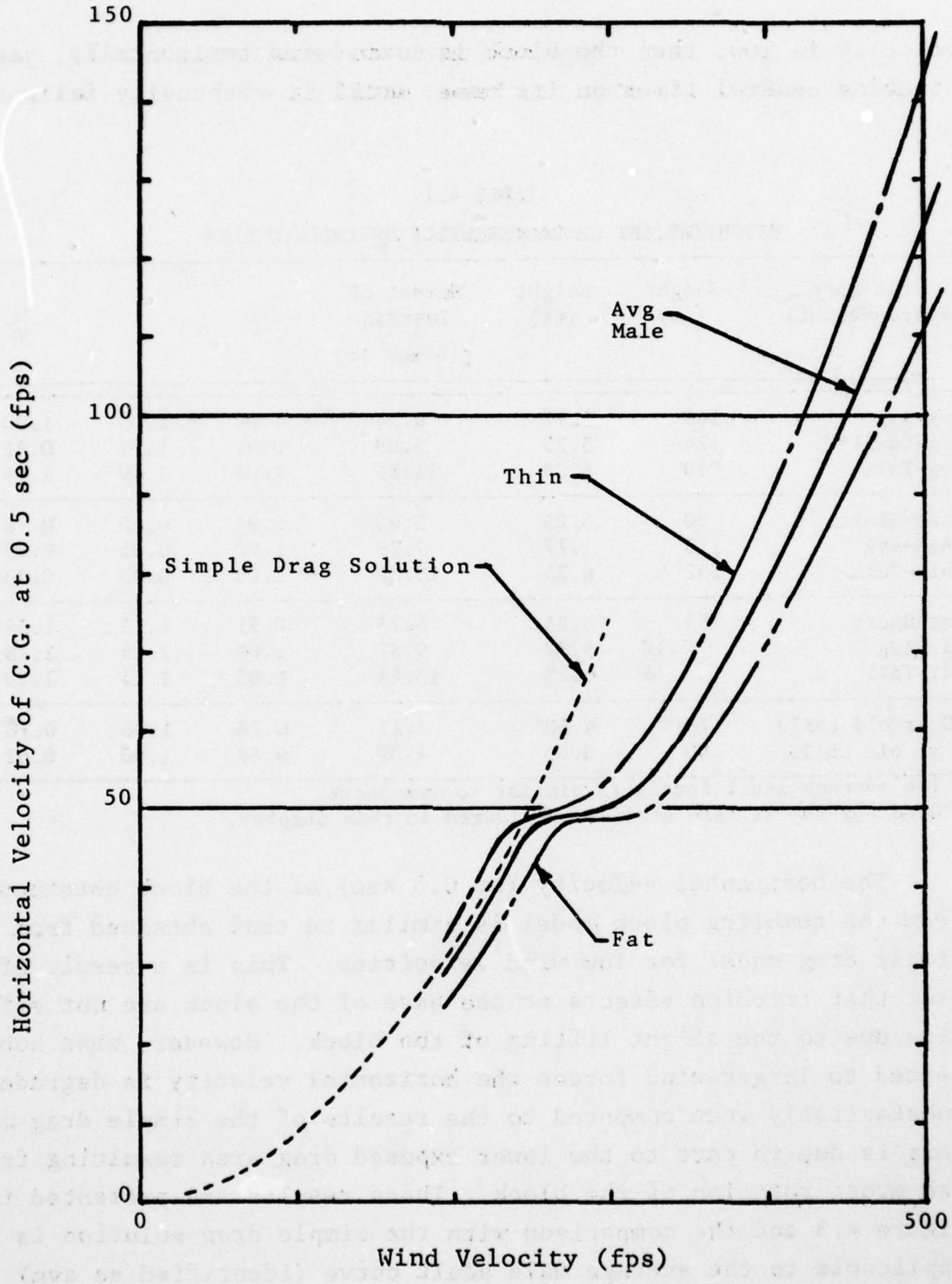

Figure 4.3 Horizontal Velocity Results - Thin/Fat

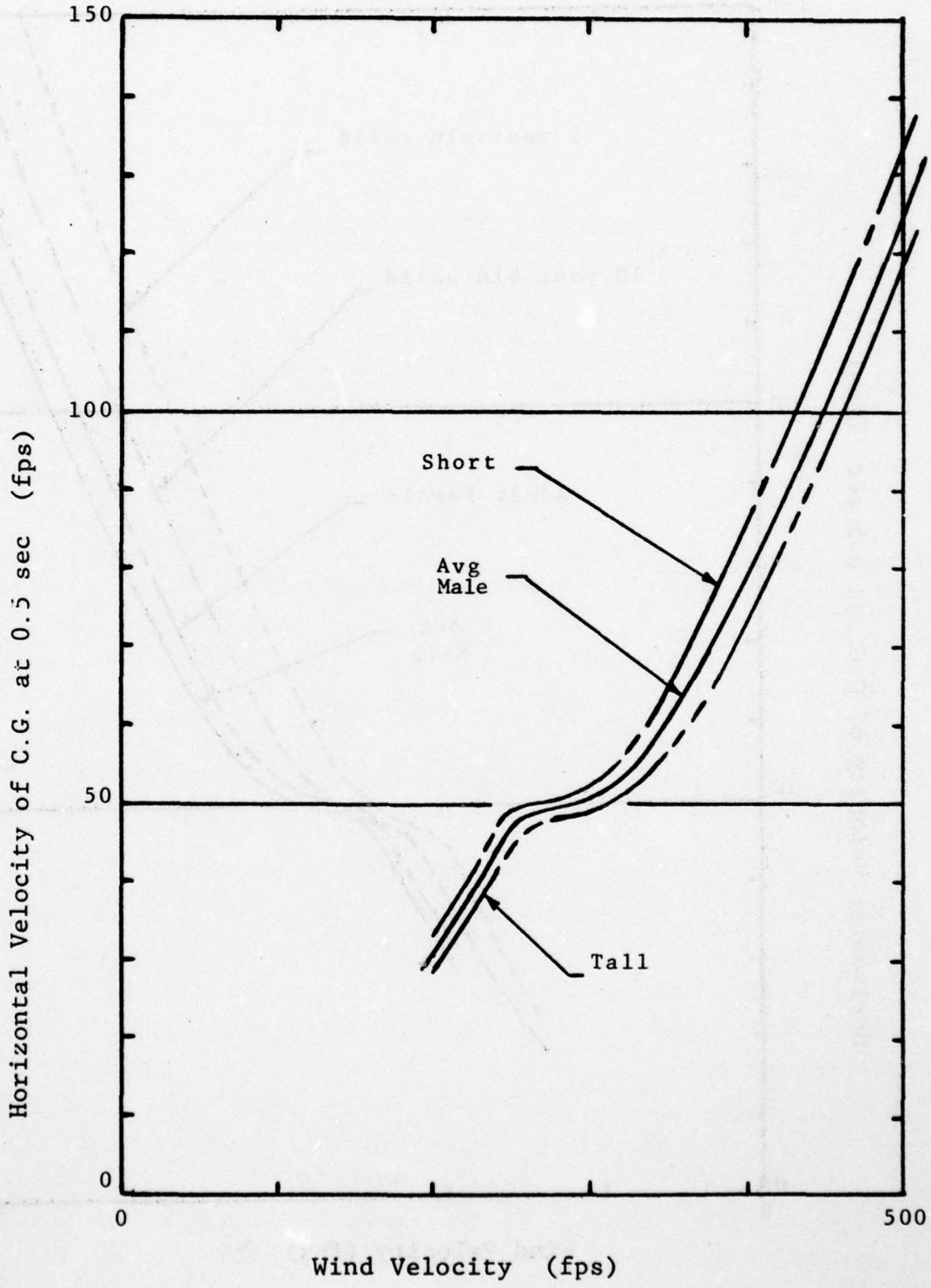

Figure 4.4 Horizontal Velocity Results - Short/Tall

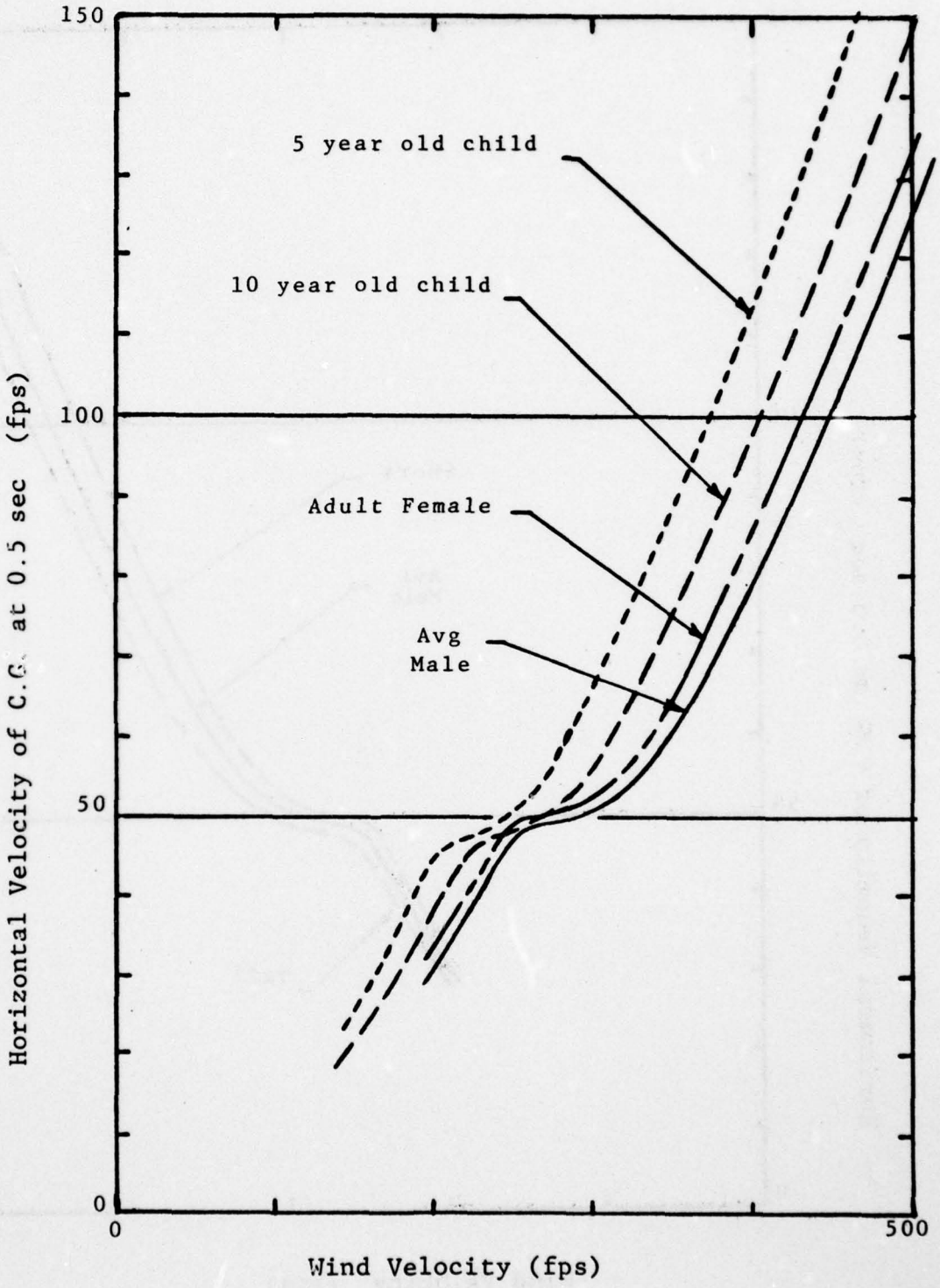

Figure 4.5 Horizontal Velocity Results - Female/Child

wind velocities behind the shock front are given in Table 4.2. The differences due to anthropometric variations are generally small, being the largest for the children groups. It should be noted that these results are for the backward facing orientation, that is, the individual faces the same direction as the direction of the wind velocity.

TABLE 4.2

SURFACE BURST CHARACTERISTICS

Peak Overpressure psi	Peak Dynamic Pressure psi	Maximum Wind Velocity fps	Range from Ground Zero (1MT) miles
2	0.09	103.83	5.00
4	0.37	197.60	3.14
6	0.83	283.31	2.46
8	1.44	362.42	2.08
10	2.21	436.02	1.84
12	3.13	504.96	1.67
14	4.19	569.90	1.53
16	5.38	631.36	1.44

The general tumbling motion of individuals for each of the groups examined are quite similar in both the nature of the tumbling as well as in the magnitude associated with the motion (i.e., translational and rotational velocities) and nature and intensity of the impact. These conclusions are borne out, in part, by examining the time at which impact occurs. Figures 4.6 and 4.7 present these results for eight groups. Finally, and most significantly are the corresponding results for the head/floor impact velocity. These results are presented in Figures 4.8 and 4.9. The onset of head/floor impact occurs at wind velocities in the range of 200 to 250 fps. It is significant that (1) the impact velocity is relatively independent upon the intensity of the wind field and (2) that anthropometric variations are not very important. Both of these observations suggest that the role of the wind (in magnitude and perhaps in time history) is to produce an unstable situation such that the rotation effect combined with gravity fall effects produces an essential constant impact velocity of approximately 16 fps. This impact magnitude for the head is a relatively dangerous magnitude

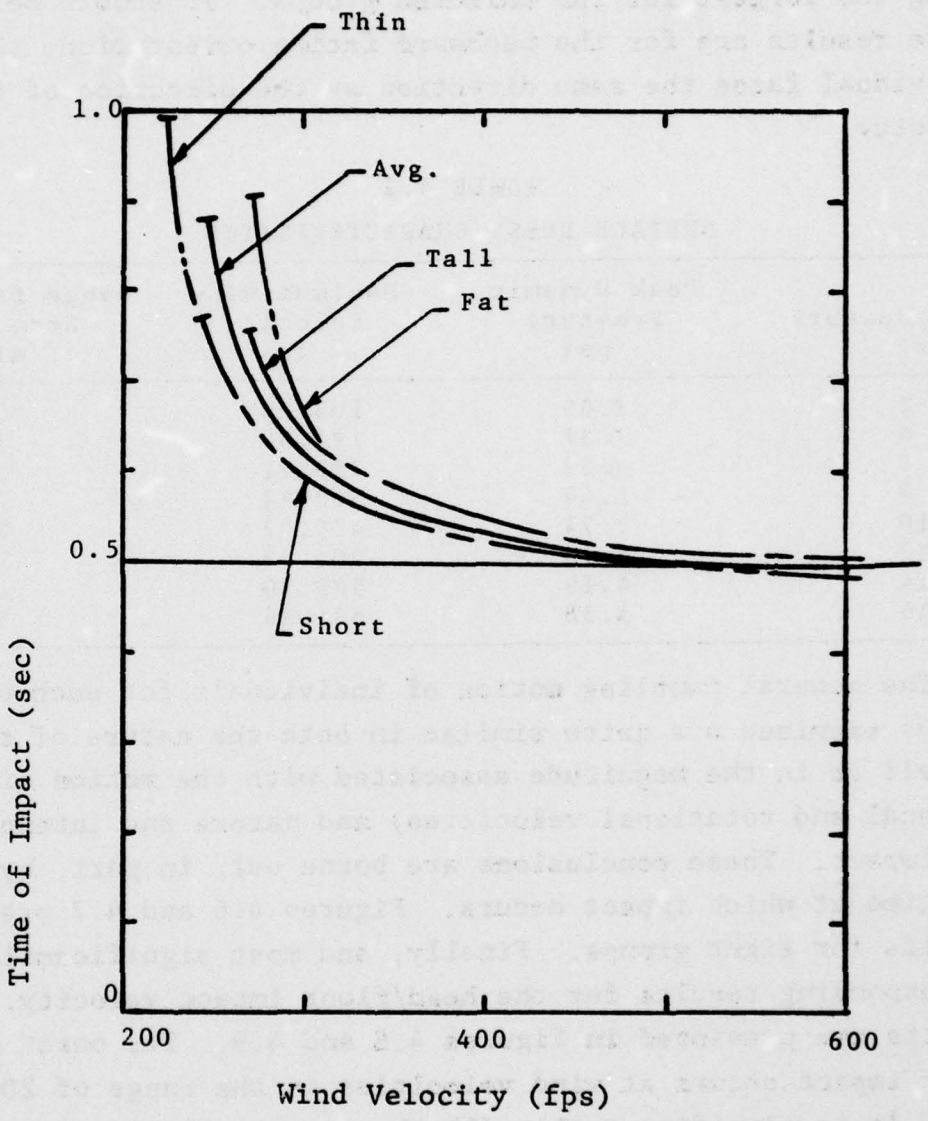

Figure 4.6 Time of Impact Variations for Male Adults

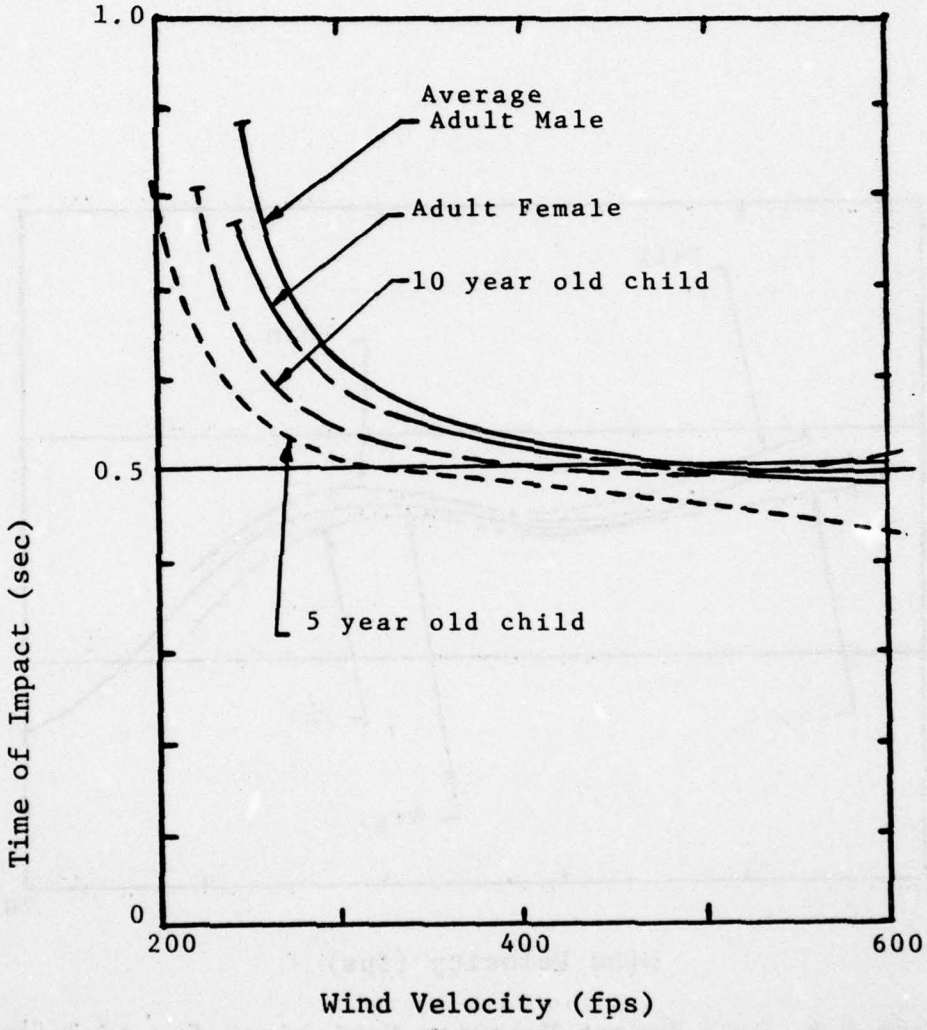

Figure 4.7 Time of Impact Variations for General Population

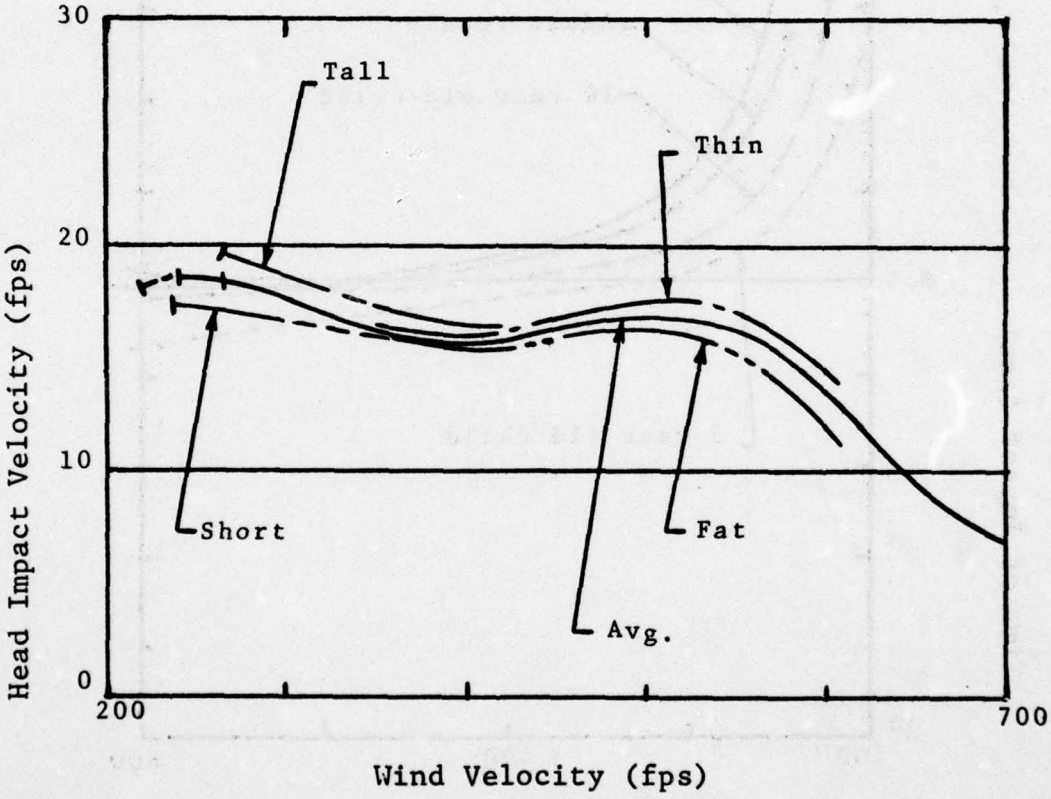

Figure 4.8 Head Impact Velocity Variations for Adult Males

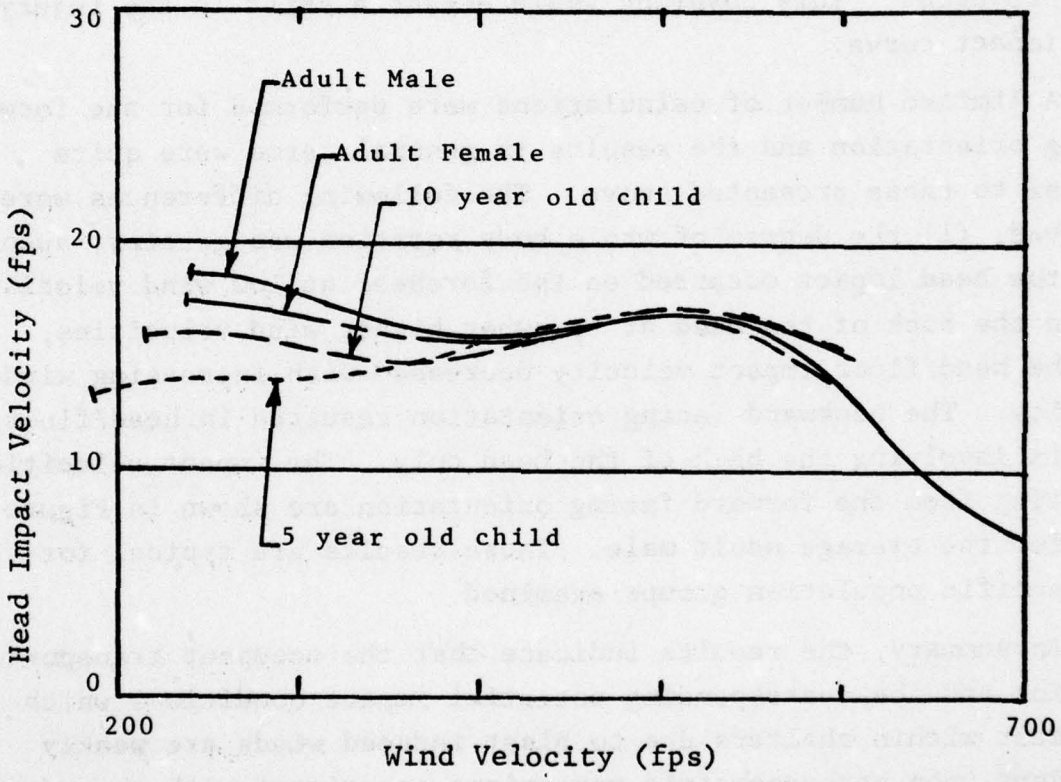

Figure 4.9 Head Impact Velocity Variations for General Population

for impact upon a hard nonresponding surface. The horizontal displacement of the c.g. of the block at the time of impact is presented in Figure 4.10. These results suggest that in large shelters the occupant will strike his or her head on the floor provided that the shelter walls are farther distant from the initial position than shown in this figure. These floor impact situations may be common and relatively severe. The survivability level of shelter occupants may be increased substantially by providing a suitable floor covering. This covering would effect a shift in the injury-head/impact curve.

A limited number of calculations were performed for the forward facing orientation and the results in general terms were quite similar to those presented above. The following differences were observed; (1) the degree of whole body rotation was greater, such that the head impact occurred on the forehead at low wind velocities and on the back of the head at somewhat higher wind velocities; (2) the head/floor impact velocity decreased with increasing wind velocity. The backward facing orientation resulted in head/floor impacts involving the back of the head only. The impact velocities resulting from the forward facing orientation are shown in Figure 4.11 for the average adult male. These results are typical for the specific population groups examined.

In summary, the results indicate that the occupant transport behavior and the corresponding potential impact conditions which can occur within shelters due to blast induced winds are weakly dependent upon anthropometric variations associated with the general population. Furthermore, the dependence upon wind intensity above approximately 200 fps is not strong. The occupant orientation is the only variable studied which had a significant influence upon the results, and then only on the vertical impact velocity magnitude. The results for the backward facing orientation are summarized in Figure 4.12 by using the wind velocity case of 400 fps. The horizontal velocity of the c.g. represents a potential wall impact situation. Thus the impact velocity of the head, feet or whole body (depending on the orientation at time of impact) with a wall ranges

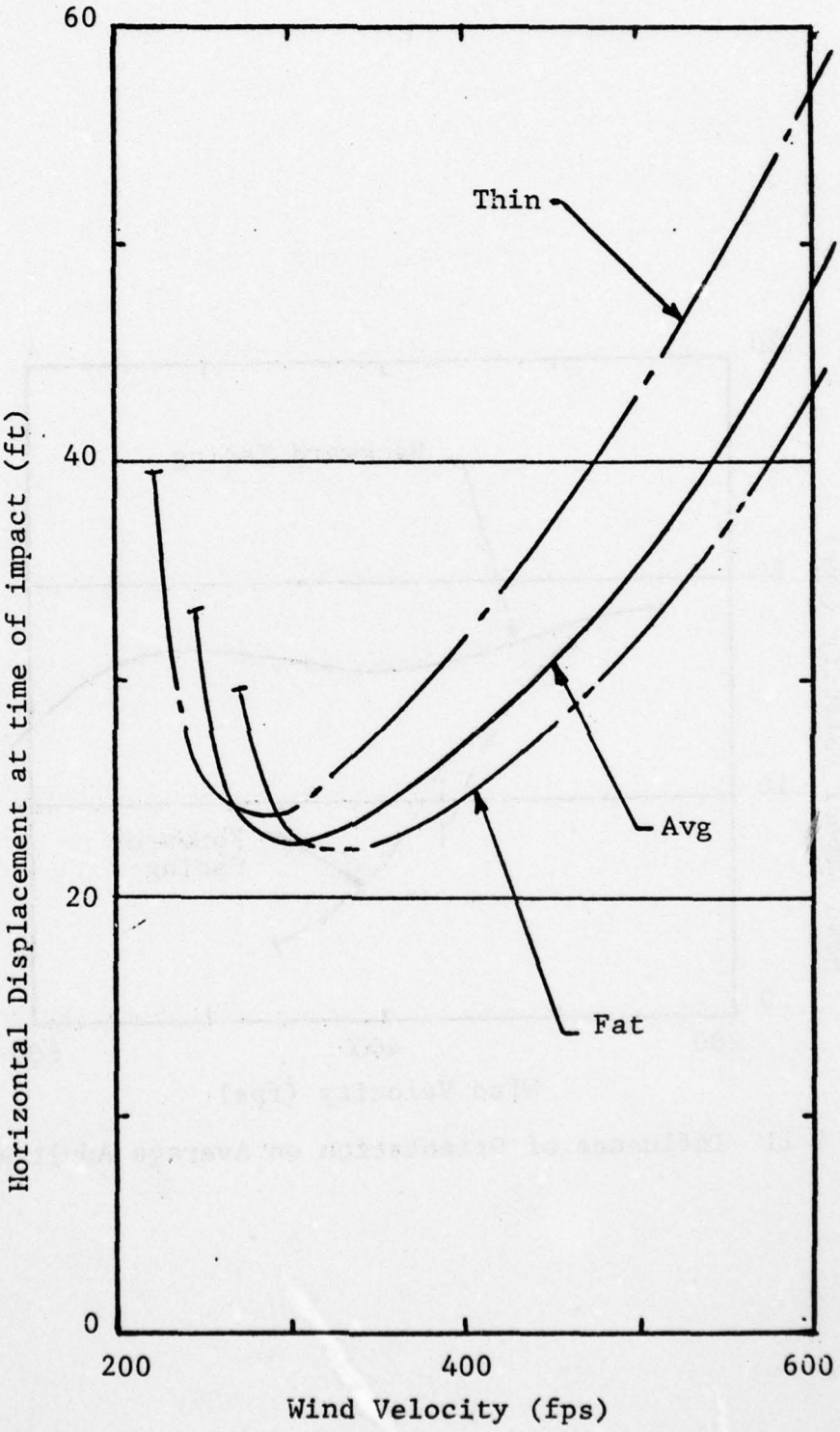

Figure 4.10 Horizontal Displacement of c.g.

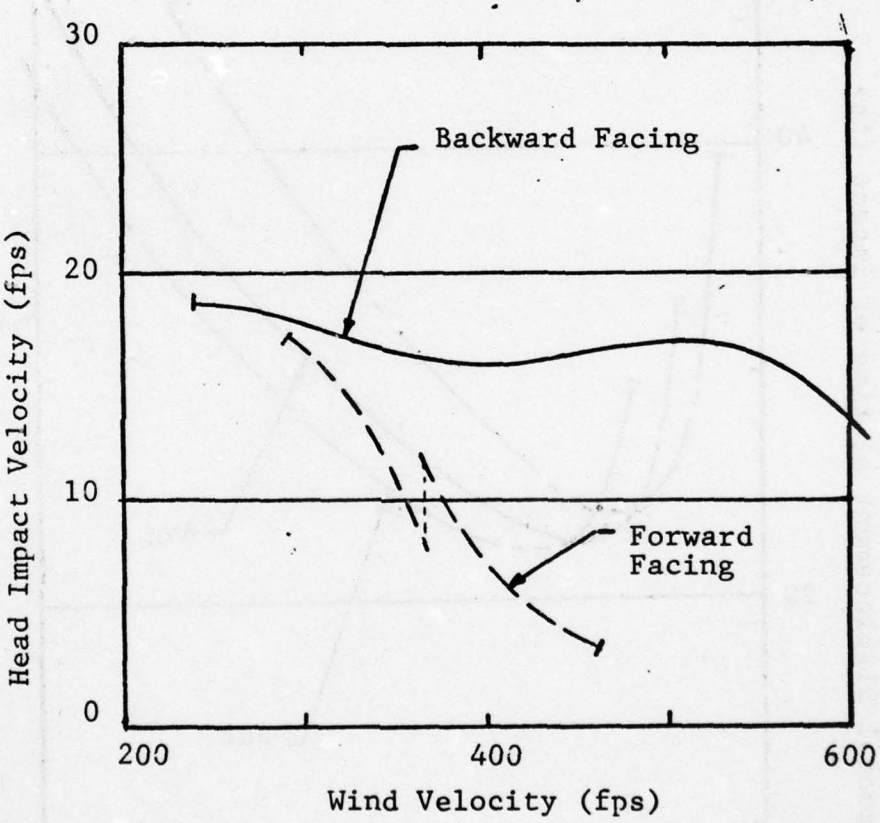

Figure 4.11 Influence of Orientation on Average Adult Male

AD-A049 040 IIT RESEARCH INST CHICAGO ILL F/G 6/21
RELATIVE STRUCTURAL CONSIDERATIONS FOR PROTECTION FROM INJURY A--ETC(U)
JUN 77 A LONGINOW, A WIEDERMANN DCPA01-75-C-0325
UNCLASSIFIED IITRI-J6365 NL

2 OF 2
AD
A049040

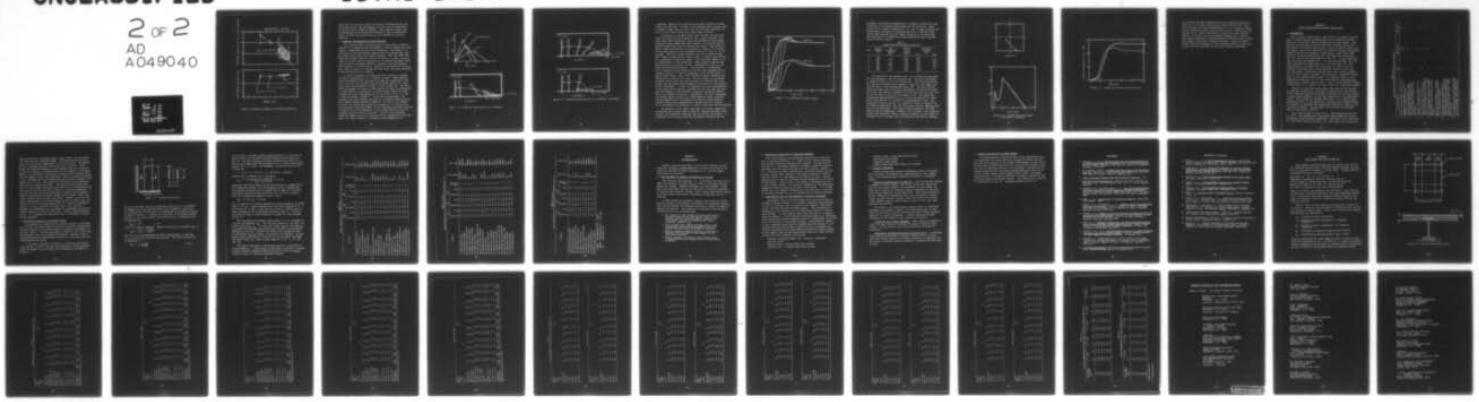

END
DATE
FILMED
3-78
DDC

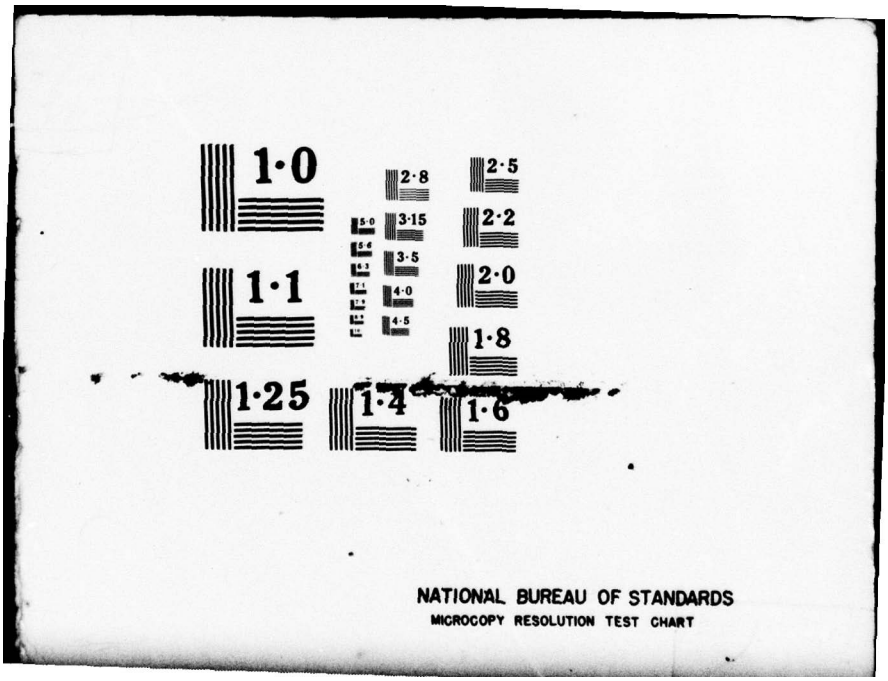
1·0
1·1
1·25
1·4
1·6
1·8
2·0
2·2
2·5
2·8
3·15
3·5
4·0
4·5
5·0
NATIONAL BUREAU OF STANDARDS
MICROCOPY RESOLUTION TEST CHART

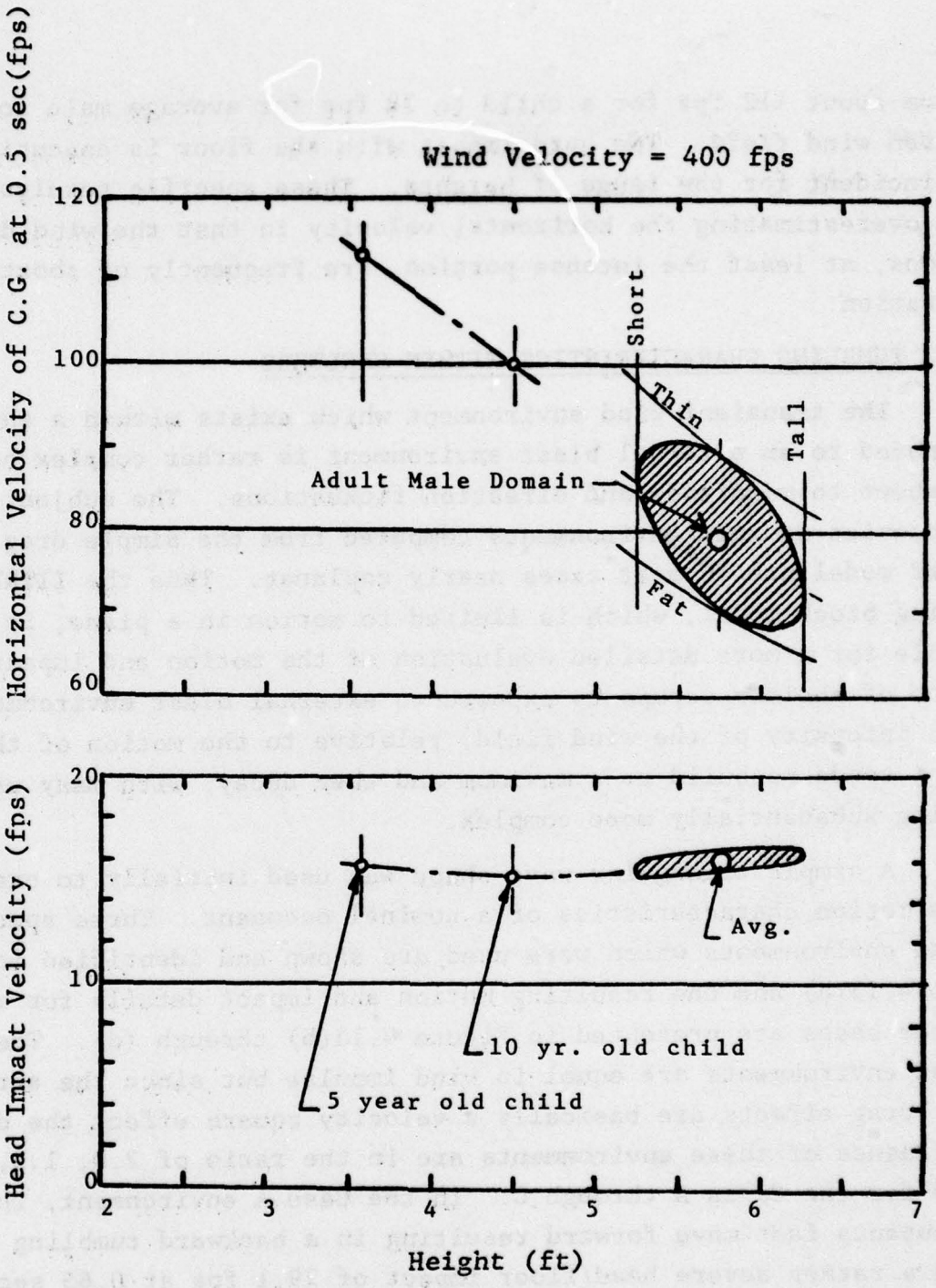

Figure 4.12 Relative Response of General Population

from about 112 fps for a child to 78 fps for average male for the given wind field. The head impact with the floor is essentially coincident for the range of heights. These specific results may be overestimating the horizontal velocity in that the wind durations, at least the intense portion, are frequently of shorter duration.

4.2 TUMBLING CHARACTERISTICS WITHIN SHELTERS

The transient wind environment which exists within a shelter exposed to an external blast environment is rather complex both with respect to magnitude and direction fluxuations. The subject trajectories in such environments computed from the simple drag transport model are in most cases nearly coplanar. Thus the IITRI tumbling block model, which is limited to motion in a plane, is applicable for a more detailed evaluation of the motion and impact condition of shelter occupants exposed to external blast environments. The intensity of the wind field, relative to the motion of the occupant tends to build to a maximum and then decay, with many waveforms being substantially more complex.

A simple triangular wave shape was used initially to examine the motion characteristics of a nominal occupant. Three specific wind environments which were used are shown and identified in Figure 4.13(a) and the resulting motion and impact details for these three cases are presented in Figure 4.13(b) through (d). The three wind environments are equal in wind impulse but since the aerodynamic drag effects are basically a velocity square effect, the drag influence of these environments are in the ratio of 2.0, 1.5, and 1.0 for the Cases A through C. In the Case A environment, the occupants feet move forward resulting in a backward tumbling motion and a rather severe head/floor impact of 29.1 fps at 0.65 second. If a wall (as shown) had existed at a location 17 ft from the initial position a foot/wall impact of 25.3 fps would also have occurred. In Cases B and C the tumbling is in the forward direction and the occupant literally falls on his face. In Case B the resulting head/floor impact occurs at 0.86 sec and has a magnitude of 22.6 fps. Again, if a wall existed at a distance of approximately 17 ft

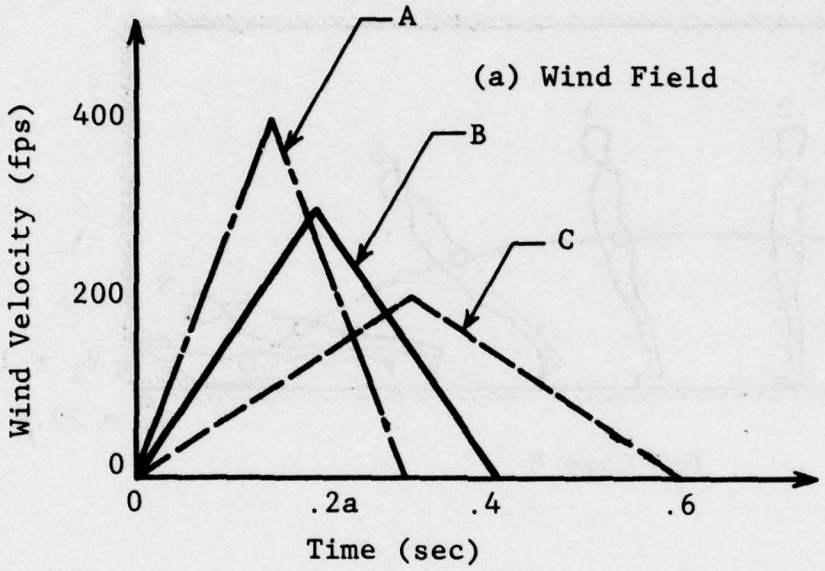

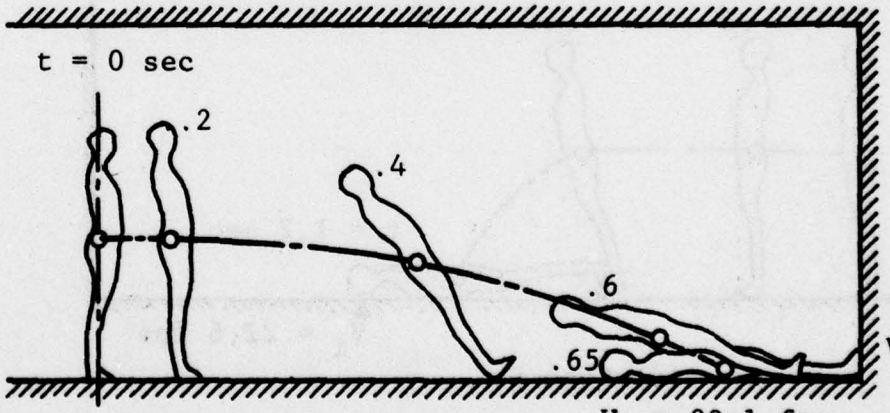

(b) Case A

Figure 4.13 Tumbling Characteristics in a Shelter

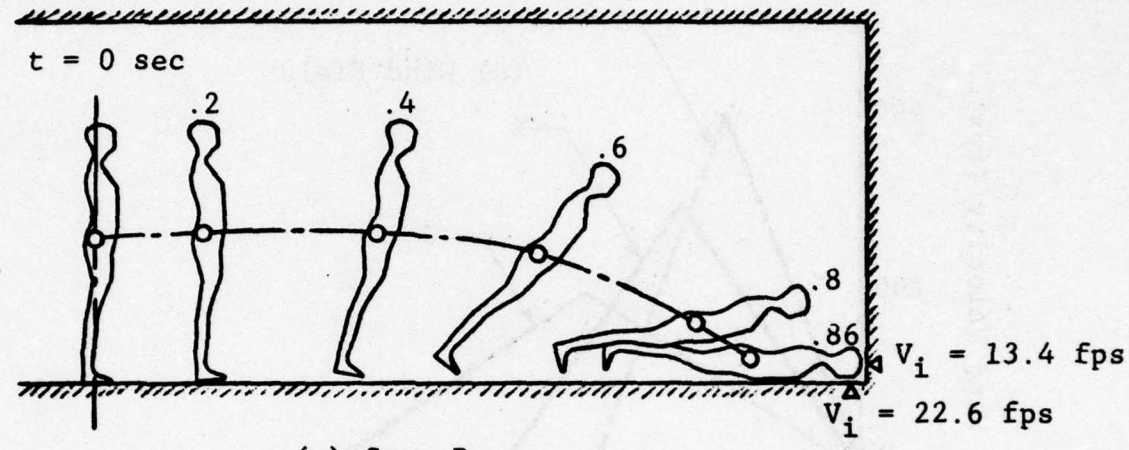

(c) Case B

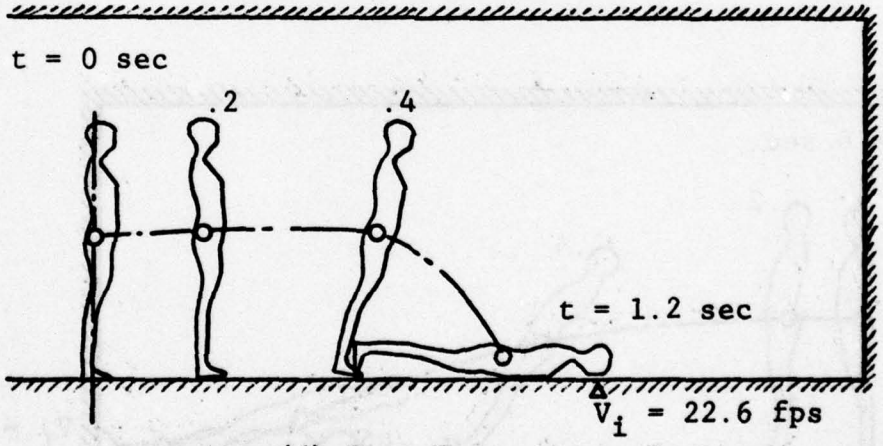

(d) Case C

Figure 4.13 Tumbling Characteristics in a Shelter (concluded)

a head/wall impact of 13.4 fps would also have occurred at essentially the same time. In Case C, the tumbling-impact process takes a somewhat longer time to occur, but the resulting head/floor impact is still rather severe (22.6 fps) impact velocity.

In addition to the above three cases in which the peak wind velocity occurred at the midpoint of the pulse duration, five other cases were evaluated to study the influence of pulse shape. Triangular pulse shapes were used, however, the relative time at which the peak wind velocity occurred was varied. The results of some of these calculations are presented in Figure 4.14 in terms of the time history of the horizontal velocity of the c.g. of the occupant. The open circles represent the time at which a head/floor impact occurs and the closed circles, of which there are but two, represents a foot/floor impact. The foot/floor impact is of no significance to this evaluation. These results indicate that wave details are of little, if any, significance at least at the lower wind velocity situations. The head/floor and head/wall (17 ft location) impact velocities for the cases examined are presented in Table 4.3. With the exception of the 400 fps wind velocity cases (cases 1 and 2) the head/floor impact velocities are identical at a value of 22.6 fps. Thus the hazard to the shelter occupant results more from the fact that he or she may fall over rather than the hazard being somewhat proportional to the intensity of the disturbance. It must be recognized that this interpretation of the above results must be corrected for the fact that the occupant can respond to the slow-fall situations and greatly improve his or her chances of survival. Nonetheless, the floor represents a potential impact surface of at least moderate impact intensity and the general level of occupant survivability within shelters should be improved by appropriately treating the floor surface, or in considering this parameter in shelter selections and evaluations.

The adequacy of the simple drag model was further examined by calculating the occupant motion using the tumbling man model using specific wind exposures resulting from the shelter calculation. A comparison of the results from the two models indicated that the

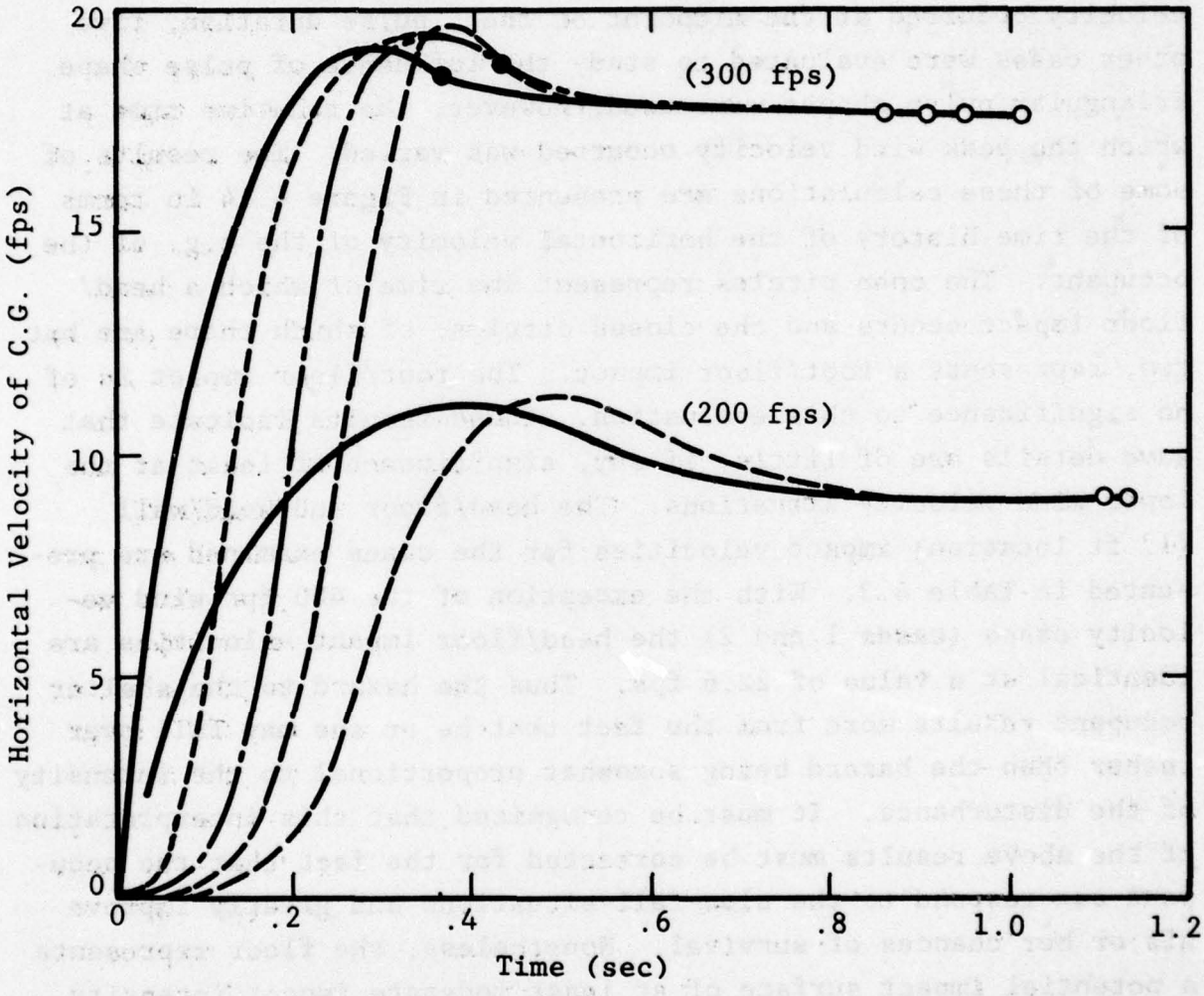

Figure 4.14 Horizontal Velocity Details

agreement was generally adequate for a situation in which the time of motion or the overall displacement was not excessive. These limits can be roughly estimated at 1 to 2 sec of time of motion and displacements in excess of approximately 20 ft. Whenever these limits were exceeded the wall impact predicted by the drag model was surplanted by a moderately intense head/floor impact as seen from the earlier results.

TABLE 4.3
TUMBLING RESPONSE TO TRIANGULAR WIND PULSE

Case	Peak Air Velocity (fps)	Time of Peak Air Velocity (sec)	Duration of Air Velocity (sec)	Head Impact Velocity (fps)	
				Floor	Wall
1	400	0	0.30	22.3	-
2	400	0.15	0.30	29.1	25.3
3	300	0	0.40	22.6	15.3
4	300	0.10	0.40	22.6	13.2
5	300	0.20	0.40	22.6	13.4
6	300	0.30	0.40	22.6	12.7
7	200	0	0.60	22.6	-
8	200	0.30	0.60	22.6	-

The results for one specific case, one in which the drag model was not applicable, will be presented here. The wind environment is shown in Figure 4.15 as the dotted line. This curve was fitted by a family of straight line segments as shown in this figure and used as input to the tumbling man model code. The wind velocity field was taken from a trajectory calculation for shelter B2 where the object was initially located 40 ft from the front wall and 10 ft off of the axis of the inlet (see Figure 4.15). The object was transported approximately 60 ft in 2.5 sec and impacted the front wall of the shelter at a velocity of approximately 13 fps. The horizontal velocity (of the c.g.) history is shown in Figure 4.16 for both the drag model case (the solid line) and the tumbling model case (the dotted line). Both calculations resulted in the same general form and magnitude. However, the drag model, which neglects gravity and rotational effects, permits the motion of the object to continue until it strikes one of the walls of the shelter, whereas

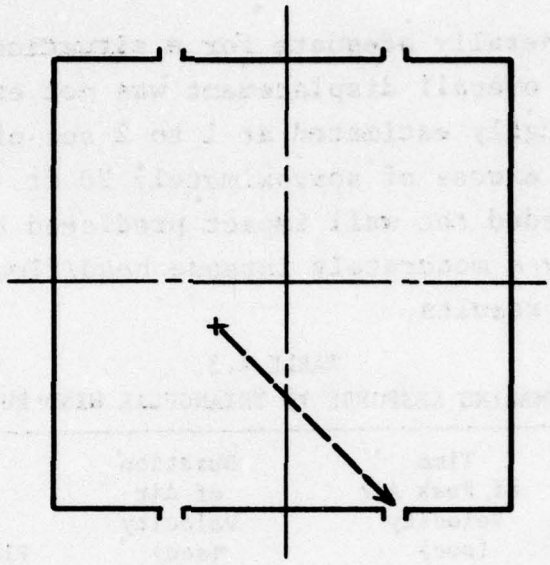

Shelter B2

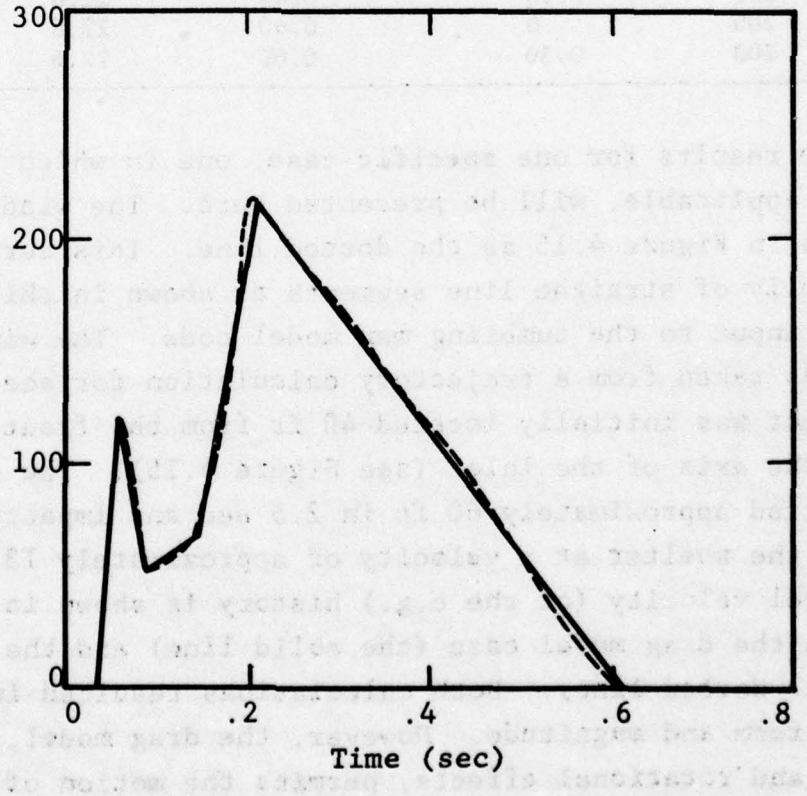

Figure 4.15 Shelter Wind Environment and Occupant Trajectory

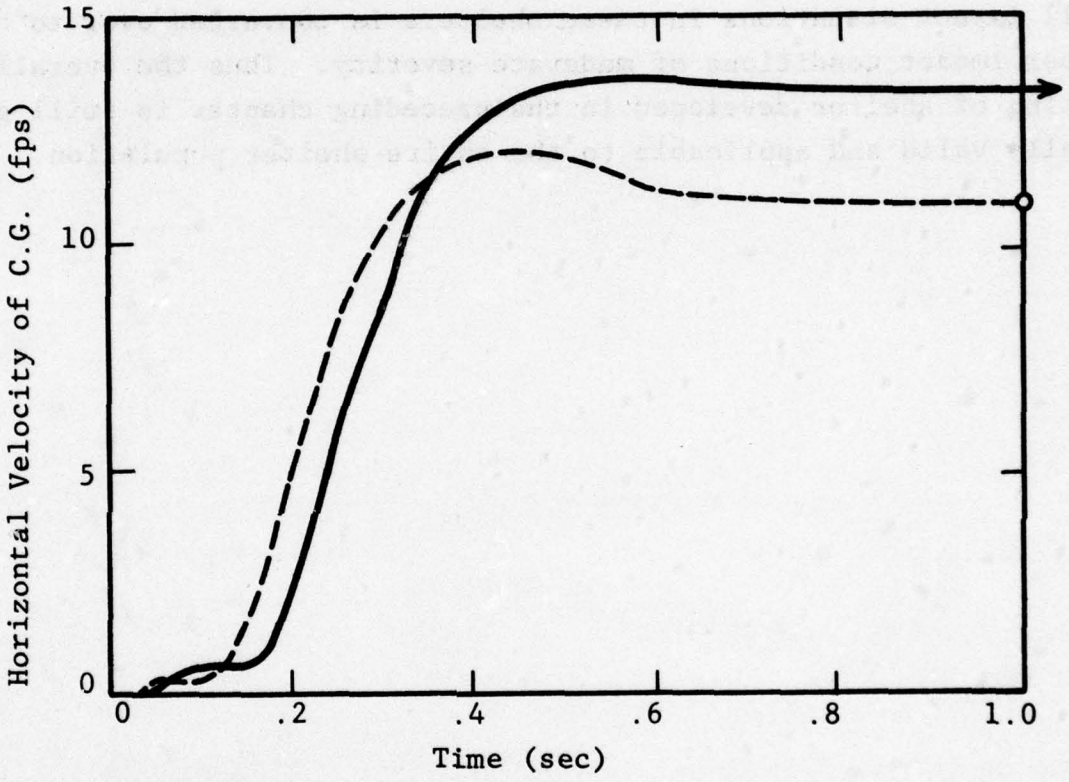

Figure 4.16 Comparison of Blast Induced Motion

the tumbling man model demonstrates that a head/floor impact will occur at 1.0 sec after the blast wave enters the shelter. The block has been translated approximately 9 ft at the time of impact and the head/floor impact velocity was 22.6 fps. Clearly the usefulness of the simple drag model is limited for large shelters, however, the results of this evaluation suggest that a group of wall impact situations in these shelters is converted over to head/floor impact conditions of moderate severity. Thus the overall rating of shelter developed in the preceding chapter is still generally valid and applicable to the entire shelter population.

CHAPTER 5
PEOPLE SURVIVABILITY IN UPPER STORY SPACES

5.1 INTRODUCTION

Over the past several years a fair amount of attention has been given to predicting the resisting capacity of building walls when subjected to the blast effects of high yield nuclear weapons. Both analytic and experimental studies have been performed and it has been found that certain types of walls, such as arching masonry walls for example, can be very effective in resisting uniformly distributed dynamic loads directed normal to their planes. Some fairly high incipient collapse overpressures have been predicted analytically (Ref. 19) and verified experimentally (Ref. 20). In one study dealing with people survivability in 50 existing buildings, wall collapse overpressures ranged from 1 psi to 38 psi (Ref. 11). For overpressures at the high end of the scale it is fair to ask if buildings containing such strong walls will survive or will fail (by overturning, instability or both) before the collapse overpressure for their walls is reached. This question is important because upper stories contain shelter space. For example, Table 5.1 was developed by DCPA (Ref. 21, 22) for the purpose of identifying and ranking best available shelter space. Four of the categories included in this table, i.e., items 5, 6, 8 and 9 deal with upper story spaces.

Analysis of building failure which takes into account possible overturning, instability of the frame and shear walls, and failure of the foundation when the building is subjected to the blast effects of large nuclear weapons, has not been considered to any significant extent. There exists one credible data point. In a limited study described in Ref. 23, an eight-story existing steel framed building was analyzed to determine the overpressure required to produce overturning or collapse. This building, the North Carolina National Bank, is described as follows.

The overall height is about 110 ft. Plan dimensions are 50 ft by 115 ft. The building has a structural steel frame with riveted and bolted column and beam connections. The ribbed floor system has a 4 inch thick concrete slab and 4 or 6 inch thick clay tile fillers.

TABLE 5.1
RELATIVE BLAST PROTECTION IN CONVENTIONAL STRUCTURES

Structure Category	Code	MLOP (psi)	MIOP (psi)
1. Subway stations, tunnels, mines and caves	A	>35	>10
2. Basements and subbasements of massive (monumental) masonry buildings	B	10	7
3. Basements and subbasements of large, fully engineered structures having any floor system over the basement other than wood, concrete flat plate, or band beam support	C	10	7
4. Basements of wood frame and brick veneer structures including residences	D	10	4
5. First three stories of buildings with "strong" walls, less than 10 aboveground stories, and less than 50 percent apertures	E	8	2
6. Fourth through ninth stories of buildings with "strong" walls, less than 10 aboveground stories, and less than 50 percent apertures	F	8	2
7. Basements and subbasements of buildings with a flat plate or band beam supported floor system over the basement	G	5	2
8. First three stories of buildings with "strong" walls, less than 10 aboveground stories, and greater than 50 percent apertures; or first three stories of buildings with "weak" walls and less than 10 aboveground stories.	H	5	2
9. All aboveground stories of buildings having 10 or more stories. Fourth through ninth stories of buildings having "weak" walls.	I	5	2

Exterior walls are of masonry (brick, terra cotta), are set within the frame and have a masonry facing. Predicted collapse overpressures for these walls ranged from 5.4 psi to 16.4 psi. The dynamic analysis performed was well within the state of the art. Both linear and nonlinear behavior of the building frame was considered as was the influence of infilled walls on the response of the frame. However, the influence of foundation response on the building frame does not appear to have been considered. Based on analyses performed it was concluded that the building would most likely collapse in the range of 4 to 5 psi. This result is sufficiently low to warrant a reevaluation of previous results. The previously mentioned study (Ref. 11) which dealt with people survivability in 50 existing buildings did not consider building collapse as a casualty mechanism. At the time when that study was performed a readily usable procedure capable of predicting building collapse did not exist. Such a procedure (method) does not exist now either. However, since the collapse overpressure for the North Carolina National Bank is low, the results for the 50-building sample (Ref. 24) should be reexamined because 16 of the buildings are higher than eight stories. Although the development of a procedure for estimating building collapse is beyond the scope of this study, a fairly crude evaluation of the 50 buildings was made herein and is described in the following paragraphs.

5.2 APPROXIMATE ANALYSIS OF BUILDING FAILURE

One approach for estimating the collapse strength of buildings is to devise a procedure based on the most reasonable collapse mode and then adjust it as necessary based on available experimental or analytic results. With one data point to adjust to, as is our case, the procedure lacks the desirable credibility. However, since a detailed analysis was well beyond the scope of this study, the following approach was taken.

If the given building is treated as a cantilever of uniform cross section, fixed at the base and subjected to uniform pressure along its height, then our model of the building is as shown in Figure 5.1.

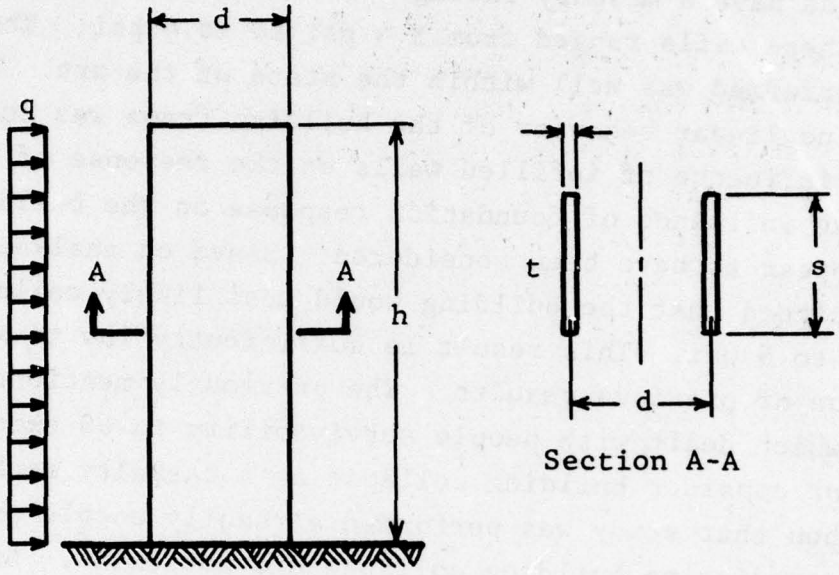

Figure 5.1 Building Idealization

The cross-sectional area of the building (section A-A) is idealized by summing the cross-sectional areas of all columns at their base and assuming that the material is concentrated in two parallel strips as shown in Figure 5.1. Basing the resistance on the plastic moment capacity of the cross section, the critical static overpressure can be expressed as

$$M_{max} = q \frac{h^2}{2} , \qquad q = ws$$

where w is the unit pressure. Then the critical unit pressure w_{ch}, is

$$w_{ch}s = 2 \frac{M_c}{h^2} = 2 \frac{(tsd\sigma_o)}{h^2}$$

where M_c is the corresponding critical bending moment at the base and σ_o is the yield stress of the material. This last equation can be expressed as

$$w_{ch} = 2 \sigma_o \left(\frac{t}{h}\right)\left(\frac{d}{h}\right) \qquad (5.1)$$

At this point we compare results using equation (5.1) with the detailed results for the North Carolina National Bank produced in Ref. 23. For this building the total cross-sectional area of columns at the ground level was estimated at 547.2 square inches which results in t = 0.2 inch. The remainder of required data for this building are:

$$h = 110 \text{ ft}, \; d = 47.33 \text{ ft}, \; \sigma_o = 36{,}000 \text{ psi (assumed)}$$

Substituting in equation (5.1), we obtain

$$w_{ch} = 2\,(36{,}000)\left(\frac{0.2}{110 \times 12}\right)\left(\frac{47.33}{110.0}\right) = 4.69 \text{ psi}$$

Assuming a step pulse blast load of long duration in comparison to the fundamental period of the building and further assuming that the building resistance can be represented by means of a bilinear resistance function having a ductility ratio of 50 at collapse, then the corresponding dynamic pressure, w_{dh} is

$$w_{dh} = (0.99)\, w_{ch} = 4.64 \text{ psi}$$

Ref. 23 predicted a collapse pressure for this building in the range from 4 to 5 psi. Being reasonably satisfied that equation (5.1) has some basis in fact, it was used as a guide to estimate the collapse strength of the 50 buildings analyzed in Ref. 11. Results are given in Table 5.2 and constitute an update of those included in Ref. 11.

Each building was analyzed using equation (5.1) to estimate its collapse overpressure, w_{dh}. This was then compared to its wall collapse overpressure, w_w. In those cases where w_{dh} was less then w_w, w_{dh} became the governing overpressure and the people survivability estimate was revised. Revision was based on the assumption that at overpressure w_{dh} and higher, no survivors are expected. On this basis, people survivability estimates for the following buildings, included in Table 5.2, were revised: Numbers 13, 35, 51, 76, 152, 160, 223.

The effort described in this chapter should be considered as very preliminary. A study should be initiated to produce a reliable, building collapse evaluation method and each of the 50 buildings listed in Table 5.2 should be analyzed in detail.

TABLE 5.2
PEOPLE SURVIVABILITY IN UPPER STORIES OF BUILDINGS (Ref. 11)

Building	50%		10%		90%		Number of Stories	Frame Type	Wall Type*
	Standing	Prone	Standing	Prone	Standing	Prone			
6 Rindge Technical School	8.0	13.5	11.7	16.7	5.1	10.2	5	Steel	LBW
7 St. Francis School	8.8	13.7	11.9	18.2	5.0	13.1	2	RC	NLBW-A
13 Leavitt's Department Store	6.0	12.8	10.6	12.8	4.3	4.6	5	Steel	NLBW-A
20 Fort Dix Barracks	4.4	6.1	8.6	12.4	3.2	4.3	3	RC	NLBW-A
29 Co-op City Building 23	4.6	5.0	8.0	9.6	3.4	3.2	33	RC	NLBW-A
33 P.S. 116	7.2	11.6	11.0	15.4	5.0	8.5	4		LBW
35 Nassau County Executive Bldg.	7.5	7.5	7.5	7.5	5.5	7.5	5	RC/Steel	NLBW-A
36 Office Building	4.3	8.5	6.9	13.5	2.5	5.0	41	Steel	NLBW-NA
37 Chase Manhattan Bank	3.7	9.3	5.7	11.6	2.4	5.9	61	Steel	NLBW-NA
44 School for the Deaf	6.7	9.6	9.5	12.0	4.8	9.0	6	Steel	NLBW-A
51 RCA Building	2.0	2.0	2.0	2.0	2.0	2.0	69	Steel	NLBW-A
55 J. C. Penney Building	3.8	8.8	6.7	10.8	2.5	5.8	46	Steel	NLBW-NA
56 Gracie Green Apartment Bldg.	3.6	6.3	6.1	10.5	2.4	3.7	21	RC	NLBW-A
62 Atlantis Building	6.4	9.4	9.5	14.1	4.3	7.1	13	RC	NLBW-A
63 Amityville Jr. High	5.8	9.2	8.3	15.0	4.2	7.6	3	Steel	NLBW-NA
66 West Dormitory Building	5.9	6.3	8.0	8.5	5.1	5.2	3		LBW
76 Garfinkel's Department Store	4.8	4.8	4.8	4.8	4.8	4.8	9	Steel	NLBW-A
81 Federal Office Building	7.0	14.0	11.2	15.6	5.1	10.6	10	RC	NLBW-NA
84 Saratoga Municipal Building	5.9	9.0	8.6	12.4	4.5	6.6	8	RC	NLBW-A
89 Water Department Building	9.1	10.5	9.8	12.0	6.2	10.0	2	Steel/RC	NLBW-A

TABLE 5.2 (contd)
PEOPLE SURVIVABILITY IN UPPER STORIES OF BUILDINGS (Ref. 11)

Building	50%		10%		90%		Number of Stories	Frame Type	Wall Type*
	Standing	Prone	Standing	Prone	Standing	Prone			
93 Sears Roebuck Store	5.8	13.4	9.4	15.5	4.5	5.6	3	RC/Steel	NLBW-A
114 Blue Mountain Academy	5.6	7.6	9.2	14.1	4.0	3.5	1	Steel	NLBW-NA
119 Royal Globe Insurance Bldg.	1.6	1.6	3.9	4.3	1.1	1.1	2	Steel	LBW
129 Harbour House South Bldg.	3.9	7.1	8.7	12.6	2.2	4.1	14	RC	NLBW-NA
130 Physics-Astronomy Building	6.2	9.8	9.4	16.6	5.2	6.4	3	RC	NLBW-A
132 Jackson Hill Church	5.3	6.2	7.3	9.9	4.2	4.4	4	Steel	LBW
136 First Federal Savings and Loan	6.9	9.5	9.5	15.0	5.2	7.2	4	RC	NLBW-A
138 U.S. Post Office Building	2.5	2.5	2.9	2.9	2.1	2.1	1		LBW
139 Davidson College Church	8.6	16.7	16.4	19.5	4.7	5.1	2	Steel	NLBW-A
140 Sunrise Towers	6.9	11.0	9.9	16.6	4.5	7.5	11	RC/Steel	NLBW-A
143 Extendicare Knoxville	6.0	9.0	9.0	14.5	4.4	6.9	1	RC	LBW
146 Marine Drive Apartments	6.1	7.8	7.6	10.0	4.2	6.6	20	RC	NLBW-A
147 Racquet Club Building	7.7	15.1	20.0	20.0	0.5	0.5	6	Steel	LBW
152 Standard Club Building	3.0	3.0	3.0	3.0	3.0	3.0	11	Steel	NLBW-A
160 Commonwealth Edison Building	8.3	8.3	8.3	8.3	6.3	8.3	3	Steel	NLBW-A
161 American Red Cross Building	6.0	8.9	8.6	11.5	5.2	6.7	1	Steel	NLBW-A
168 National Brewing Co. Bldg.	4.9	5.9	8.7	12.6	4.2	4.3	3	Steel	NLBW-A
171 Maple Manor Building	7.2	8.8	9.0	11.5	4.5	7.0	1	RC	LBW
177 Willmar High School	1.6	1.6	5.5	8.1	1.1	1.1	3	RC	LBW
179 City-County Building	4.8	6.6	8.4	13.2	4.2	4.3	8	Steel	NLBW-A

TABLE 5.2 (concl)
PEOPLE SURVIVABILITY IN UPPER STORIES OF BUILDINGS (Ref. 11)

	Building	50%		10%		90%		Number of Stories	Frame Type	Wall Type*
		Standing	Prone	Standing	Prone	Standing	Prone			
195	May Advertising Building	5.7	8.6	8.7	11.9	4.3	4.9	1	RC	LBW
198	Kallison Towers Building	7.2	15.0	10.2	16.7	4.4	7.1	10	RC	RC
202	Instrumentation Office Bldg.	6.8	7.0	20.0	20.0	6.2	6.2	1	Steel	LBW
204	Brady Moving and Storage	11.5	12.4	15.7	15.9	7.7	11.2	6	RC	NLBW-A
207	Hanover Public School	7.6	11.3	9.7	14.7	5.0	8.3	2	RC	LBW
212	Edison Brothers Stores Bldg.	5.8	7.6	8.7	12.6	4.4	5.4	13	RC	NLBW-A
223	Biltmore Hotel	10.0	12.4	12.4	12.4	5.7	12.4	14	Steel	NLBW-A
228	Starkman Building	4.3	10.2	8.9	15.4	2.6	6.4	5	Steel	NLBW-NA
239	Stanford Hospital-West	8.4	8.6	8.9	9.0	7.3	8.1	3	RC	NLBW-A
250N	Arthur Hall Dormitory	4.4	7.9	8.8	15.2	2.5	4.6	4	RC	LBW

* NLBW-A Nonloadbearing wall - arching
NLBW-NA Nonloadbearing wall - nonarching
LBW Loadbearing wall

CHAPTER 6

RECOMMENDATIONS

Based on the work described in the previous chapters of this study the following recommendations as to future directions of research in the area of people survivability in a nuclear weapon environment are provided.

6.1 THE INFLUENCE OF CHANGES IN BUILDINGS ON SHELTER

Over the past three decades, i.e., since about the time of the NFSS, the character of urban areas in terms of buildings and their makeup has changed. Numerous buildings have been removed. Those that took their place are for the most part of different character in terms of their physical makeup. Since energy conservation appears to be the trend of the future, the makeup of buildings will be affected.

A study should be initiated to monitor construction to determine how changes in the makeup of buildings and associated construction practices affect the existing inventory of shelter in terms of quantity and quality. This would be a continuous study and would include at least the following tasks.

1. On a selective basis monitor building construction and obtain data on new buildings in terms of use classes, type of structural system, quantity of floor space, quantity of basement floor space, occupancy, location, etc.
2. On a periodic basis obtain building plans of new construction from selected geographic areas and perform detailed people survivability analyses.
3. Monitor changes in applied building technology to determine the influence of such changes on the sheltering potential.
4. Monitor changes in selected local building codes to determine how such changes affect the sheltering potential.

6.2 SHELTERING CAPABILITIES OF EXISTING BASEMENTS

This study examined the sheltering capabilities of one category of existing basements, i.e., those in steel framed buildings with two-way reinforced concrete floor systems. The previous effort (Ref. 1) considered basements in framed, reinforced concrete buildings with flat plate and flat slab floor systems. Results, i.e., estimates of people survivability, from both studies are consistent, however when compared to the same categories of results reported in Ref. 11, they appear to be distinctly lower. Results reported here are based on building designs generated in the course of this effort. Those of Ref. 11 are based on building data collected in field surveys. The analysis procedure and the underlying assumptions were essentially the same in both cases. It is recommended that this apparent difference be resolved since it can lead to erroneous estimates as to the capabilities of existing shelters.

6.3 EXPERIMENTAL DATA ON THE RESPONSE OF BUILDING COMPONENTS

Experimental data on the full-range (from initial yielding to ultimate collapse) behavior of structural components when subjected to static or dynamic loads is currently very limited. That which exists, has been produced with DCPA support. Such information is necessary for the evaluation of the sheltering potential of existing buildings. It also becomes useful when the task is to upgrade existing shelters. A study should be initiated which on a continuous basis identifies building components which in "significant" quantities enter the inventory of existing buildings. Representative samples of such components would then be obtained from the industry or constructed and then tested under controlled static and dynamic conditions representative of blast effects produced by nuclear weapons. At the present time, we need experimental data on at least the following structural components and systems.

Precast, prestressed beams (e.g., Flexicore, Spancrete)
Open web joists
Concrete slab - concrete beam floor systems
Concrete joist - concrete beam floor systems

Concrete joist - steel beam floor systems
Prestressed steel beams
Laminated timber beams
Common timber beams and timber floor systems

6.4 CASUALTY ESTIMATION

Studies dealing with casualty estimation should be continued with the object of broadening our understanding of this complex field. The following topics should be considered in subsequent studies.

Tumbling Characteristics in Shelters - This problem was examined in Chapter 4 of this report. One of the conclusions reached was that the head impact velocity of individuals at first impact was essentially constant and therefore mostly independent of the wave-form and peak magnitude of the wind field. This problem should be further examined by considering other body orientations (forward facing, rearward facing, sitting, prone) and taking into account a more complete range of wind fields in terms of rise time, peak magnitude and duration.

The bounce or the second impact problem should be considered. Depending on the angle of impact, the second impact may in some cases be more severe than the first and therefore becomes extremely important in casualty estimation. A simple approach has been formulated in the course of this study but not applied.

Casualties due to Glass Fragments - This casualty mechanism is likely the major source of injuries for people located in upper stories. It has received very little attention and should be considered.

Examination of Related Sources for Casualty Data - A continuous effort should be maintained to monitor ongoing work in related areas where people safety and casualty estimation is important with the object of updating casualty estimation procedures and data used by DCPA.

6.5 PEOPLE SURVIVABILITY IN UPPER STORIES

A building analysis reported in Ref. 23 has demonstrated that tall buildings with strong walls may collapse at fairly low overpressures when compared to the failure overpressures of their walls. The analysis described represents the first serious attempt to predict the overturning/collapse of tall buildings. Because the overpressure predicted for the single building analyzed in Ref. 23 is low and because upper stories contain shelter space, the effort started in Ref. 23 should be continued to produce a method for predicting building overturning/collapse. This should then be applied to the analysis of the 50 buildings analyzed in Ref. 11.

REFERENCES

1. Longinow, A., et al, Debris Motion and Injury Relationships in All Hazard Environments, for Defense Civil Preparedness Agency, Contract DCPA01-74-C-0251, DCPA Work Unit 1614 E, IIT Research Institute, July 1976

2. ACI Standard 318-63 - Building Code Requirements for Reinforced Concrete, (ACI 318-63), American Concrete Institute, P.O. Box 4754, Redford Station, Detroit, Michigan 48219

3. City of Chicago Building Code and Contractors Register, 1975

4. Manual of Steel Construction, American Institute of Steel Construction, Inc. 101 Park Avenue, New York, N.Y. 10017 (Seventh Edition)

5. Newmark, N. M. and Haltiwanger, J. D., Air Force Design Manual; Principles and Practices for Design of Hardened Structures, Technical Documentary Report AFSWC-TDR-62-138, Air Force Special Weapons Center, Kirtland Air Force Base, New Mexico, December 1962

6. Biggs, J. M., Introduction to Structural Dynamics, McGraw-Hill Book Company, 1964

7. Wiehle, C. K. and Bockholt, J. L., Dynamic Analysis of Reinforced Concrete Floor Systems, Contract DAHC20-71-C-0292, DCPA Work Unit 1154 I, for Defense Civil Preparedness Agency, Stanford Research Institute, May 1973

8. Jensen, G. F., Summary of Existing Structures Evaluation Part III: Structural Steel Connections, Contract No. OCD-DAHC20-67-C-0136, OCD Work Unit 1126C for Office of Civil Defense, Stanford Research Institute, December 1969

9. Huff, W. J., Collapse Strength of a Two-Way Reinforced Concrete Slab Contained Within a Steel Frame Structure, Technical Report N-75-2, U.S. Army Engineer Waterways Experiment Station, CE, Vicksburg, Mississippi, June 1975

10. Tolman, D. F., et al, Estimated Characteristics of NFSS Inventory - Final Building Classification Report, Contract DAHC20-72-C-0277 for DCPA, Research Triangle Institute, 27 November 1972

11. Longinow, A., "Survivability in a Direct Effects Environment (Analysis of 50 NFSS Buildings), for Defense Civil Preparedness Agency, Contract DAHC20-73-C-0227, IIT Research Institute, July 1974

12. Air Blast Attenuation, Construction Engineering Research Laboratory, Technical Manuscript S-1 R, February 1971

13. White, C. S., et al, The Biodynamics of Airblast, for Defense Nuclear Agency, Washington, D.C. 20305, Contract DASA 01-70-C-0075, Lovelace Foundation, DNA 2738T, July 1, 1971

14. Longinow, A., et al, People Survivability in a Direct Effects Environment and Related Topics, for Defense Civil Preparedness Agency, Contract DAHC20-68-C-0126, DCPA Work Unit 1614D, IIT Research Institute, May 1973

15. Coulter, G. A., Flow in Model Rooms Caused by Air Shock Waves, BRL Report BRLMR 2044, July 1970

16. Coulter, G. A., Blast Loading of Objects in Basement Shelter Models, BRL Report BRLMR 2348, January 1974

17. Coulter, G. A., Blast Loading on Model Dummies in Two-Room Shelters, BRL Report BRLMR 2674, September 1976

18. Damon, A., The Human Body in Equipment Design, Harvard University Press, 1971

19. Wiehle, C. K. and Bockholt, J. L., "Existing Structures Evaluation, Part V: Applications", for Office of Civil Defense, Contract DAHC20-67-C-0136, Stanford Research Institute, July 1971

20. Gabrielsen, B. and Wilton, C., "Shock Tunnel Tests of Arched Wall Panels", for Defense Civil Preparedness Agency, Contract DAHC20-71-C-0223, URS Research Company, URS7030-19, December 1974

21. "DCPA Attack Environment Manual", Chapter 2, Research Directorate, Defense Civil Preparedness Agency, June 1972

22. Private communication from Mr. G. N. Sisson, Research Directorate Defense Civil Preparedness Agency, January 1977

23. Wiehle, C. K., "Dynamic Analysis of a Building and Building Elements", for Defense Civil Preparedness Agency, Contract DAHC20-71-C-0292, Stanford Research Institute, April 1974

APPENDIX
SLAB DESIGNS AND SLAB FAILURE DATA

This appendix contains design data and failure data for two-way reinforced concrete slabs and steel supporting beams (see Figure A-1) presented in Chapter 2 of this report. Design parameters considered are given as follows:

Slab span: 12, 16, 20, 24, and 28 - ft
Compressive strength of concrete: 3000 and 4000 psi
Yield strength of reinforcing steel: 40,000 and 60,000 psi
Design live load: 50, 80, 100, 125, 200 and 250 psf
A36 steel is assumed for the steel framing members

Table A-1 contains corresponding slab thicknesses, required reinforcing steel, beam and column sizes and other supporting information. It should be noted that minimum thickness governs in all cases and therefore there is no difference between 3000 psi and 4000 psi concrete.

Results of the failure analyses are presented in Tables A-2, A-3 and A-4. Table A-2 contains failure overpressures for the two-way reinforced concrete slabs. Labels identifying various assumed failure modes are described as:

P_i - Incipient collapse overpressure

P_f - Ultimate collapse overpressure, no membrane resistance

P_{ft} - Ultimate collapse overpressure, with membrane resistance

P_{si} - Overpressure producing incipient shear failure

P_{su} - Overpressure producing ultimate shear failure

Failure overpressures for steel beams are given in Table A-3 and those for connections in A-4. In Table A-3, PI refers to incipient failure overpressure and PU refers to ultimate failure overpressure. Entries in Table A-4 are ultimate failure overpressure values.

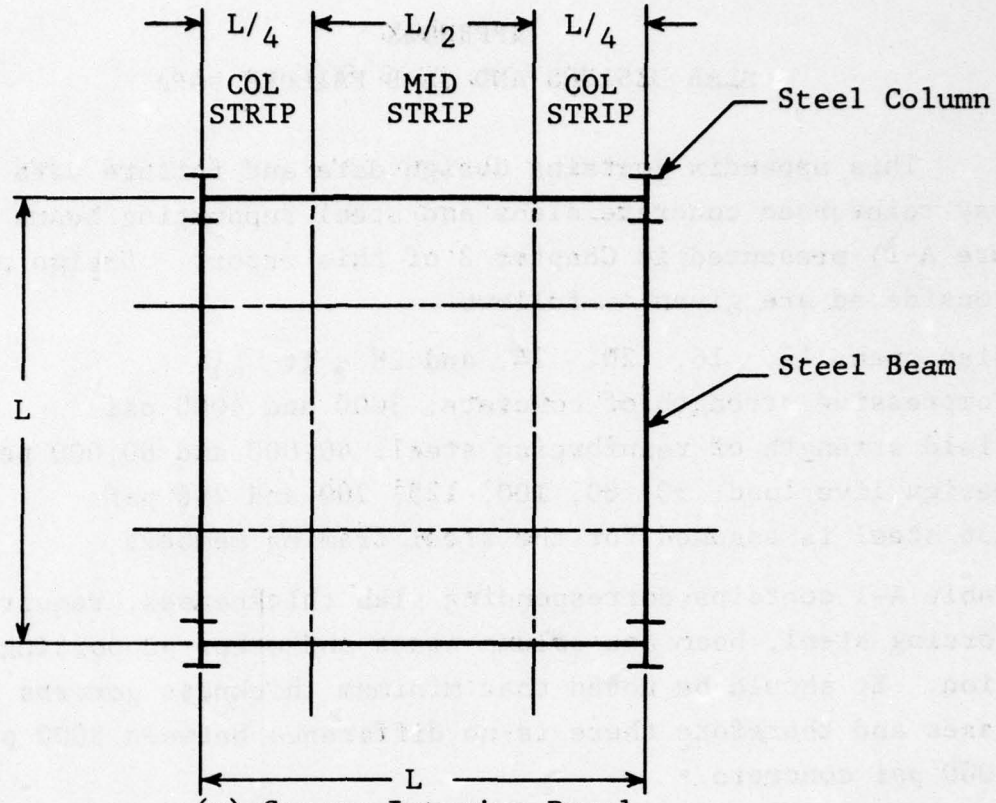

(a) Square Interior Panel

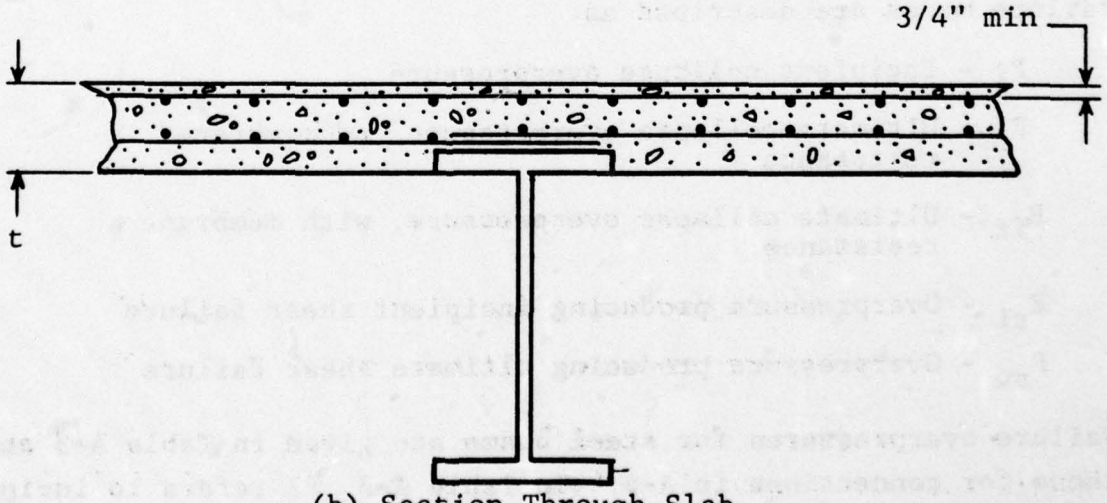

(b) Section Through Slab

Figure A-1 Floor System Characteristics

TABLE A-1

DESIGN DATA ON TWO-WAY REINFORCED CONCRETE SLAB, STEEL BEAM AND COLUMN

Span (ft)	12											
Design	W S D											
f'_c (ksi)	3											
F_y (ksi)	40						60					
Dead load (psf)	60	60	60	60	60	60	60	60	60	60	60	60
Live load (psf)	50	80	100	125	200	250	50	80	100	125	200	250
Reduced Live Load (psf)	48	76	95	119	190	238	48	76	95	119	190	238
DL + Red LL (psf)	108	138	155	179	250	298	108	138	155	179	250	298
Mid Strip + M (k-ft)*	0.39	0.49	0.56	0.64	0.90	1.07	0.39	0.49	0.56	0.64	0.90	1.07
Mid Strip - M (k-ft)	0.51	0.65	0.74	0.85	1.19	1.42	0.51	0.65	0.74	0.85	1.19	1.42
Col Strip + M (k-ft)	0.26	0.33	0.37	0.43	0.60	0.72	0.26	0.33	0.37	0.43	0.60	0.72
Col Strip - M (k-ft)	0.34	0.43	0.49	0.57	0.79	0.94	0.34	0.43	0.49	0.57	0.79	0.94
Slab t (in.)	4	4	4	4	4	4	4	4	4	4	4	4
d (in.)	2.75	2.75	2.75	2.75	2.75	2.75	2.75	2.75	2.75	2.75	2.75	2.75
Mid Strip + A_s $(in.)^2$*	0.098	0.12	0.14	0.16	0.23	0.27	0.086	0.10	0.12	0.13	0.19	0.22
Mid Strip - A_s $(in.)^2$	0.13	0.16	0.19	0.21	0.30	0.36	0.11	0.13	0.15	0.18	0.25	0.29
Col Strip + A_s $(in.)^2$	0.096	0.096	0.096	0.11	0.15	0.18	0.086	0.086	0.086	0.086	0.12	0.15
Col Strip - A_s $(in.)^2$	0.096	0.11	0.12	0.14	0.20	0.24	0.086	0.086	0.10	0.12	0.16	0.20
Steel Beam Size	W10x11.5	W10x11.5	W10x15	W10x15	W12x16.5	W12x22	W10x11.5	W10x11.5	W10x15	W10x15	W12x16.5	W12x22
Steel Column Size	W8x24	W8x28	W8x31	W8x35	W8x48	W8x58	W8x24	W8x28	W8x31	W8x35	W8x48	W8x58

*Moments and Steel Areas are per foot of Slab

TABLE A-1 (continued)

Span (ft)	16											
Design	W S D											
f'_c (ksi)	3											
F_y (ksi)	40						60					
Dead load (psf)	80	80	80	80	80	80	80	80	80	80	80	80
Live load (psf)	50	80	100	125	200	250	50	80	100	125	200	250
Reduced live load (psf)	45	72	90	112	180	224	45	72	90	112	180	224
DL + Red LL (psf)	125	152	170	192	260	304	125	152	170	192	260	304
Mid Strip + M (k-ft)*	0.80	0.97	1.09	1.23	1.66	1.95	0.80	0.97	1.09	1.23	1.66	1.95
Mid Strip - M (k-ft)	1.06	1.28	1.44	1.62	2.20	2.57	1.06	1.28	1.44	1.62	2.20	2.57
Col Strip + M (k-ft)	0.53	0.65	0.73	0.82	1.11	1.30	0.53	0.65	0.73	0.82	1.11	1.30
Col Strip - M (k-ft)	0.70	0.86	0.96	1.08	1.46	1.71	0.70	0.86	0.96	1.08	1.46	1.71
Slab t (in.)	5.5	5.5	5.5	5.5	5.5	5.5	5.5	5.5	5.5	5.5	5.5	5.5
d (in.)	4.25	4.25	4.25	4.25	4.25	4.25	4.25	4.25	4.25	4.25	4.25	4.25
Mid Strip + A_s $(in.)^2$*	0.13	0.16	0.18	0.20	0.27	0.32	0.12	0.13	0.15	0.16	0.22	0.26
Mid Strip - A_s $(in.)^2$	0.17	0.21	0.24	0.26	0.36	0.42	0.14	0.17	0.19	0.22	0.29	0.34
Col Strip + A_s $(in.)^2$	0.13	0.13	0.13	0.13	0.18	0.21	0.12	0.12	0.12	0.12	0.15	0.17
Col Strip - A_s $(in.)^2$	0.13	0.14	0.16	0.18	0.24	0.28	0.12	0.12	0.13	0.14	0.20	0.23
Steel Beam Size	W10x25	W12x27	W14x26	W14x26	W16x31	W18x35	W10x25	W12x27	W14x26	W14x26	W16x31	W18x35
Steel Column Size	W10x49	W10x54	W10x60	W10x66	W10x89	W10x100	W10x49	W10x54	W10x60	W10x66	W10x89	W10x100

*Moments and Steel Areas are per foot of Slab

TABLE A-1 (continued)

Span (ft)	20											
Design	W S D											
f'_c (ksi)	3											
F_y (ksi)	40						60					
Dead load (psf)	98	98	98	98	98	98	98	98	98	98	98	98
Live load (psf)	50	80	100	125	200	250	50	80	100	125	200	250
Red Live load (psf)	43	68	85	106	170	212	43	68	85	106	170	212
DL + Red LL (psf)	141	166	183	204	268	310	141	166	183	204	268	310
Mid Strip + M (k-ft)*	1.41	1.66	1.83	2.04	2.68	3.10	1.41	1.66	1.83	2.04	2.68	3.10
Mid Strip - M (k-ft)	1.86	2.19	2.42	2.69	3.54	4.09	1.86	2.19	2.42	2.69	3.54	4.09
Col Strip + M (k-ft)	0.94	1.11	1.22	1.36	1.79	2.07	0.94	1.11	1.22	1.36	1.79	2.07
Col Strip - M (k-ft)	1.24	1.46	1.61	1.79	2.36	2.73	1.24	1.46	1.61	1.79	2.36	2.73
Slab t (in.)	7	7	7	7	7	7	7	7	7	7	7	7
d (in.)	5.75	5.75	5.75	5.75	5.75	5.75	5.75	5.75	5.75	5.75	5.75	5.75
Mid Strip + A_s $(in.)^2$*	0.17	0.20	0.22	0.25	0.32	0.37	0.15	0.16	0.18	0.20	0.26	0.31
Mid Strip - A_s $(in.)^2$	0.22	0.26	0.29	0.32	0.43	0.49	0.18	0.22	0.24	0.27	0.35	0.40
Col Strip + A_s $(in.)^2$	0.17	0.17	0.17	0.17	0.22	0.25	0.15	0.15	0.15	0.15	0.18	0.20
Col Strip - A_s $(in.)^2$	0.17	0.18	0.19	0.22	0.29	0.33	0.15	0.15	0.16	0.18	0.23	0.27
Steel Beam Size	W16x31	W18x35	W18x40	W18x40	W21x49	W21x55	W16x31	W18x35	W18x40	W18x40	W21x49	W21x55
Steel Column Size	W12x85	W12x99	W12x106	W12x120	W12x133	W12x161	W12x85	W12x99	W12x106	W12x120	W12x133	W12x161

*Moments and Steel Areas are per foot of Slab

TABLE A-1 (continued)

Span (ft)	24											
Design	W S D											
f'_c (ksi)	3											
F_y (ksi)	40						60					
Dead load (psf)	110	110	110	110	110	110	110	110	110	110	110	110
Live load (psf)	50	80	100	125	200	250	50	80	100	125	200	250
Red live load (psf)	43	68	85	106	170	213	43	68	85	106	170	213
DL + Red LL (psf)	153	178	195	216	280	323	153	178	195	216	280	323
Mid Strip + M (k-ft)*	2.20	2.56	2.81	3.11	4.03	4.65	2.20	2.56	2.81	3.11	4.03	4.65
Mid Strip - M (k-ft)	2.91	3.38	3.71	4.11	5.32	6.14	2.91	3.38	3.71	4.11	5.32	6.14
Col Strip + M (k-ft)	1.47	1.71	1.87	2.07	2.69	3.10	1.47	1.71	1.87	2.07	2.69	3.10
Col Strip - M (k-ft)	1.94	2.25	2.47	2.74	3.55	4.09	1.94	2.25	2.47	2.74	3.55	4.09
Slab t (in.)	8	8	8	8	8	8	8	8	8	8	8	8
d (in.)	6.75	6.75	6.75	6.75	6.75	6.75	6.75	6.75	6.75	6.75	6.75	6.75
Mid Strip + A_s $(in.)^2$	0.23	0.26	0.29	0.32	0.41	0.48	0.19	0.22	0.24	0.26	0.34	0.39
Mid Strip - A_s $(in.)^2$	0.30	0.35	0.38	0.42	0.55	0.63	0.24	0.28	0.31	0.35	0.45	0.52
Col Strip + A_s $(in.)^2$	0.19	0.19	0.19	0.21	0.28	0.32	0.17	0.17	0.17	0.17	0.23	0.26
Col Strip - A_s $(in.)^2$	0.20	0.23	0.25	0.28	0.37	0.42	0.17	0.19	0.21	0.23	0.30	0.34
Steel Beam Size	W21x49	W21x55	W24x61	W24x61	W24x76	W24x84	W21x49	W21x55	W24x61	W24x61	W24x76	W24x84
Steel Column Size	W14x136	W14x150	W14x158	W14x167	W14x202	W14x228	W14x136	W14x150	W14x158	W14x167	W14x202	W14x228

*Moments and Steel Areas are per foot of Slab

TABLE A-1 (concluded)

Span (ft)	28											
Design	W S D											
f'_c (ksi)	3											
F_y (ksi)	40						60					
Dead load (psf)	129	129	129	129	129	129	129	129	129	129	129	129
Live load (psf)	50	80	100	125	200	250	50	80	100	125	200	250
Red Live load (psf)	43	68	85	106	170	213	43	68	85	106	170	213
DL + Red LL (psf)	172	197	214	235	299	342	172	197	214	235	299	342
Mid Strip + M (k-ft)*	3.37	3.86	4.19	4.61	5.86	6.70	3.37	3.86	4.19	4.61	5.86	6.70
Mid Strip - M (k-ft)	4.45	5.10	5.54	6.08	7.74	8.85	4.45	5.10	5.54	6.08	7.74	8.85
Col Strip + M (k-ft)	2.25	2.57	2.79	3.07	3.91	4.47	2.25	2.57	2.79	3.07	3.91	4.47
Col Strip - M (k-ft)	2.97	3.40	3.79	4.05	5.16	5.90	2.97	3.40	3.69	4.05	5.16	5.90
Slab t (in.)	9½	9½	9½	9½	9½	9½	9½	9½	9½	9½	9½	9½
d (in.)	8.25	8.25	8.25	8.25	8.25	8.25	8.25	8.25	8.25	8.25	8.25	8.25
Mid Strip + A_s $(in.)^2$	0.28	0.32	0.35	0.39	0.49	0.56	0.23	0.27	0.29	0.32	0.40	0.46
Mid Strip - A_s $(in.)^2$	0.37	0.43	0.47	0.51	0.65	0.74	0.31	0.35	0.38	0.42	0.53	0.61
Col Strip + A_s $(in.)^2$	0.23	0.23	0.23	0.26	0.33	0.38	0.21	0.21	0.21	0.21	0.27	0.31
Col Strip - A_s $(in.)^2$	0.25	0.29	0.31	0.34	0.43	0.50	0.21	0.23	0.25	0.28	0.36	0.41
Steel Beam Size	W24x76	W24x84	W24x84	W24x94	W30x108	W30x116	W24x76	W24x84	W24x84	W24x94	W30x108	W30x116
Steel Column Size	W14x202	W14x219	W14x228	W14x246	W14x314	W14x342	W14x202	W14x219	W14x228	W14x246	W14x314	W14x342

*Moments and Steel Areas are per foot of Slab

TABLE A-2

FAILURE OVERPRESSURES FOR TWO-WAY REINFORCED CONCRETE SLABS, (psi)

Span (ft)	12											
Design	W S D											
f'_c (ksi)	3											
f_y (ksi)	40						60					
Live load (psf)	50	80	100	125	200	250	50	80	100	125	200	250
Slab t (in.)	4.0	4.0	4.0	4.0	4.0	4.0	4.0	4.0	4.0	4.0	4.0	4.0
P_e (psi)	0.87	1.06	1.23	1.43	2.13	2.58	1.25	1.39	1.61	1.85	2.65	3.19
P_f (psi)	2.05	2.41	2.73	3.13	4.45	5.27	2.79	3.06	3.49	3.96	5.49	6.50
P_{ft} (psi)	2.07	2.43	2.76	3.16	4.53	5.39	2.79	3.07	3.50	3.97	5.52	6.55
P_{se} (psi)	4.78	4.78	4.78	4.78	4.78	4.78	4.78	4.78	4.78	4.78	4.78	4.78
P_{su} (psi)	7.81	7.80	7.80	7.79	7.77	7.76	7.78	7.78	7.77	7.77	7.74	7.73

TABLE A-2 (continued)

Span (ft)	12											
Design	W S D											
f'_c (ksi)	4											
f_y (ksi)	40						60					
Live load (psf)	50	80	100	125	200	250	50	80	100	125	200	250
Slab t (in.)	4.0	4.0	4.0	4.0	4.0	4.0	4.0	4.0	4.0	4.0	4.0	4.0
P_i (psi)	0.88	1.07	1.24	1.45	2.17	2.63	1.26	1.40	1.63	1.88	2.71	3.27
P_f (psi)	2.07	2.44	2.76	3.16	4.52	5.37	2.81	3.09	3.54	4.02	5.60	6.65
P_{ft} (psi)	2.09	2.45	2.79	3.20	4.60	5.49	2.82	3.10	3.54	4.02	5.63	6.70
P_{si} (psi)	5.58	5.58	5.58	5.58	5.58	5.58	5.58	5.58	5.58	5.58	5.58	5.58
P_{su} (psi)	9.06	9.06	9.06	9.05	9.02	9.01	9.04	9.04	9.03	9.02	8.99	8.97

TABLE A-2 (continued)

Span (ft)	16											
Design	W S D											
f'_c (ksi)	3											
f_y (ksi)	40						60					
Live load (psf)	50	80	100	125	200	250	50	80	100	125	200	250
Slab t (in.)	5.5	5.5	5.5	5.5	5.5	5.5	5.5	5.5	5.5	5.5	5.5	5.5
P_i (psi)	0.94	1.14	1.31	1.46	2.13	2.55	1.41	1.56	1.74	1.92	2.69	3.18
P_f (psi)	2.32	2.70	3.04	3.32	4.60	5.40	3.24	3.52	3.88	4.23	5.73	6.65
P_{ft} (psi)	2.34	2.73	3.07	3.35	4.67	5.50	3.26	3.54	3.90	4.25	5.76	6.70
P_{si} (psi)	5.45	5.45	5.45	5.45	5.45	5.45	5.45	5.45	5.45	5.45	5.45	5.45
P_{su} (psi)	8.96	8.95	8.95	8.95	8.93	8.92	8.93	8.94	8.93	8.93	8.91	8.90

TABLE A-2 (continued)

Span (ft)	16											
Design	W S D											
f'_c (ksi)	4											
f_y (ksi)	40						60					
Live load (psf)	50	80	100	125	200	250	50	80	100	125	200	250
Slab t (in.)	5.5	5.5	5.5	5.5	5.5	5.5	5.5	5.5	5.5	5.5	5.5	5.5
P_i (psi)	0.95	1.15	1.33	1.47	2.16	2.59	1.43	1.57	1.76	1.94	2.74	3.24
P_f (psi)	2.33	2.73	3.06	3.35	4.66	5.48	3.27	3.56	3.92	4.28	5.82	6.77
P_{ft} (psi)	2.36	2.75	3.09	3.38	4.73	5.58	3.28	3.58	3.94	4.30	5.85	6.81
P_{si} (psi)	6.37	6.37	6.37	6.37	6.37	6.37	6.37	6.37	6.37	6.37	6.37	6.37
P_{su} (psi)	10.42	10.41	10.41	10.40	10.38	10.37	10.39	10.39	10.39	10.38	10.36	10.35

TABLE A-2 (continued)

Span (ft)	20											
Design	W S D											
f'_c (ksi)	3											
f_y (ksi)	40						60					
Live load (psf)	50	80	100	125	200	250	50	80	100	125	200	250
Slab t (in.)	7.0	7.0	7.0	7.0	7.0	7.0	7.0	7.0	7.0	7.0	7.0	7.0
P_i (psi)	1.00	1.17	1.30	1.49	2.12	2.49	1.46	1.62	1.77	1.99	2.67	3.16
P_f (psi)	2.55	2.89	3.14	3.51	4.71	5.42	3.45	3.76	4.07	4.50	5.83	6.76
P_{ft} (psi)	2.58	2.92	3.17	3.54	4.78	5.51	3.48	3.79	4.10	4.53	5.86	6.81
P_{si} (psi)	5.80	5.80	5.80	5.80	5.80	5.80	5.80	5.80	5.80	5.80	5.80	5.80
P_{su} (psi)	9.59	9.59	9.59	9.58	9.57	9.56	9.57	9.57	9.57	9.57	9.55	9.54

TABLE A-2 (continued)

Span (ft)	20											
Design	W S D											
f'_c (ksi)	4											
f_y (ksi)	40						60					
Live load (psf)	50	80	100	125	200	250	50	80	100	125	200	250
Slab t (in.)	7.0	7.0	7.0	7.0	7.0	7.0	7.0	7.0	7.0	7.0	7.0	7.0
P_i (psi)	1.01	1.18	1.31	1.50	2.14	2.52	1.47	1.63	1.79	2.02	2.71	3.21
P_f (psi)	2.57	2.91	3.16	3.54	4.77	5.49	3.48	3.80	4.11	4.55	5.91	6.86
P_{ft} (psi)	2.60	2.94	3.19	3.57	4.83	5.58	3.51	3.83	4.14	4.58	5.94	6.91
P_{si} (psi)	6.79	6.79	6.79	6.79	6.79	6.79	6.79	6.79	6.79	6.79	6.79	6.79
P_{su} (psi)	11.17	11.16	11.16	11.16	11.14	11.13	11.14	11.15	11.14	11.14	11.12	11.11

TABLE A-2 (continued)

Span (ft)	24											
Design	W S D											
f'_c (ksi)	3											
f_y (ksi)	40						60					
Live load (psf)	50	80	100	125	200	250	50	80	100	125	200	250
Slab t (in.)	8.0	8.0	8.0	8.0	8.0	8.0	8.0	8.0	8.0	8.0	8.0	8.0
P_i (psi)	0.95	1.14	1.28	1.49	2.13	2.53	1.36	1.59	1.77	1.97	2.75	3.21
P_f (psi)	2.54	2.92	3.19	3.59	4.82	5.58	3.35	3.80	4.15	4.55	6.05	6.94
P_{ft} (psi)	2.57	2.95	3.22	3.63	4.89	5.68	3.37	3.83	4.18	4.57	6.09	6.99
P_{si} (psi)	5.57	5.57	5.57	5.57	5.57	5.57	5.57	5.57	5.57	5.57	5.57	5.57
P_{su} (psi)	9.28	9.28	9.28	9.27	9.26	9.25	9.27	9.26	9.26	9.26	9.24	9.23

TABLE A-2 (continued)

Span (ft)	24											
Design	W S D											
f'_c (ksi)	4											
f_y (ksi)	40						60					
Live load (psf)	50	80	100	125	200	250	50	80	100	125	200	250
Slab t (in.)	8.0	8.0	8.0	8.0	8.0	8.0	8.0	8.0	8.0	8.0	8.0	8.0
P_i (psi)	0.96	1.15	1.30	1.50	2.16	2.57	1.38	1.61	1.79	2.00	2.79	3.27
P_f (psi)	2.56	2.94	3.22	3.62	4.88	5.65	3.38	3.84	4.20	4.60	6.14	7.05
P_{ft} (psi)	2.59	2.97	3.25	3.66	4.95	5.75	3.40	3.86	4.22	4.63	6.18	7.11
P_{si} (psi)	6.54	6.54	6.54	6.54	6.54	6.54	6.54	6.54	6.54	6.54	6.54	6.54
P_{su} (psi)	10.83	10.82	10.82	10.82	10.80	10.79	10.81	10.80	10.80	10.80	10.77	10.76

TABLE A-2 (continued)

Span (ft)	28											
Design	W S D											
f'_c (ksi)	3											
f_y (ksi)	40						60					
Live load (psf)	50	80	100	125	200	250	50	80	100	125	200	250
Slab t (in.)	9.5	9.5	9.5	9.5	9.5	9.5	9.5	9.5	9.5	9.5	9.5	9.5
P_i (psi)	0.99	1.21	1.35	1.56	2.18	2.60	1.47	1.70	1.86	2.09	2.83	3.34
P_f (psi)	2.75	3.17	3.45	3.86	5.03	5.83	3.70	4.15	4.46	4.91	6.35	7.38
P_{ft} (psi)	2.78	3.21	3.48	3.91	5.11	5.94	3.73	4.18	4.49	4.94	6.39	7.38
P_{si} (psi)	5.74	5.74	5.74	5.74	5.74	5.74	5.74	5.74	5.74	5.74	5.74	5.74
P_{su} (psi)	9.62	9.62	9.61	9.61	9.60	9.59	9.60	9.60	9.60	9.59	9.58	9.57

TABLE A-2 (concluded)

Span (ft)	28											
Design	W S D											
f'_c (ksi)	4											
f_y (ksi)	40						60					
Live load (psf)	50	80	100	125	200	250	50	80	100	125	200	250
Slab t (in.)	9.5	9.5	9.5	9.5	9.5	9.5	9.5	9.5	9.5	9.5	9.5	9.5
P_i (psi)	1.00	1.22	1.36	1.58	2.21	2.64	1.49	1.73	1.89	2.12	2.88	3.40
P_f (psi)	2.77	3.20	3.48	3.90	5.09	5.91	3.73	4.19	4.51	4.97	6.44	7.44
P_{ft} (psi)	2.80	3.24	3.52	3.95	5.17	6.02	3.76	4.22	4.54	5.00	6.48	7.50
P_{si} (psi)	6.75	6.75	6.75	6.75	6.75	6.75	6.75	6.75	6.75	6.75	6.75	6.75
P_{su} (psi)	11.24	11.23	11.23	11.22	11.21	11.20	11.22	11.21	11.21	11.20	11.18	11.17

TABLE A-3

FAILURE OVERPRESSURES FOR STEEL BEAMS SUPPORTING CONCRETE SLABS (psi)

Slab Design live load psf	12 ft Span		16 ft Span		20 ft Span		24 ft Span		28 ft Span	
	PI	PU	PI	PU	PI	PU	PI	PU	PI	PU
50	0.75	1.41	0.70	1.31	0.60	1.13	0.70	1.31	0.85	1.59
80	0.65	1.22	0.90	1.69	0.75	1.41	0.80	1.50	0.95	1.78
100	0.90	1.69	0.95	1.78	0.90	1.69	1.05	1.97	0.90	1.69
125	0.80	1.50	0.85	1.59	0.80	1.50	0.95	1.78	1.20	2.25
200	1.00	1.88	1.15	2.16	1.20	2.25	1.30	2.44	1.45	2.72
250	1.60	3.00	1.50	2.81	1.40	2.63	1.40	2.63	1.50	2.81

TABLE A-4

FAILURE OVERPRESSURES FOR BOLTED CONNECTIONS (psi)

Slab Design live load psf	12 ft Span		16 ft Span		20 ft Span		24 ft Span		28 ft Span	
	F*	S*	F	S	F	S	F	S	F	S
50	2.4	1.5	1.6	2.2	1.7	3.9	2.2	3.9	1.7	3.2
80	2.2	1.8	1.3	2.7	1.7	3.6	2.1	3.8	2.7	5.2
100	3.0	1.7	1.4	3.2	1.7	3.5	3.3	3.6	2.6	4.4
125	2.8	3.2	2.2	3.0	2.6	5.8	3.2	4.4	2.6	4.2
200	2.3	4.9	2.3	5.7	4.0	5.3	3.2	6.9	3.4	5.2
250	2.5	6.8	2.3	5.4	3.8	3.4	4.7	7.6	4.2	6.4

* Framed Connection

** Seated Connection

STANDARD DISTRIBUTION LIST FOR RESEARCH REPORTS

(Number of Copies - One unless otherwise indicated)

Defense Civil Preparedness Agency
Research
Washington, D.C. 20301
Attention: Administrative Officer (50)

Assistant Secretary of the Army (R&D)
Washington, D.C. 20310
Attention: Assistant for Research

Chief of Naval Research
Washington, D.C. 20360

Commander, Naval Supply Systems
Command (0421G)
Department of the Navy
Washington, D.C. 20376

Commander
Naval Facilities Engineering Command
Research & Development (Code 0322C)
Department of the Navy
Washington, D.C. 20390

Defense Documentation Center
Cameron Station
Alexandria, Virginia 22314 (12)

Civil Defense Research Project
Oak Ridge National Laboratory
P.O. Box X
Oak Ridge, Tennessee 37830
Attention: Librarian

Mr. Edward L. Hill
Research Triangle Institute
P.O. Box 12194

Mr. H. L. Murphy
Stanford Research Institute
333 Ravenswood Avenue
Menlo Park, California 94025

Chief of Engineers
Attn: ENGME-RD
Department of the Army
Washington, D.C. 20314

Commanding Officer
U.S. Naval Civil Engineering Laboratory
Attn: Document Library
Port Hueneme, California 93041

AFWL/Civil Engineering Division
Attn: Technical Library
Kirtland Air Force Base
Albuquerque, New Mexico 87117

Chief, Joint Civil Defense Support Group
Attn: ENGMC-D
Office, Chief of Engineers
Department of the Army
Washington, D.C. 20314

Director, U.S. Army Engineer
Waterways Experiment Station
Attn: Nuclear Weapons Effects Branch
P.O. Box 631
Vicksburg, Mississippi 39180

Mr. William H. Van Horn
URS Research Company
155 Bovet Road
San Mateo, California 94402

Mr. Carl K. Wiehle
Stanford Research Insitute
333 Ravenswood Avenue
Menlo Park, California 94025

Mr. Anatole Longinow
IIT Research Institute
10 West 35th Street
Chicago, Illinois 60616

Mr. Samuel Kramer, Chief
Office of Federal Building Technology
Center for Building Technology
National Bureau of Standards
Washington, D.C. 20234

Director, Defense Nuclear Agency
Attn: Mr. Jack R. Kelso
Washington, D.C. 20305

Mr. Bert Greenglass
Director, Office of Administration
Program Planning and Control
Department of Housing & Urban Development
Washington, D.C. 20410

Los Alamos Scientific Laboratory
Attn: Document Library
Los Alamos, New Mexico 87544

Mr. George N. Sisson
Research Directorate
Defense Civil Preparedness Agency
Washington, D.C. 20301

Director
Ballistic Research Laboratory
Attn: Document Library
Aberdeen Proving Ground, Maryland 21005

Civil Engineering Center/AF/PRECET
Attn: Technical Library
Wright-Patterson Air Force Base
Dayton, Ohio 45433

Director, Army Materials & Mechanics
Research Center
Attn: Technical Library
Watertown, Massachusetts 02172

Commanding Officer
U.S. Army Combat Developments
Command
Institute of Nuclear Studies
Fort Bliss, Texas 79916

Director, U.S. Army Engineer
Waterways Experiment Station
Attn: Document Library
P.O. Box 631
Vicksburg, Mississippi 39180

Mr. Donald A. Bettge
Research Directorate
Defense Civil Preparedness Agency
Washington, D.C. 20301

Dr. Lewis V. Spencer
Radiation Theory Section 4.3
National Bureau of Standards
Washington, D.C. 20234

Professor Robert Bailey
Nuclear Engineering Department
Duncan Annex
Purdue University
Lafayette, Indiana 47907

Director, Defense Nuclear Agency
Attn: Technical Library
Washington, D.C. 20305

Peter K. Dai, R1/2170
TRW Defense & Space Systems Group
1 Space Park
Redondo Beach, California 90278
(213)536-3253